Institute of Paper Science and Technology

SLIDE MATERIAL

To The

PAPERMAKING

PROJECT ADVISORY COMMITTEE

April 4, 1991
Institute of Paper Science and Technology
Atlanta, GA

Atlanta, Georgia

SLIDE MATERIAL

To The

PAPERMAKING

PROJECT ADVISORY COMMITTEE

April 4, 1991
Institute of Paper Science and Technology
Atlanta, GA

FUNDAMENTALS OF DRYING
PROJECT 3470

April 4, 1991
Institute of Paper Science and Technology
Atlanta, Georgia

FUNDAMENTALS OF DRYING

IMPULSE DRYING OF HEAVY WEIGHT GRADES

OBJECTIVES

- Demonstrate and evaluate pilot scale impulse drying of 42 lb linerboard using prototype ceramic coated press roll.

- Develop an understanding of the mechanism of operation of low thermal mass press surfaces by measuring heat flux during impulse drying.

PILOT SCALE DEMONSTRATION AND EVALUATION

PILOT SCALE IMPULSE DRIER

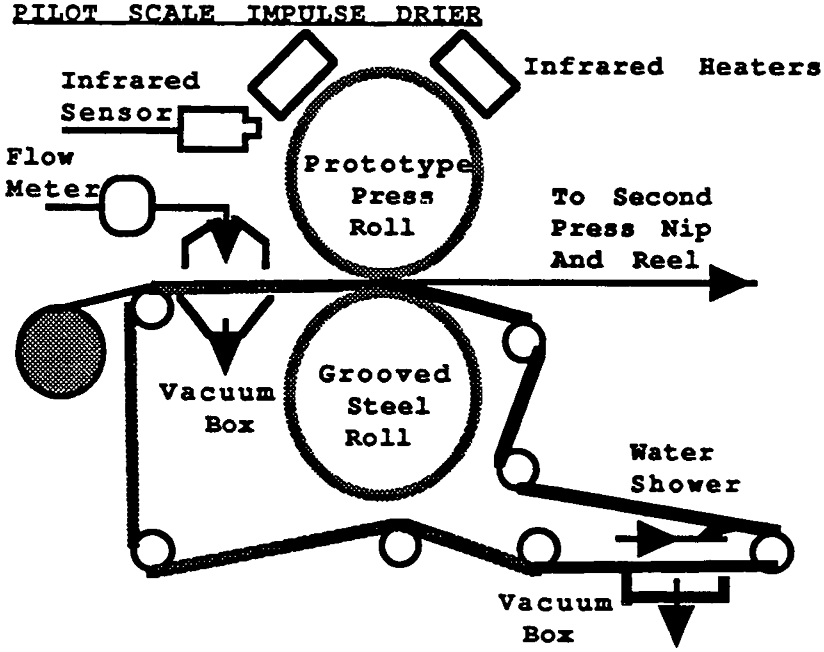

PILOT SCALE STEAM PREHEATING EXPERIMENTS

Sheet Conditions:	
Basis Weight	205 gsm
Entering Solids	30 to 50%
Entering Temperature	25°C
Steam Box and Vacuum Box:	
Steam Flow rate	214 kg/h
Steam Temperature	112°C
Vacuum	28 cm Hg
Pilot Conditions:	
Pilot Speed	30 and 60 m/min

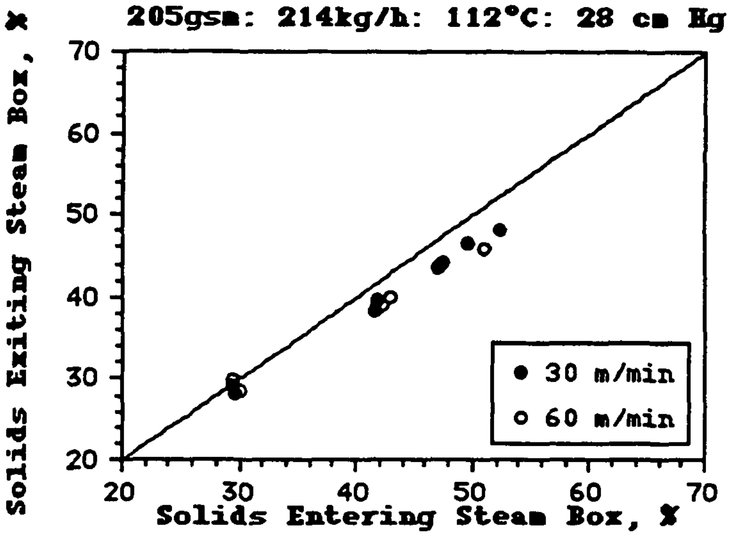

PILOT SCALE IMPULSE DRYING EXPERIMENTAL CONDITIONS

Sheet Conditions:	
Unbleached Softwood Kraft, Kappa # 73.5	
Refined To 650 ml CSF, WebFormer	
Basis Weight	205 gsm
Steam Box and Vacuum Box:	
Steam Flow Rate	214 kg/h
Steam Temperature	112°C
Vacuum	28 cm Hg
Impulse Drying Conditions:	
Ingoing Temperature	~100°C
Peak Pressure	6.2 MPa
Pilot Speed	30 and 60 m/min
Nip Residence Time	40 and 20 ms
Roll Temperature	106, 371 and 426°C
Ingoing Solids	41.5 and 43.5%

PILOT SCALE: CERAMIC COATED PRESS ROLL
205gsm:41.5%Sin:6.2MPa:214kg/h Steam

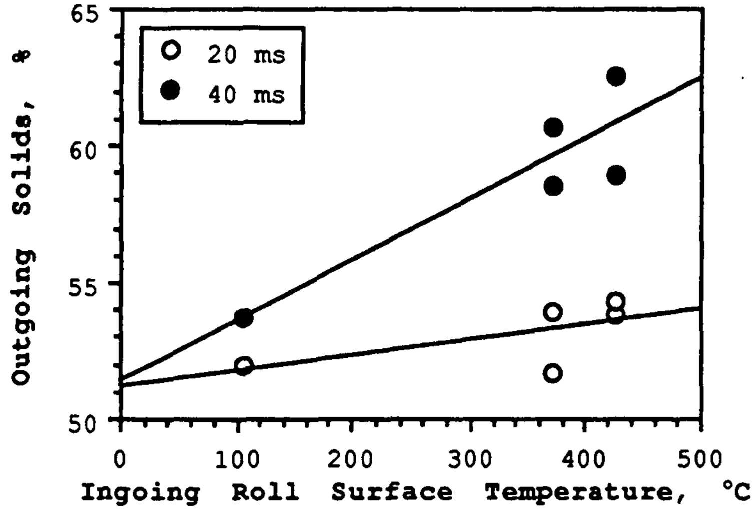

PILOT SCALE: CERAMIC COATED PRESS ROLL
205gsm:43.5%Sin:6.2MPa:214kg/h Steam

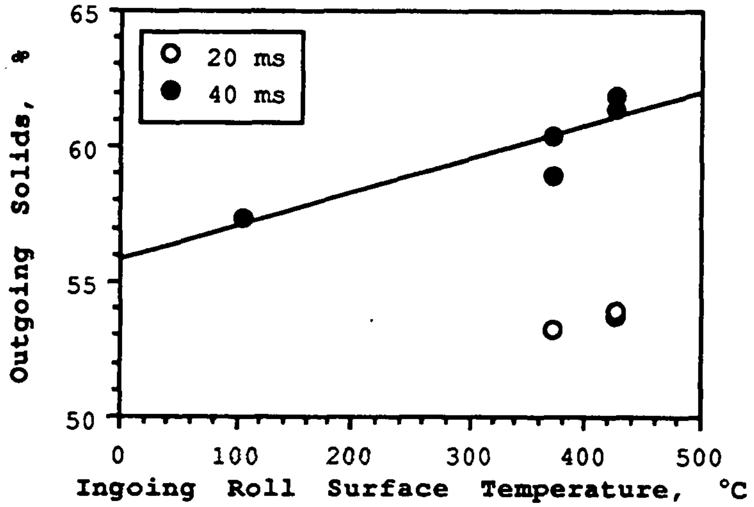

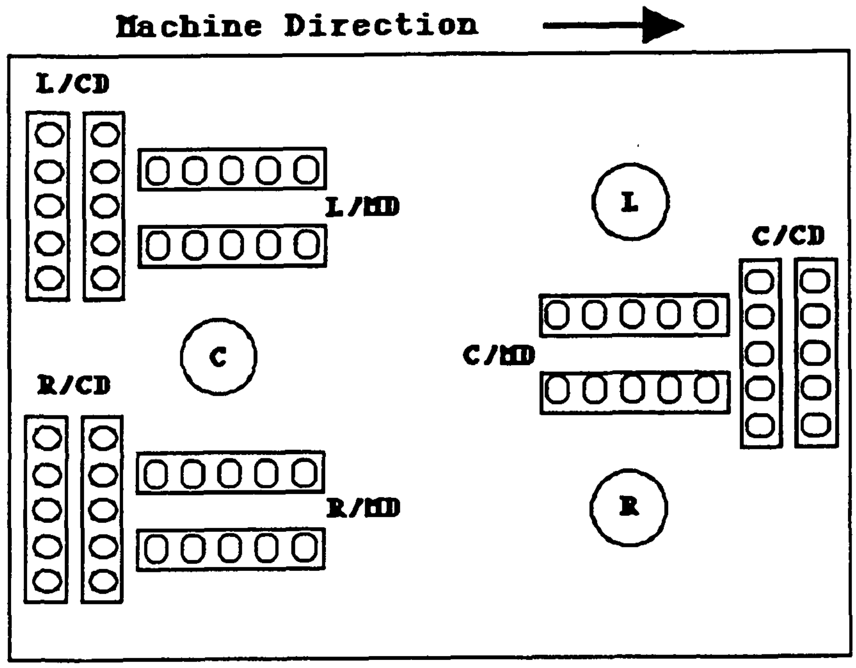

PHYSICAL TESTS PERFORMED ON PILOT SCALE IMPULSE DRIED SAMPLES

LOCATION	TEST PERFORMED	TESTS PER LOCATION
L/CD	Z - Ultrasound STFI Compression OD Basis Weight	10 10 2
L/MD	Z - Ultrasound STFI Compression OD Basis Weight	10 10 2
C/CD	Z - Ultrasound STFI Compression OD Basis Weight	10 10 2
C/MD	Z - Ultrasound STFI Compression OD Basis Weight	10 10 2
R/CD	Z - Ultrasound STFI Compression OD Basis Weight	10 10 2
R/MD	Z - Ultrasound STFI Compression OD Basis Weight	10 10 2
L	Burst	1
C	Burst	1
R	Burst	1

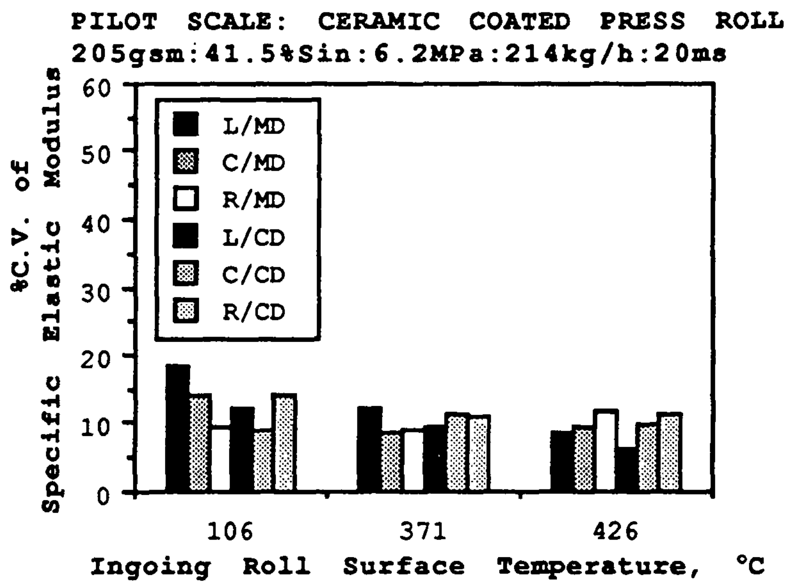
PILOT SCALE: CERAMIC COATED PRESS ROLL
205gsm:41.5%Sin:6.2MPa:214kg/h:20ms
Specific Elastic Modulus %C.V. of
60
50
40
30
20
10
0
L/MD
C/MD
R/MD
L/CD
C/CD
R/CD
106
371
426
Ingoing Roll Surface Temperature, °C

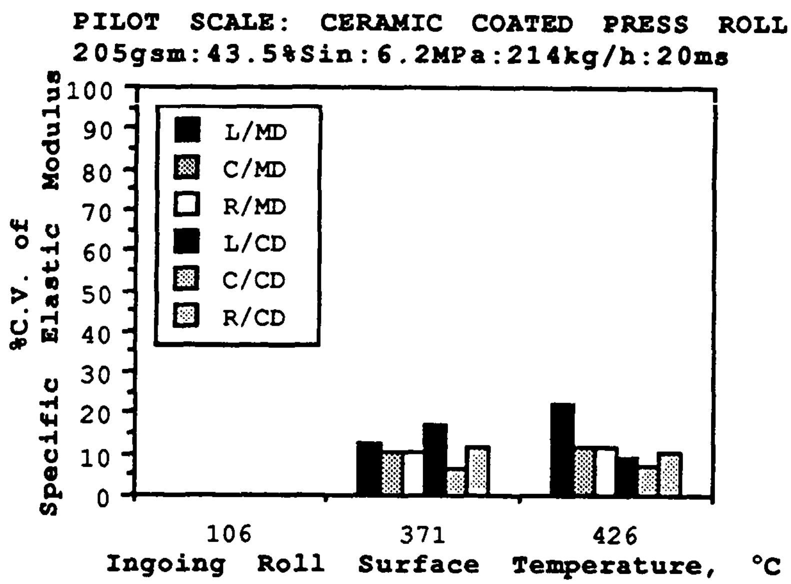
PILOT SCALE: CERAMIC COATED PRESS ROLL
205gsm:43.5%Sin:6.2MPa:214kg/h:20ms
Specific Elastic Modulus %C.V. of
100
90
80
70
60
50
40
30
20
10
0
L/MD
C/MD
R/MD
L/CD
C/CD
R/CD
106
371
426
Ingoing Roll Surface Temperature, °C

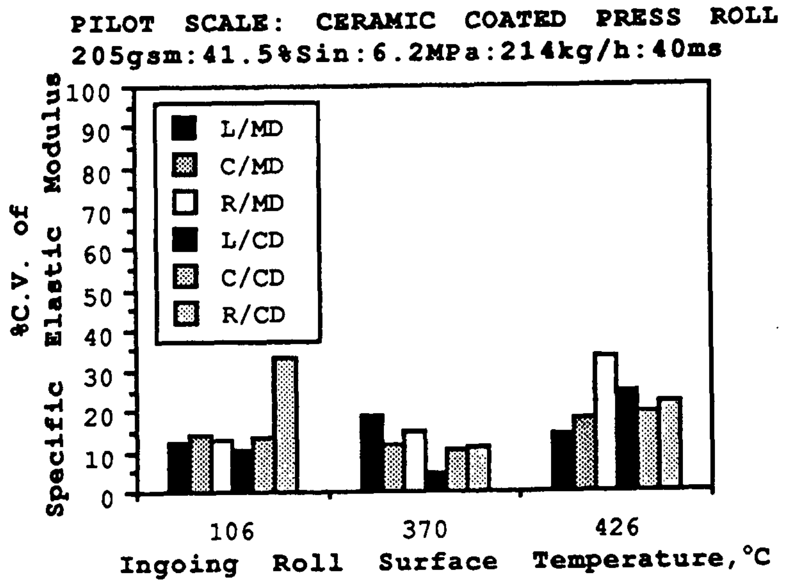
PILOT SCALE: CERAMIC COATED PRESS ROLL
205gsm:41.5%Sin:6.2MPa:214kg/h:40ms
Specific Elastic Modulus %C.V. of
100
90
80
70
60
50
40
30
20
10
0
L/MD
C/MD
R/MD
L/CD
C/CD
R/CD
106
370
426
Ingoing Roll Surface Temperature,°C

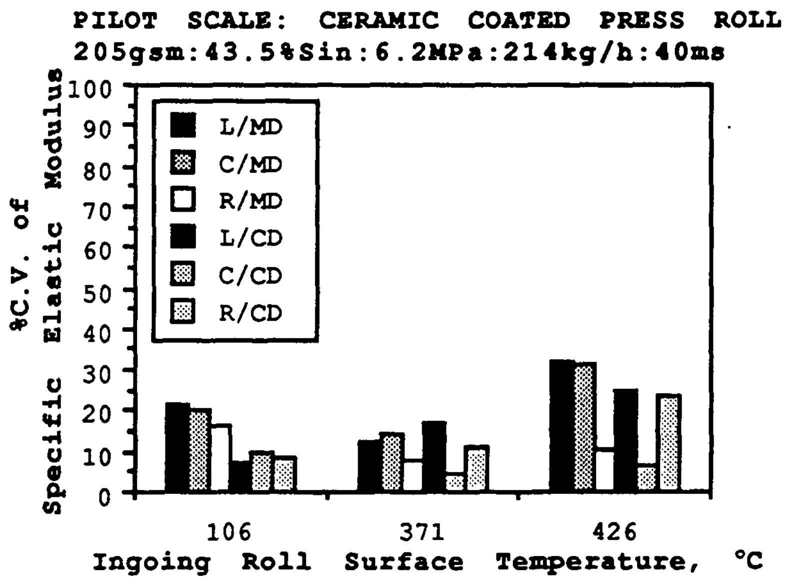
PILOT SCALE: CERAMIC COATED PRESS ROLL
205gsm:43.5%Sin:6.2MPa:214kg/h:40ms
Specific Elastic Modulus %C.V. of
100
90
80
70
60
50
40
30
20
10
0
L/MD
C/MD
R/MD
L/CD
C/CD
R/CD
106
371
426
Ingoing Roll Surface Temperature, °C

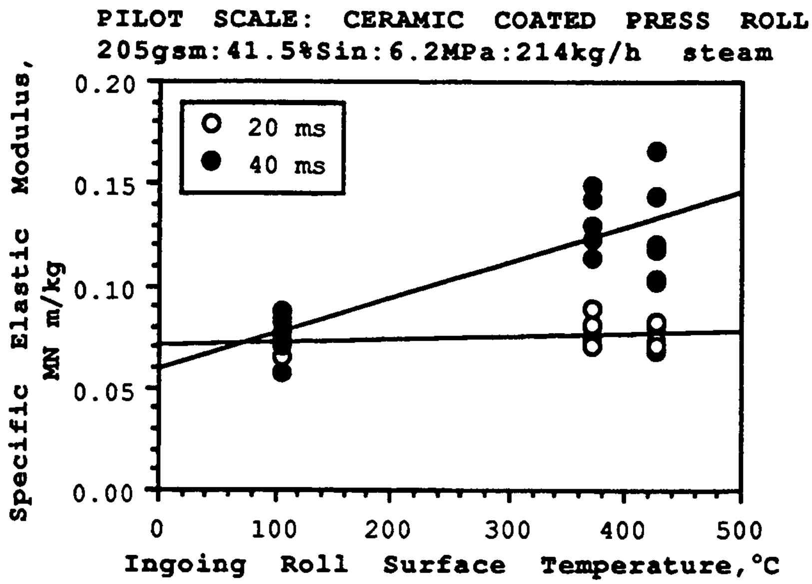
PILOT SCALE: CERAMIC COATED PRESS ROLL
205gsm:41.5%Sin:6.2MPa:214kg/h steam
Specific Elastic Modulus, MN m/kg
0.20
0.15
0.10
0.05
0.00
20 ms
40 ms
0
100
200
300
400
500
Ingoing Roll Surface Temperature,°C

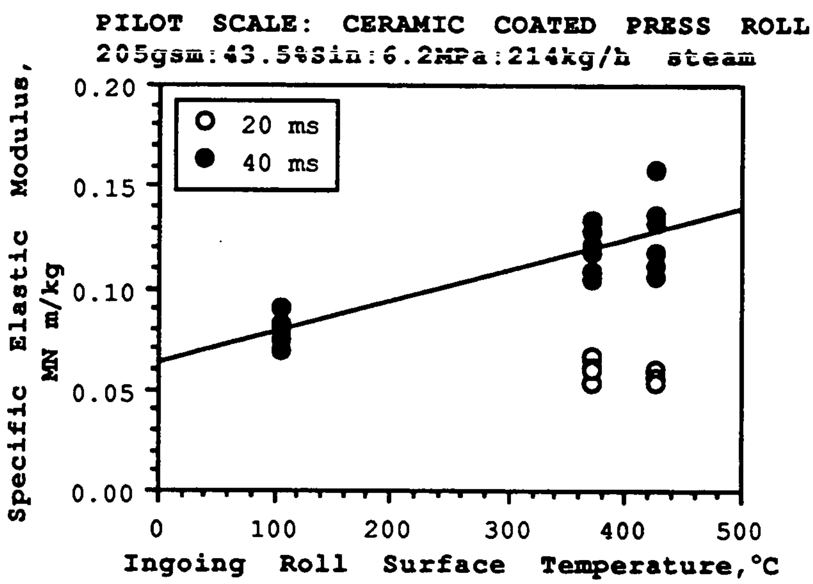
PILOT SCALE: CERAMIC COATED PRESS ROLL
205gsm:43.5%Sin:6.2MPa:214kg/h steam
Specific Elastic Modulus, MN m/kg
0.20
0.15
0.10
0.05
0.00
20 ms
40 ms
0
100
200
300
400
500
Ingoing Roll Surface Temperature,°C

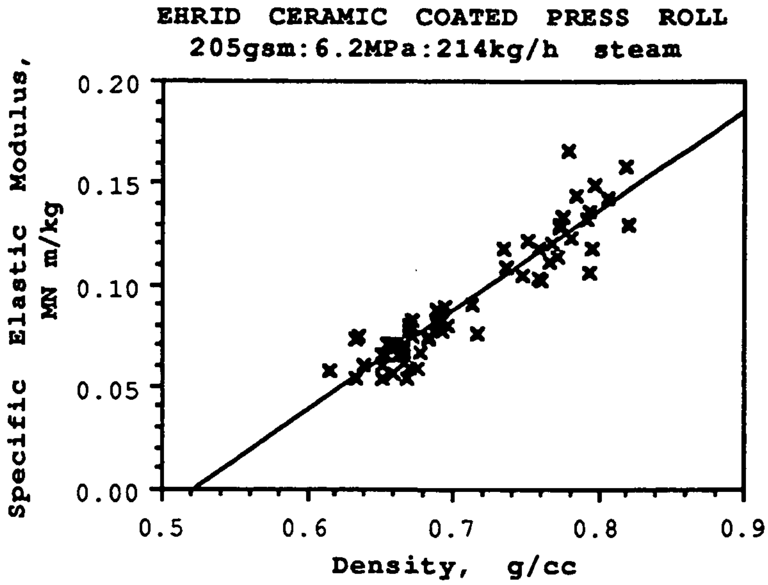
EHRID CERAMIC COATED PRESS ROLL
205gsm:6.2MPa:214kg/h steam
Specific Elastic Modulus, MN m/kg
0.20
0.15
0.10
0.05
0.00
0.5
0.6
0.7
0.8
0.9
Density, g/cc

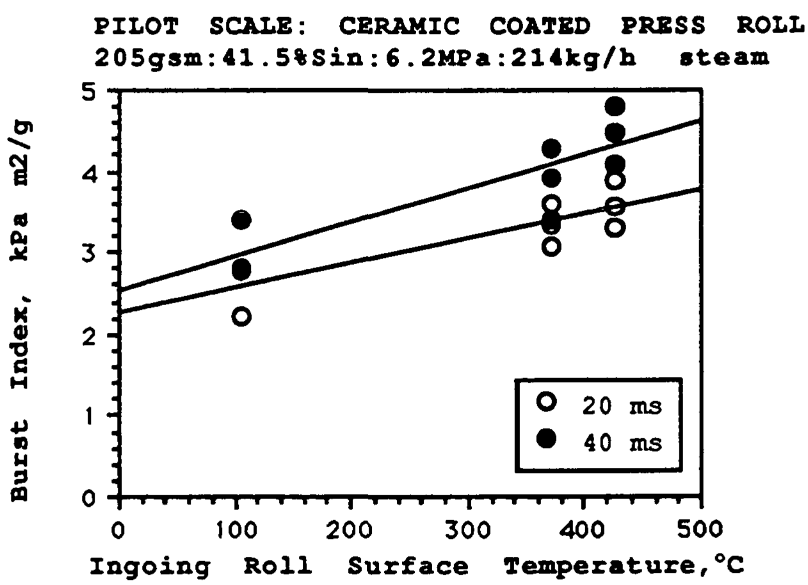
PILOT SCALE: CERAMIC COATED PRESS ROLL
205gsm:41.5%Sin:6.2MPa:214kg/h steam
Burst Index, kPa m2/g
5
4
3
2
1
0
0
100
200
300
400
500
Ingoing Roll Surface Temperature,°C
20 ms
40 ms

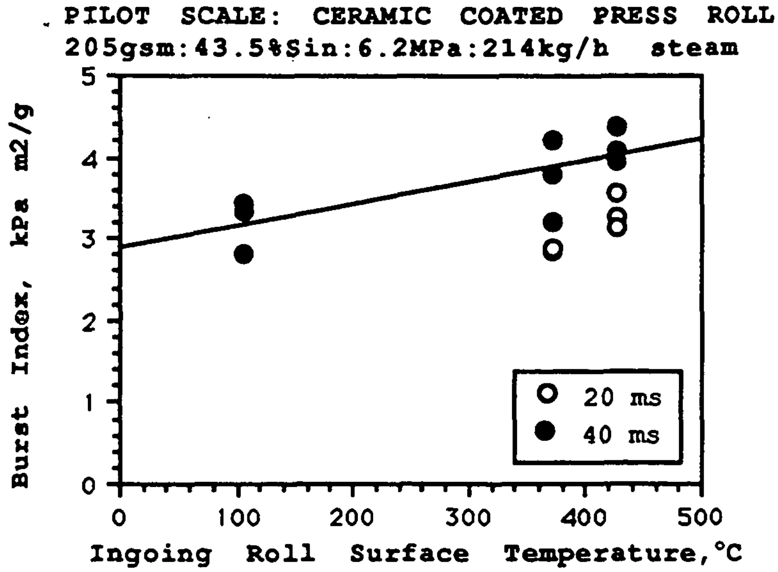
PILOT SCALE: CERAMIC COATED PRESS ROLL
205gsm:43.5%Sin:6.2MPa:214kg/h steam
Burst Index, kPa m2/g
Ingoing Roll Surface Temperature,°C
20 ms
40 ms

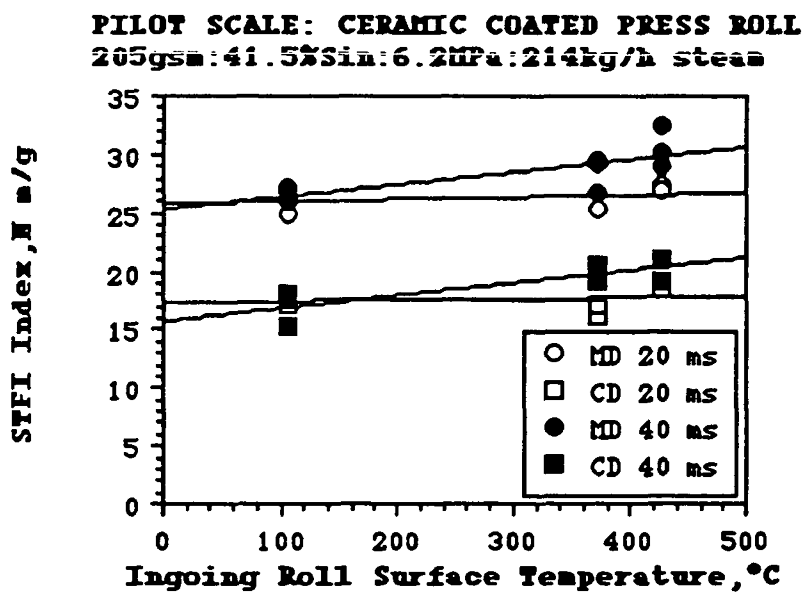
PILOT SCALE: CERAMIC COATED PRESS ROLL
205gsm:41.5%Sin:6.2MPa:214kg/h steam
STFI Index,N m/g
Ingoing Roll Surface Temperature,°C
MD 20 ms
CD 20 ms
MD 40 ms
CD 40 ms

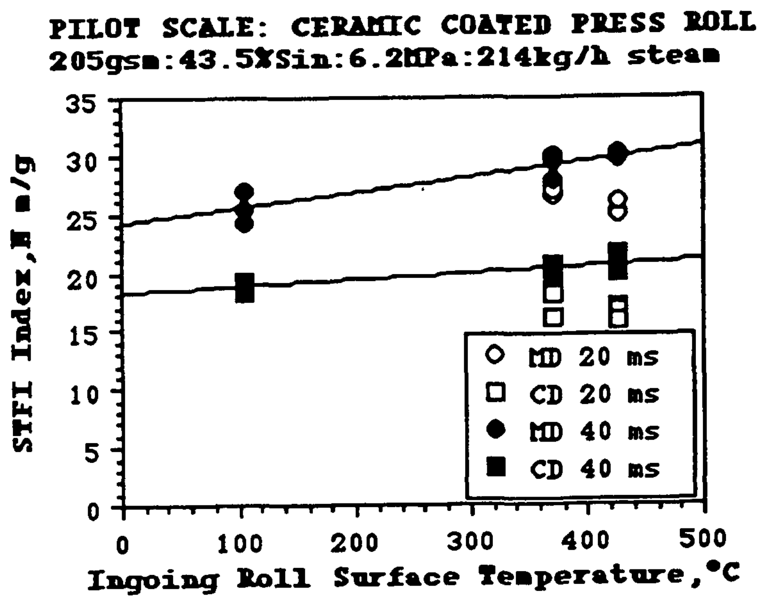

SUMMARY OF RESULTS OF PILOT SCALE EXPERIMENTS				
	WET PRESS 20 ms	IMPULSE DRY 427°C 20ms	WET PRESS 40 ms	IMPULSE DRY 371°C 40ms
Solids Out, %	52	54	54	60
Modulus, MN m/kg	0.07	0.07	0.07	0.12
Burst Index, kPa m2/g	2.6	3.5	3.0	4.0
MD STFI Index, N m/g	26	26	26	29
CD STFI Index, N m/g	17	17	17	20

LABORATORY SCALE HEAT FLUX MEASUREMENTS

LAB SCALE IMPULSE DRYING SIMULATOR

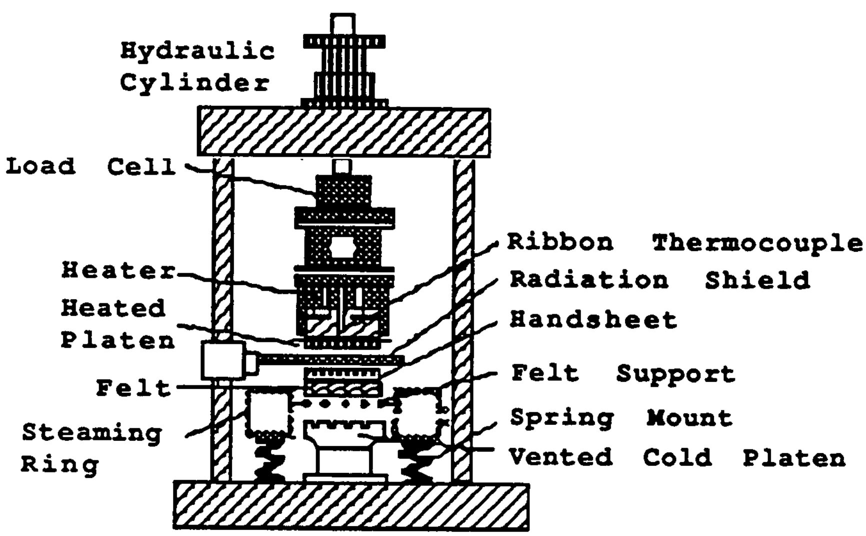

LAB SCALE IMPULSE DRYING EXPERIMENTAL CONDITIONS

Sheet Conditions:
Unbleached Softwood Kraft, Kappa # 73.5
Refined To 650 ml CSF, British Sheet Mold

Basis Weight	205 gsm

Post Steaming Conditions:

Radiation Shield	Used
Ingoing Solids	30 %
Ingoing Temperature	85°C

Impulse Drying Conditions:

Platen Type	Steel and Prototype
Peak Pressure	3.1 and 6.2 MPa
Dwell Time	20 ms
Platen Temperature	88, 150, 260, 371°C

LAB SCALE IMPULSE DRYING PRELIMINARY RESULTS

o Sheets with more water at the heated surface absorb more energy during impulse drying.

o Heat flux vs time curves show two peak heat flux, during compression and during decompression.

o At a given ingoing platen surface temperature the prototype platen tranfered less energy than the steel platen.

o Energy transfer from the steel platen increased with peak pressure, while energy transfer from the prototype platen was pressure independent.

PLANS FOR THE NEXT REPORTING PERIOD

- For a range of linerboard furnishes, determine the impulse drying pilot scale operating conditions resulting in maximum water removal without sheet delamination.

- Evaluate lower thermal mass ceramic coatings and the concept of a low surface energy synthetic diamond outer coating on lab scale.

- Expand lab scale heat flux measurements to higher ingoing solids and longer dwell times. Explore influence of sheet permeability and various felt variables. Further develop an understanding of the mechanism of operation.

- Coat second press roll with advanced ceramic coating and demonstrate concept of continuous polymer re-coating and/or durability and function of synthetic diamond outer coating.

FUNDAMENTALS OF WATER REMOVAL PROCESSES
PROJECT 3480

April 4, 1991
Institute of Paper Science and Technology
Atlanta, Georgia

Project 3480

Title:

Fundamentals of Water Removal Processes

Objective:

To assist water removal technologies by improving the fundamental understanding of water flow in paper.

Anisotropic Permeability

Relevant to:

- Wet pressing
- Displacement dewatering
- Impulse drying
- Coating application
- Edge penetration

Project 3480 Activities

- Anisotropic permeability measurements
- Modeling of displacement dewatering and impulse drying
- Measurements and analysis of effective porosity in paper
- Studies of vapor-liquid flow in fibrous media

Definitions

- Permeability

  Not a flow rate of air, but an intrinsic property of a porous medium tied to Darcy's law. (Units are meters-squared.)

- Porosity

  Also not a flow rate of air. Porosity is the fraction of the sample volume not occupied by solid. (Dimensionless.)

Hypotheses

Fiber orientation in the plane will cause the in-plane permeability to be greater than the transverse permeability ($\alpha > 1$).

Furthermore, permeability in the machine direction should exceed permeability in the cross-direction ($\beta > 1$).

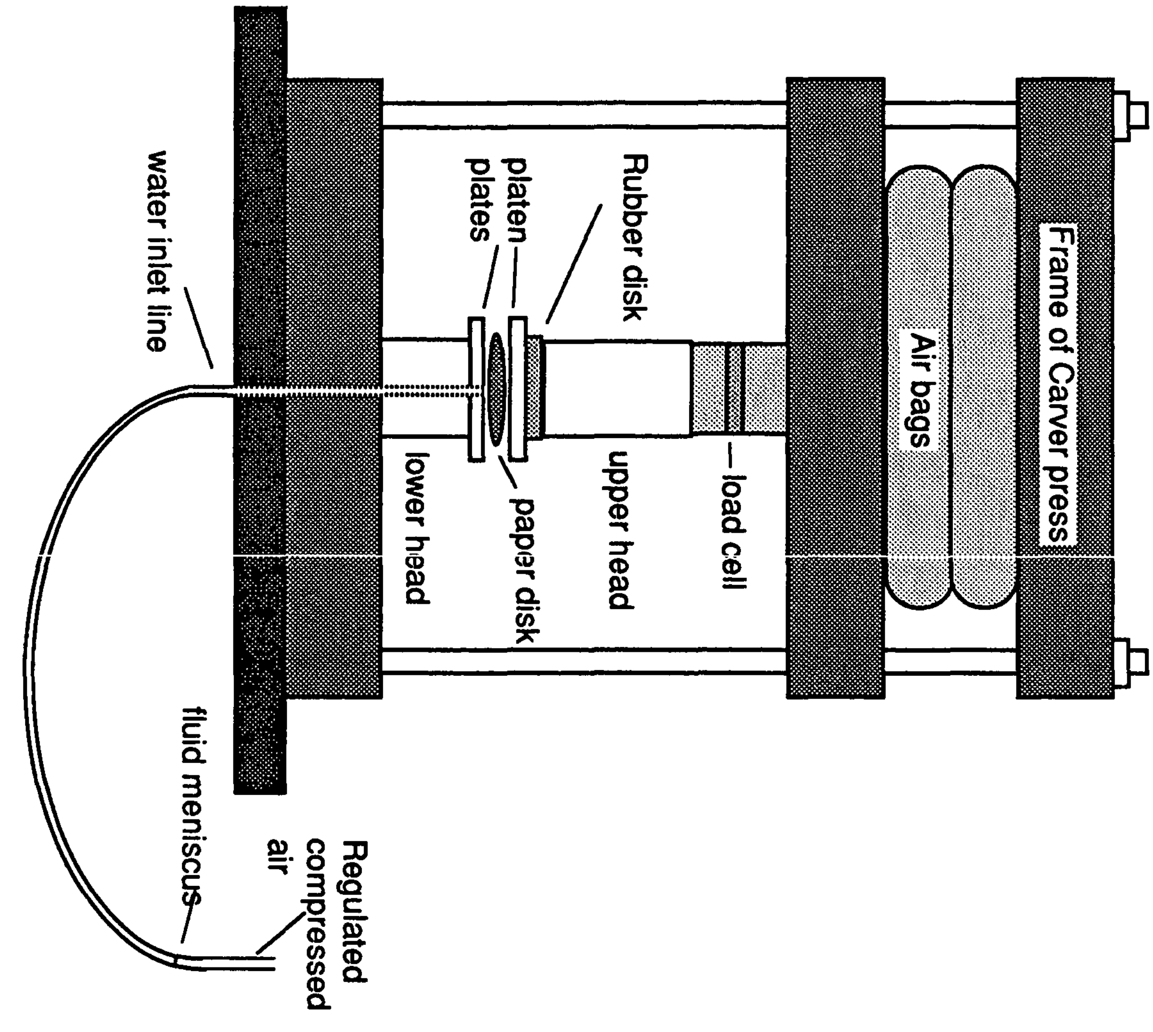
Frame of Carver press
Air bags
load cell
upper head
Rubber disk
platen
plates
paper disk
lower head
water inlet line
fluid meniscus
Regulated
compressed
air

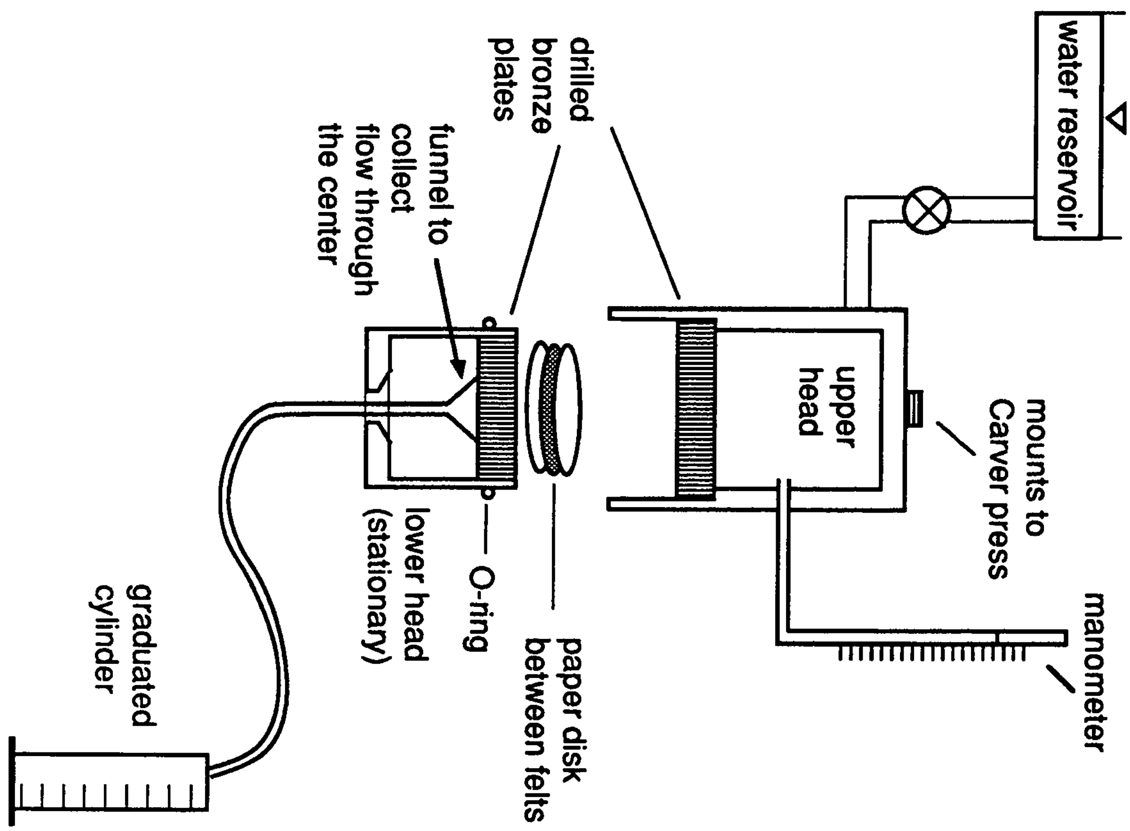
water reservoir
mounts to Carver press
upper head
manometer
drilled bronze plates
funnel to collect flow through the center
paper disk between felts
O-ring
lower head (stationary)
graduated cylinder

Lateral Perm. in 200 gsm West Coast Sulfite

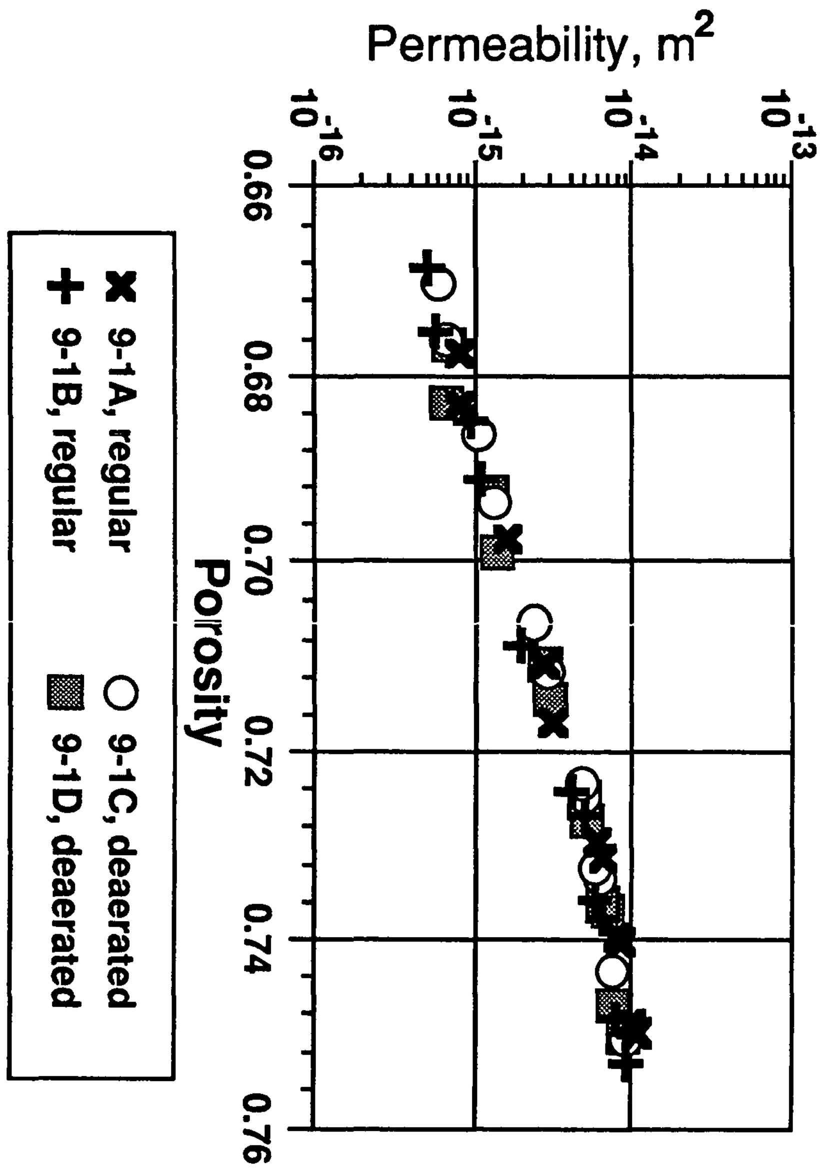

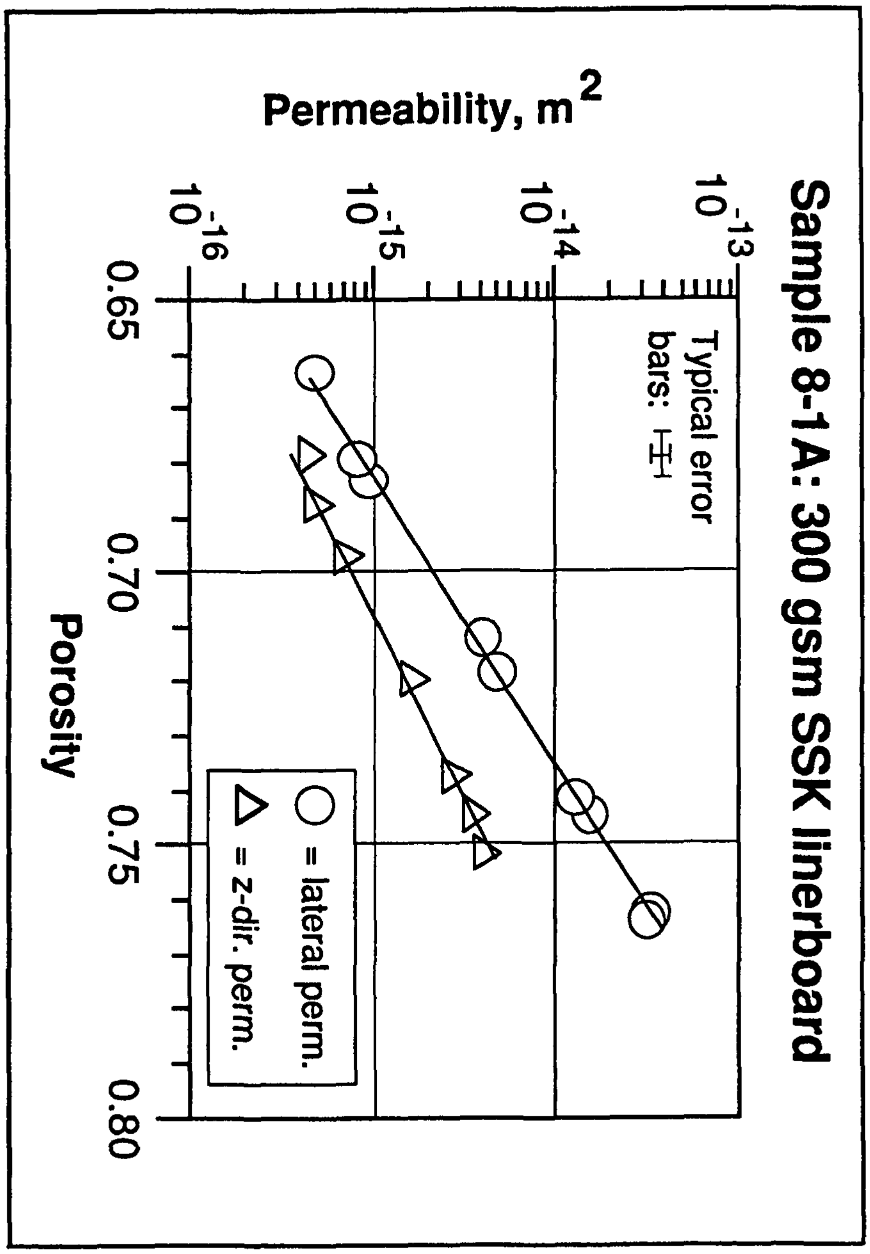
Sample 8-1A: 300 gsm SSK linerboard
Permeability, m^2
10^{-13}
10^{-14}
10^{-15}
10^{-16}
Porosity
0.65
0.70
0.75
0.80
Typical error bars:
○ = lateral perm.
△ = z-dir. perm.

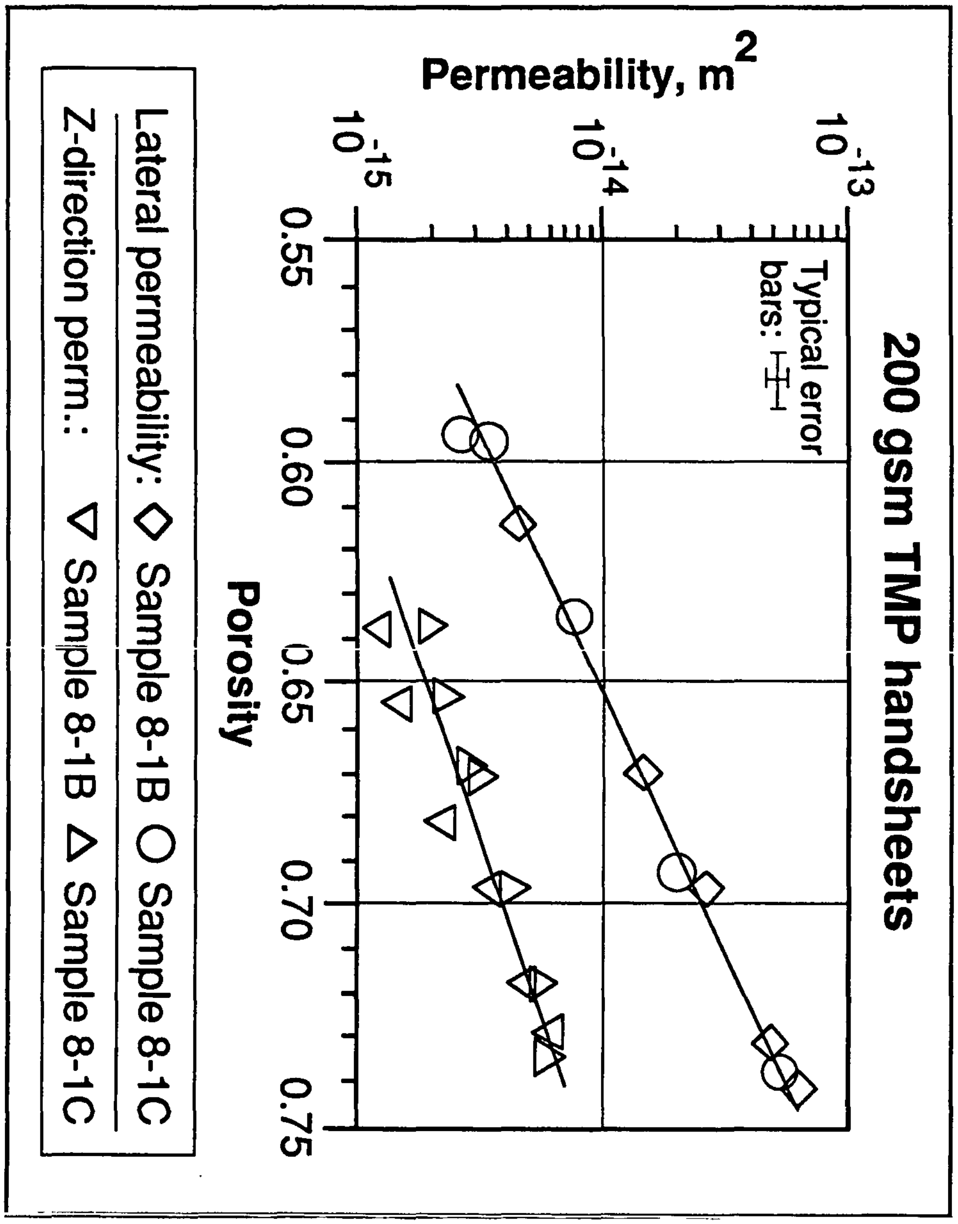

200 gsm TMP handsheets
Permeability, m2
10-13
10-14
10-15
Typical error bars:
0.55
0.60
0.65
0.70
0.75
Porosity
Lateral permeability: ◇ Sample 8-1B ○ Sample 8-1C
Z-direction perm.: ▽ Sample 8-1B △ Sample 8-1C

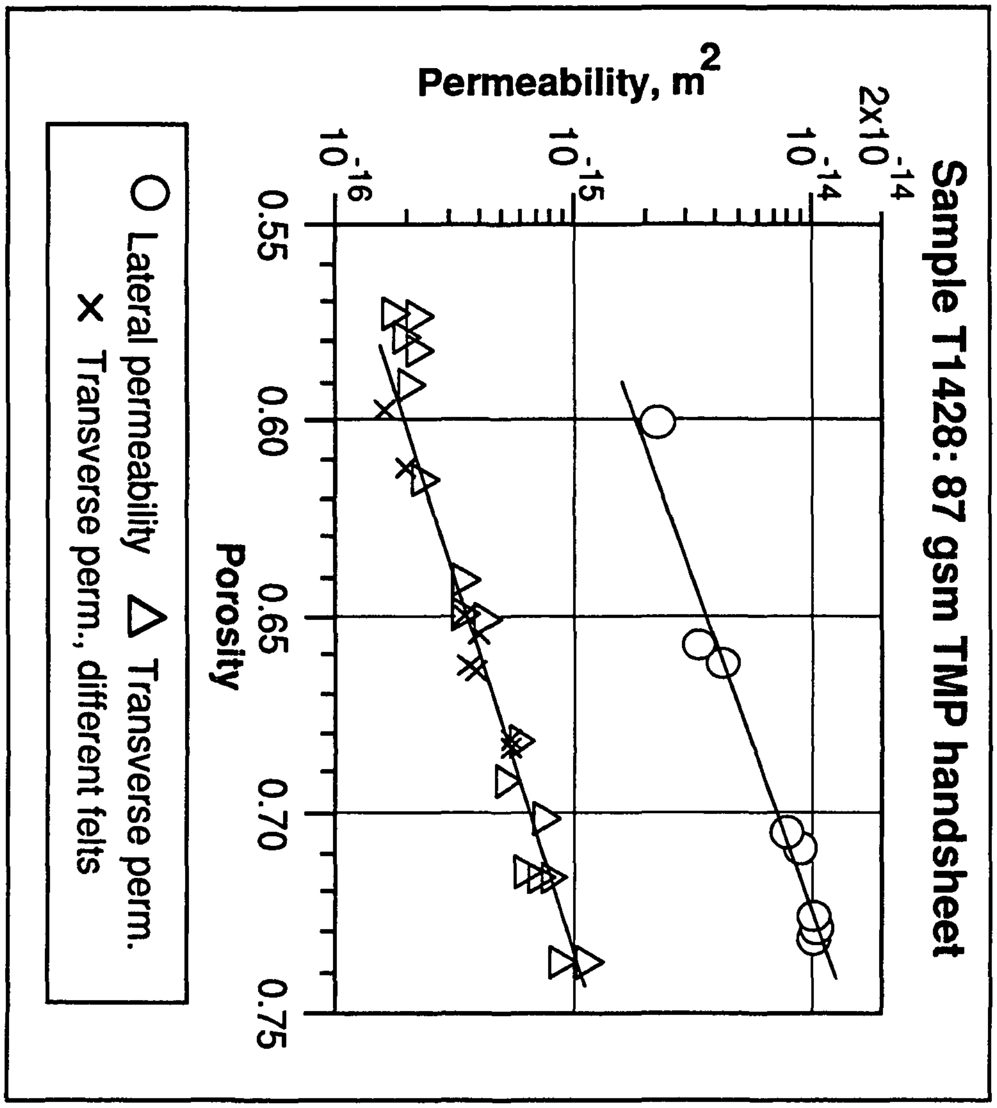
Sample T1428: 87 gsm TMP handsheet
Permeability, m^2
2x10^{-14}
10^{-14}
10^{-15}
10^{-16}
0.55
0.60
0.65
0.70
0.75
Porosity
○ Lateral permeability △ Transverse perm.
× Transverse perm., different felts

Specific Surface and Volume in an Anisotropic Sheet

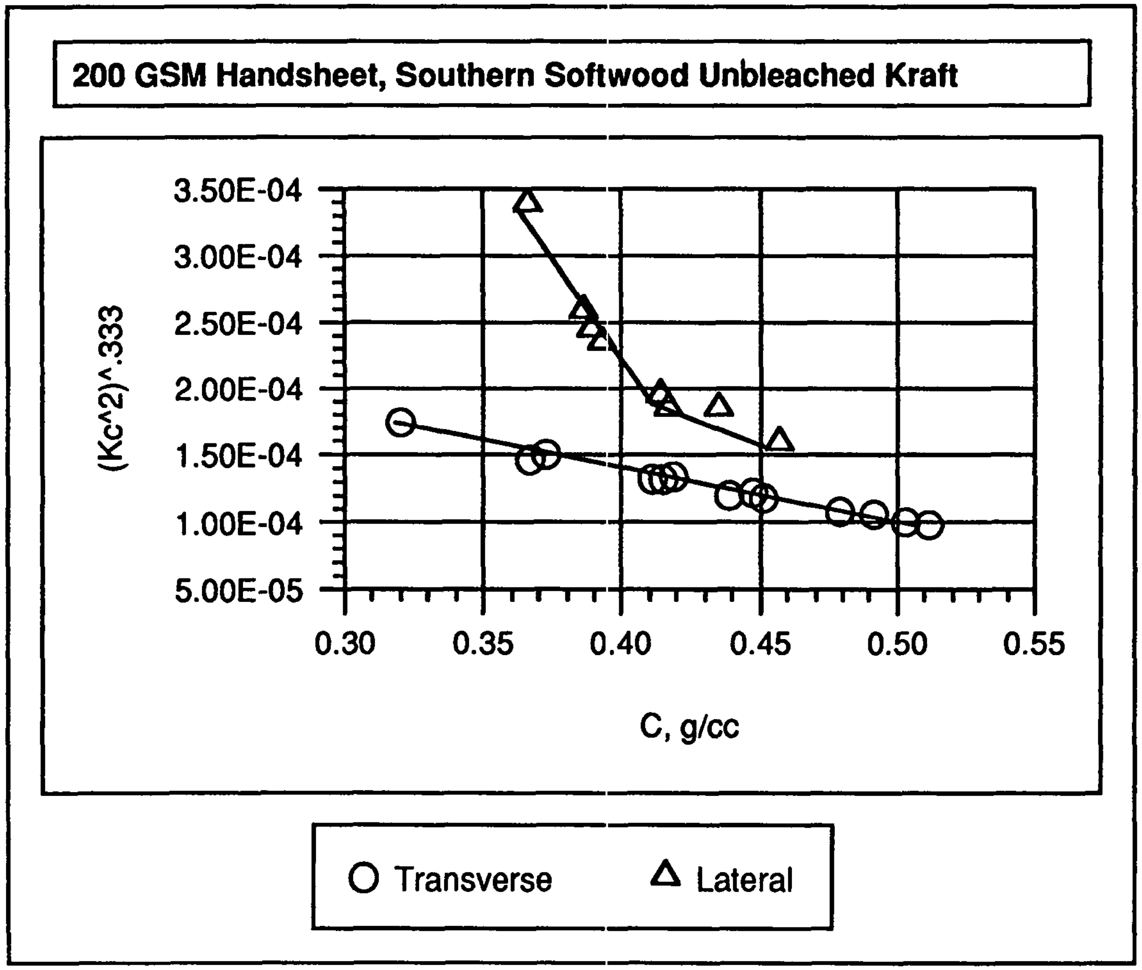

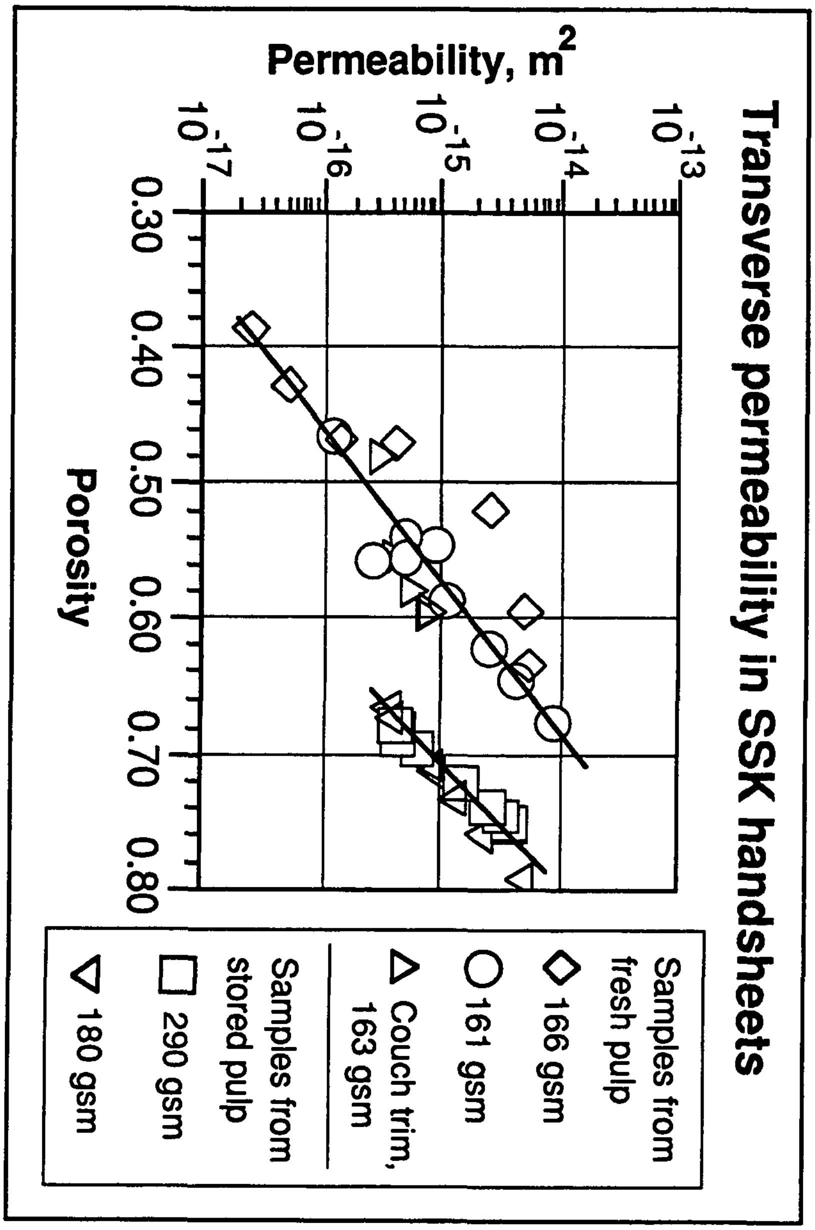
Transverse permeability in SSK handsheets
Permeability, m^2
10^{-13}
10^{-14}
10^{-15}
10^{-16}
10^{-17}
0.30
0.40
0.50
0.60
0.70
0.80
Porosity
Samples from fresh pulp
166 gsm
161 gsm
Couch trim, 163 gsm
Samples from stored pulp
290 gsm
180 gsm

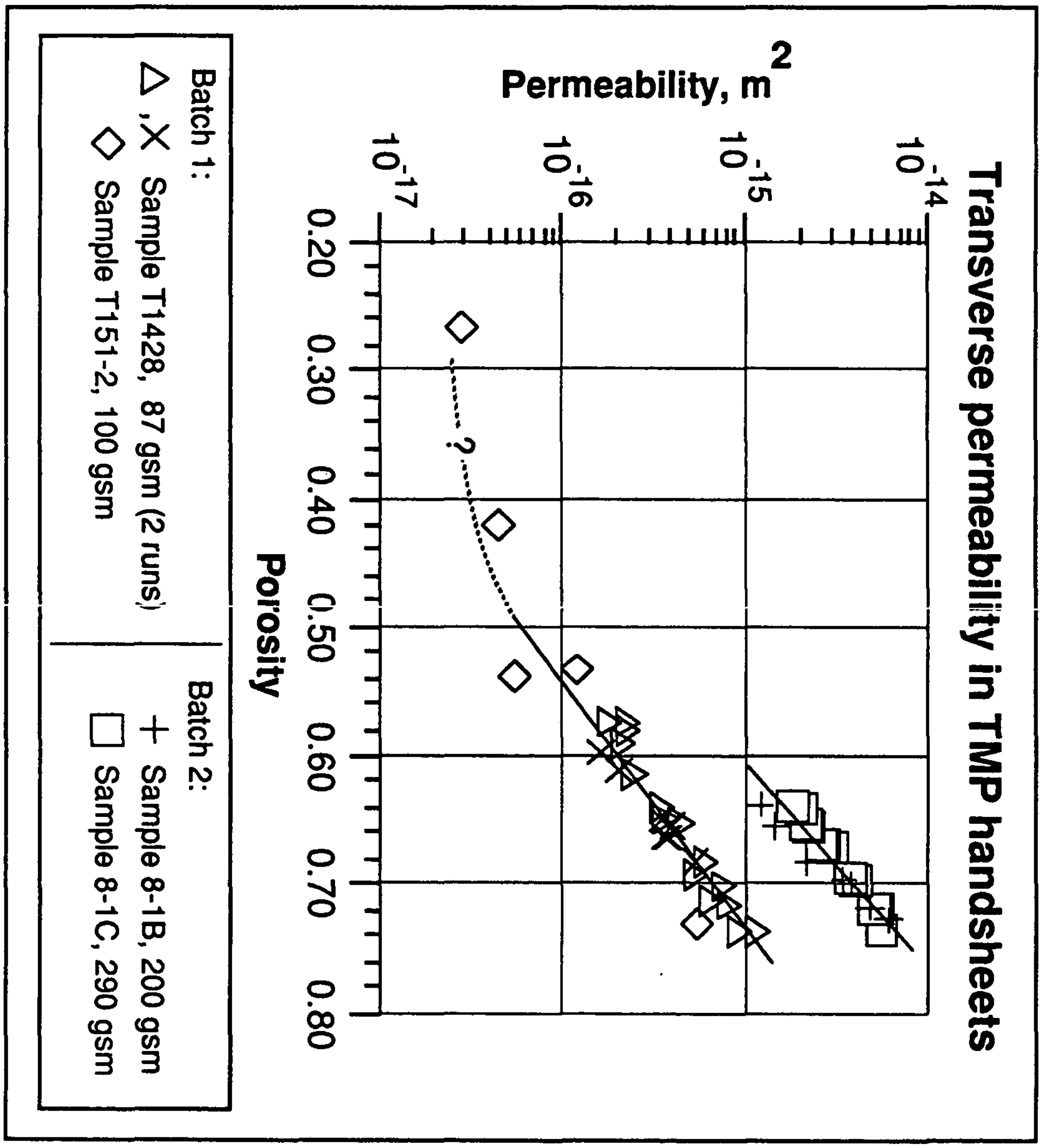
Transverse permeability in TMP handsheets
Permeability, m2
10-14
10-15
10-16
10-17
0.20
0.30
0.40
0.50
0.60
0.70
0.80
Porosity
?
Batch 1:
△ ,X Sample T1428, 87 gsm (2 runs)
◇ Sample T151-2, 100 gsm
Batch 2:
+ Sample 8-1B, 200 gsm
□ Sample 8-1C, 290 gsm

Current Related Work

Cush Hamlen, Univ. of Minnesota:

3-D model of fibrous media helps explain experimental observations at IPST.

Increasing fiber stiffness leads to higher anisotropy.

Conclusions

- Lateral permeability exceeds transverse permeability by a factor of roughly 2-10
- Permeability is a sensitive indicator of changes in fiber and sheet structure
- Fiber characteristics strongly affect the degree of anisotropy

Physics of Vapor-Liquid Flows

- Relative permeability issues
- Saturation measurement
- Phase-change heat transfer (boiling) in fibrous media
- Numerical modeling

Applications

- Displacement dewatering
- Impulse drying
- Rewetting in wet pressing
- Many other processes

Relative Permeability

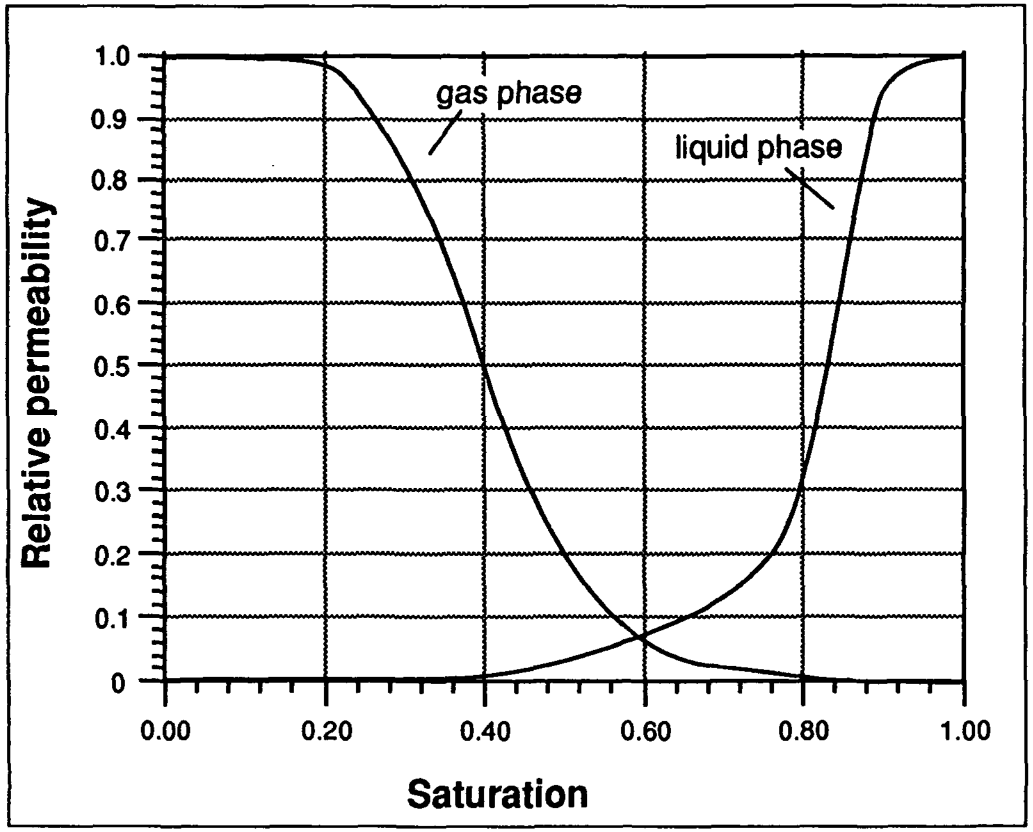

Numerical Modeling

- Impulse drying and displacement dewatering
- MIPPS-II as a basis
- Extensions for consolidation and two-phase counter-current flow

Possible Impulse Drying Implementation

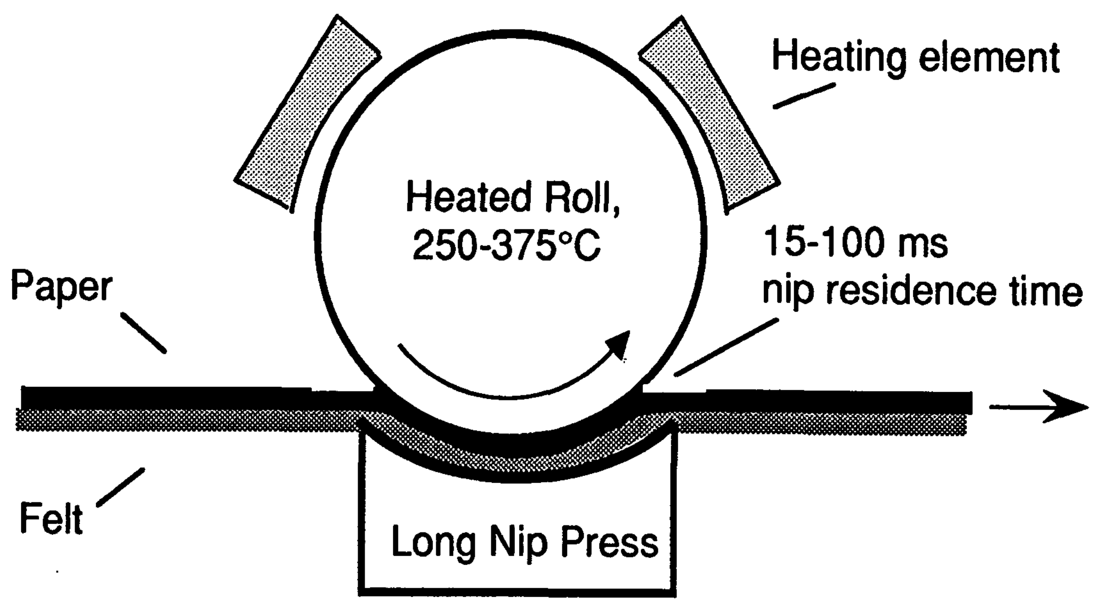

Predicted Density Gradient During Dynamic Compression of a Saturated Sheet

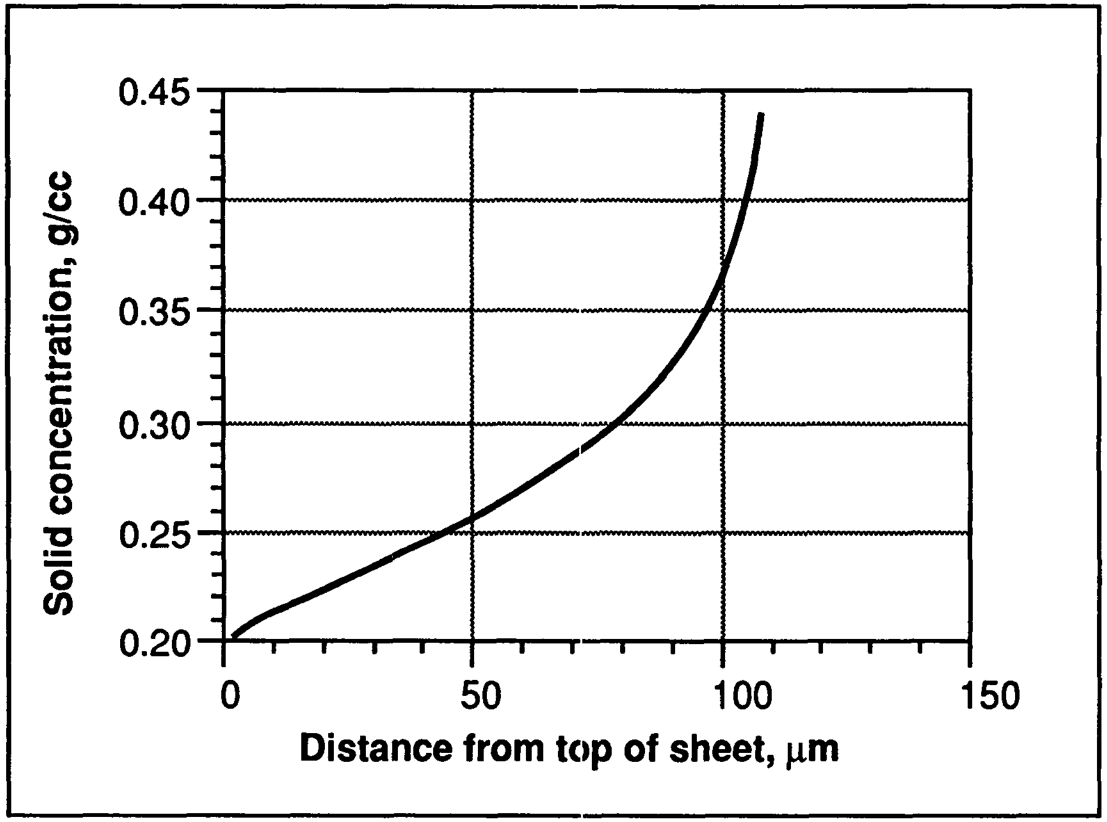

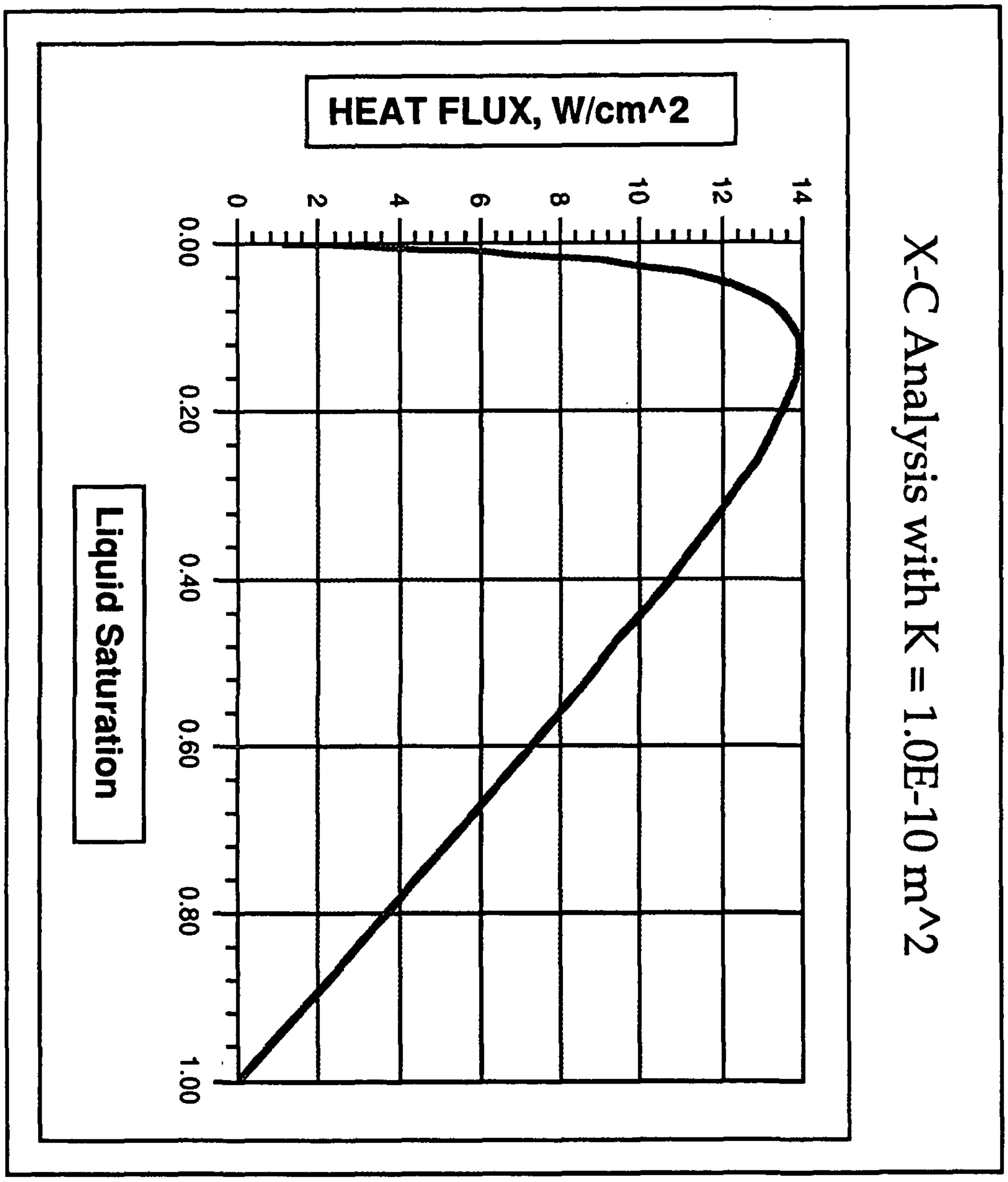
X-C Analysis with K = 1.0E-10 m^2
HEAT FLUX, W/cm^2
0
2
4
6
8
10
12
14
0.00
0.20
0.40
0.60
0.80
1.00
Liquid Saturation

Proposed Platen Assembly for Relative Permeability Work

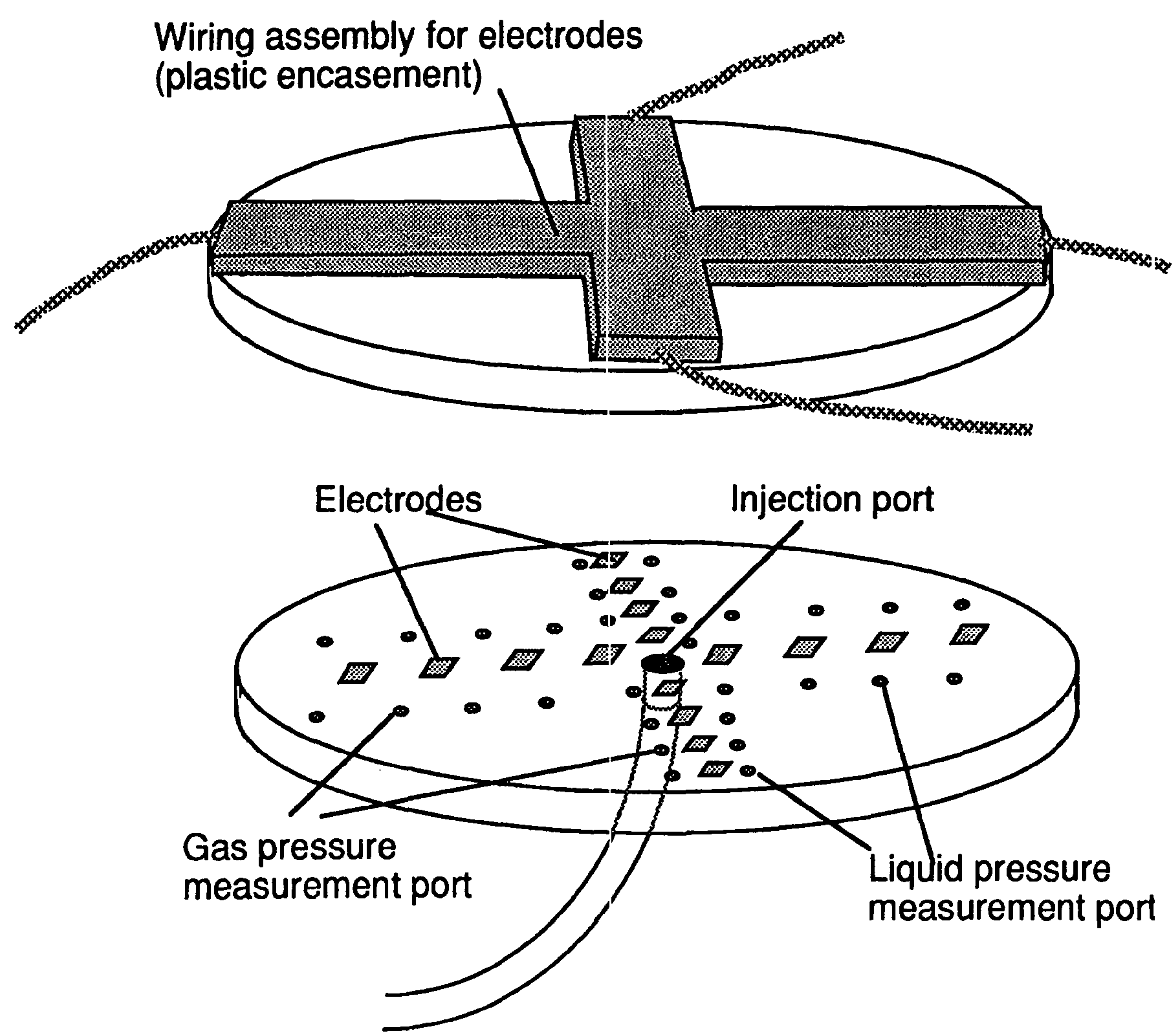

Relative Porosity

The fraction of the total **void** volume available for flow.

Effective Porosity

The fraction of the total volume available for flow.

Effective Porosity Measurement

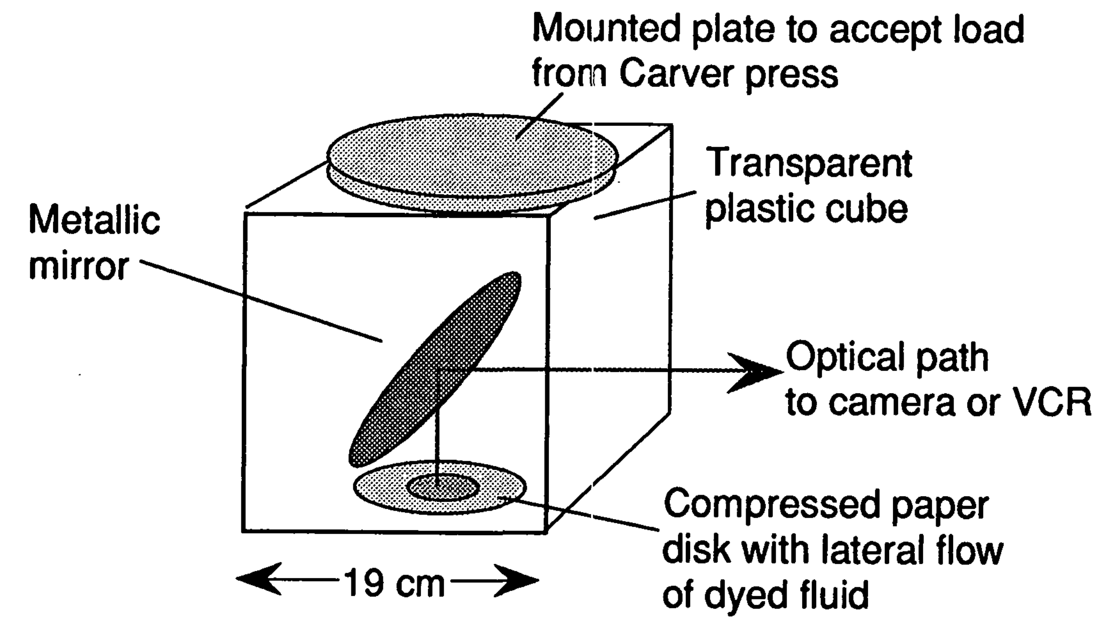

Student Research

A190 Projects:

Marty Hoskins - Saturation Profiles During Boiling in Fibrous Media

John Frazier - Z-direction Hydraulic Pressure Gradients in Wet Pressing

Ph.D. Projects:

James Burns - Z-direction Dynamic Density Gradients During Pressing

Project 3480 Plans

- Continue measurements of anisotropic permeability
- Examine permeability as a process control parameter
- Begin measurements of effective porosity
- Submit an NSF proposal for funding of relative permeability measurements
- Add wet pressing and heat pipe modules to MIPPS for more realistic modeling of impulse drying and displacement processes

APPLICATION OF FLASH X-RAY TO WEB CONSOLIDATION

(FINAL REPORT)

PROJECT STAFF: CYRUS AIDUN

OBJECTIVE

INVESTIGATE THE FEASIBILITY OF USING THE FLASH X-RAY TECHNIQUE FOR MEASUREMENT OF SHEET DEFORMATION IN A ROLL PRESS a)

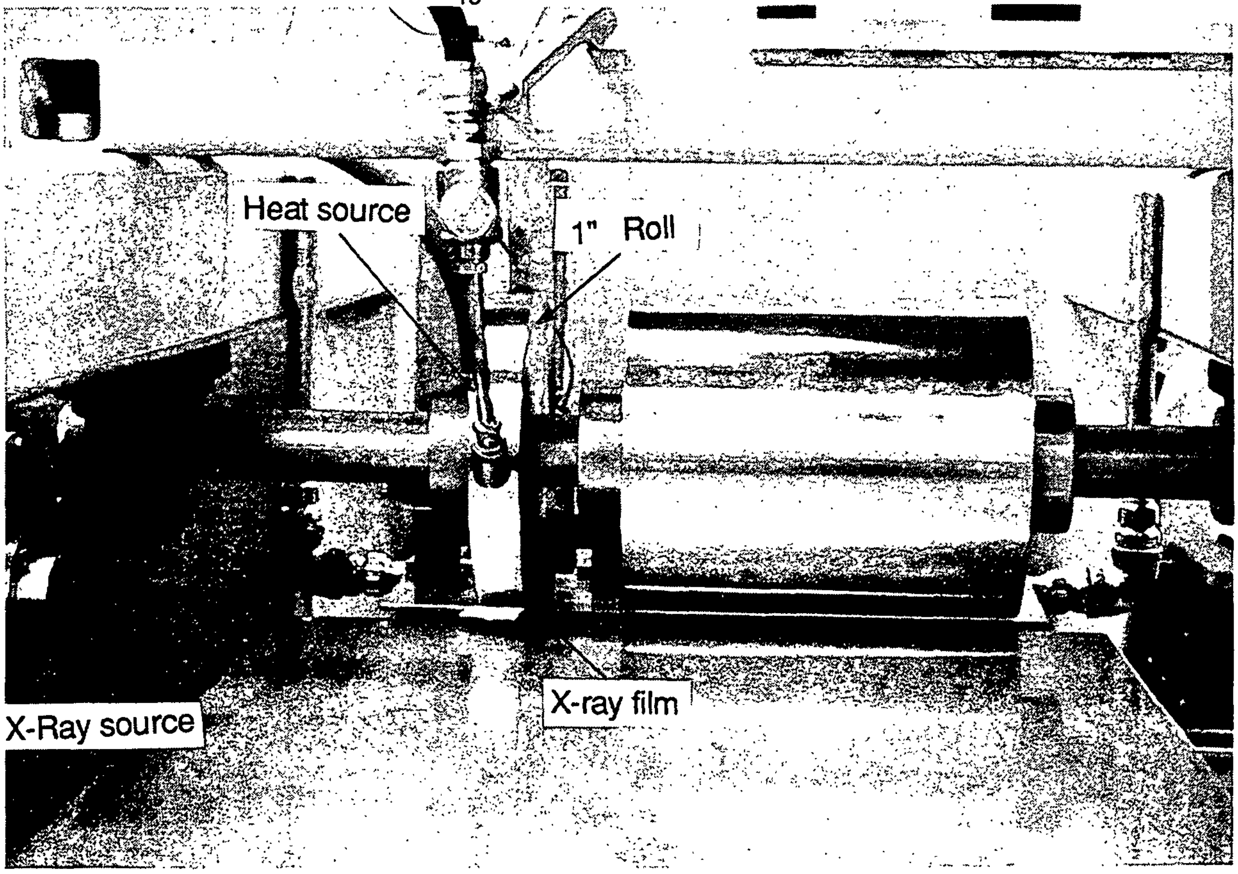

b)

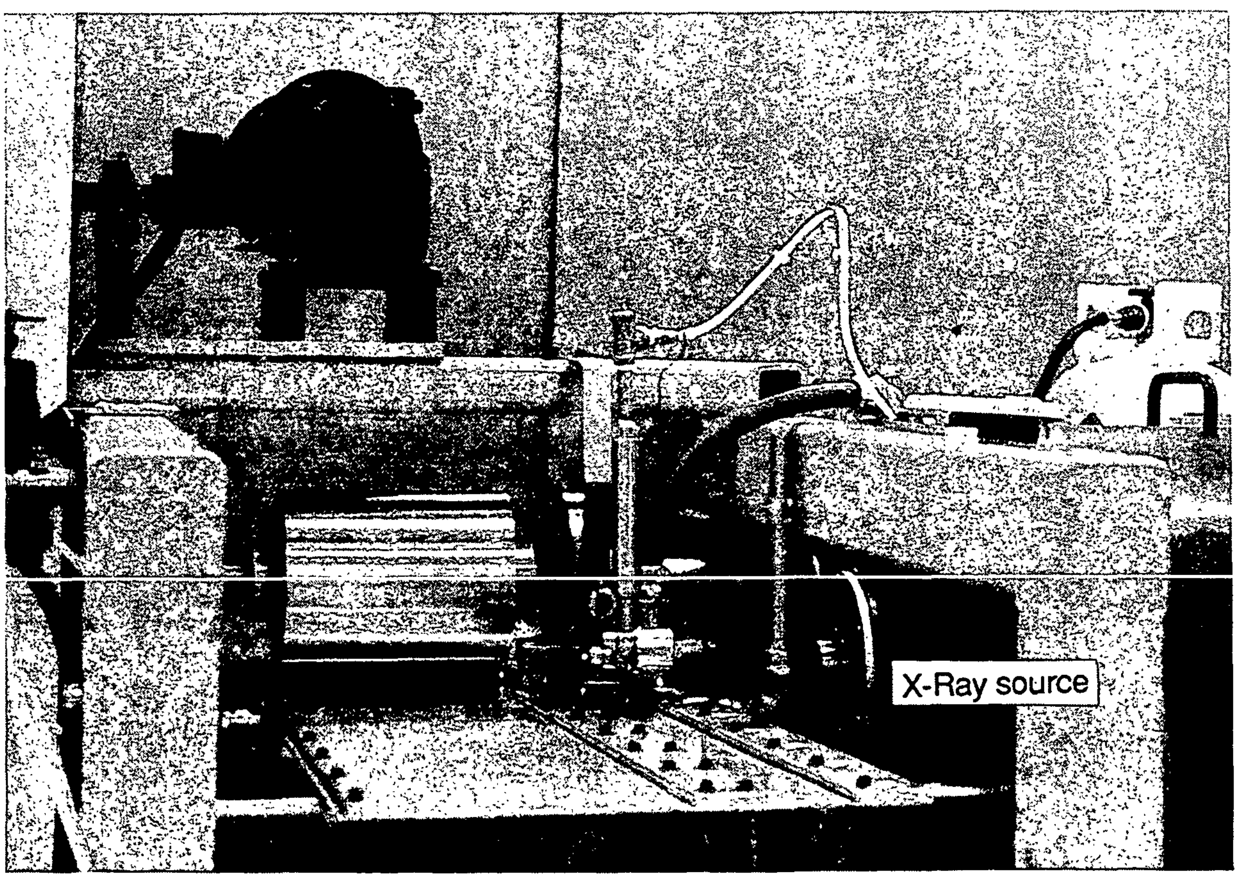

Figure 1. X-Ray Roll Press a) exit side b) entering side

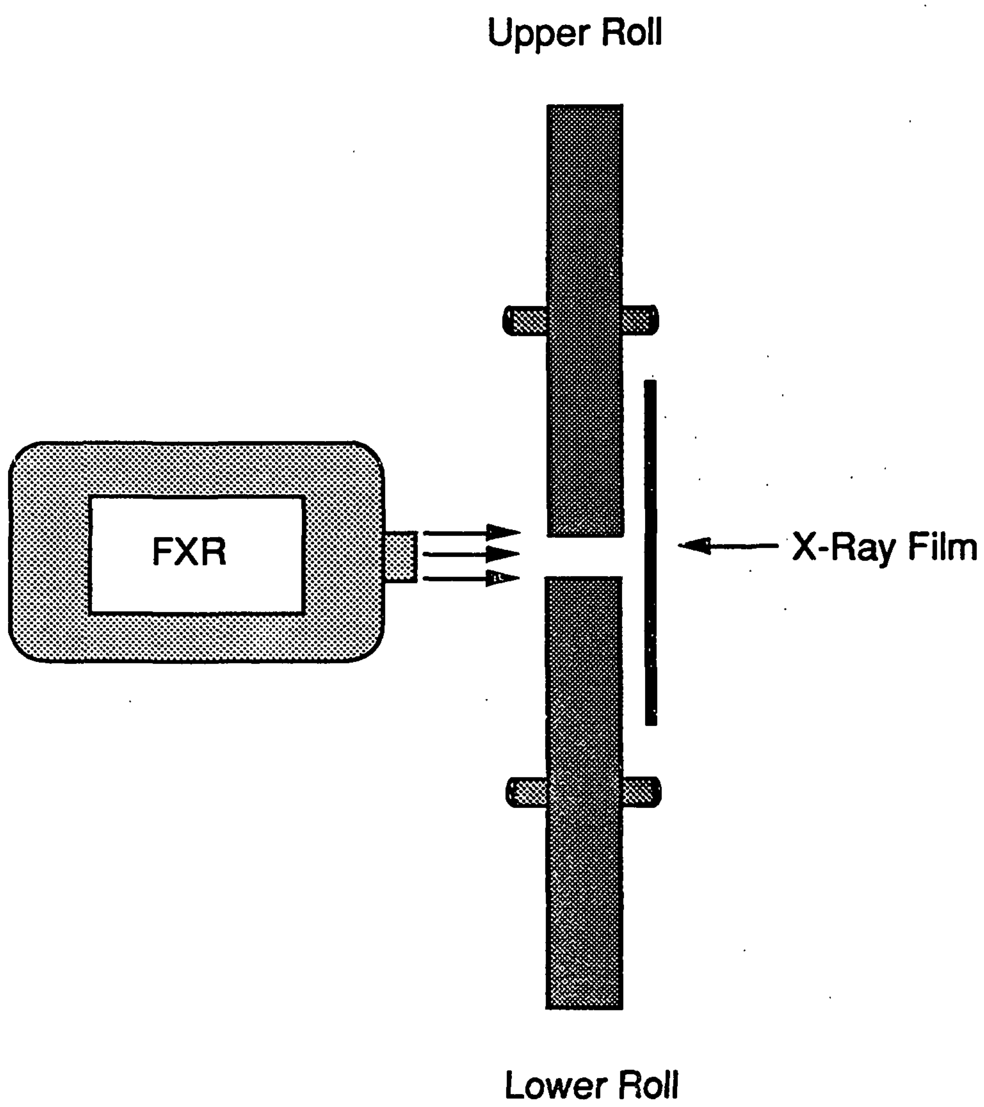

Figure 2. Schematic diagram of the relative position of the x-ray source, x-ray film, and the rolls.

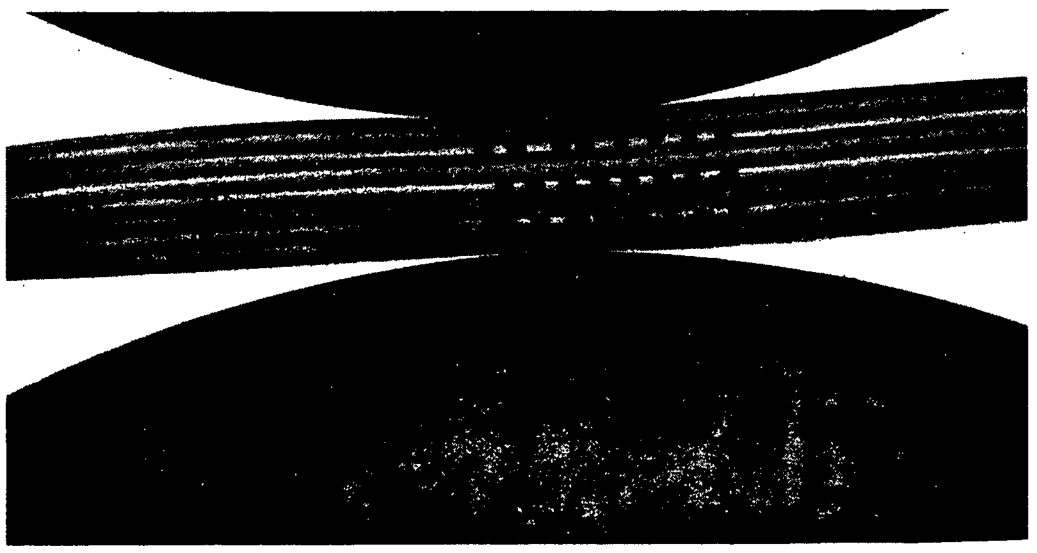

Figure 3a. Flash X-ray Radiograph of Target Particles (zero load)

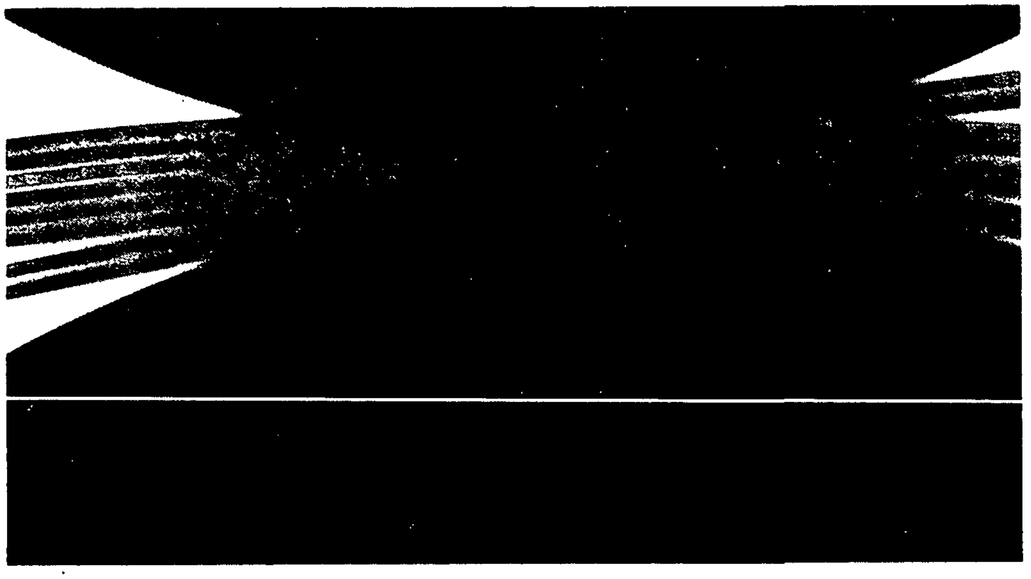

Figure 3b. Flash X-Ray Radiograph of Target Particles (compressed)

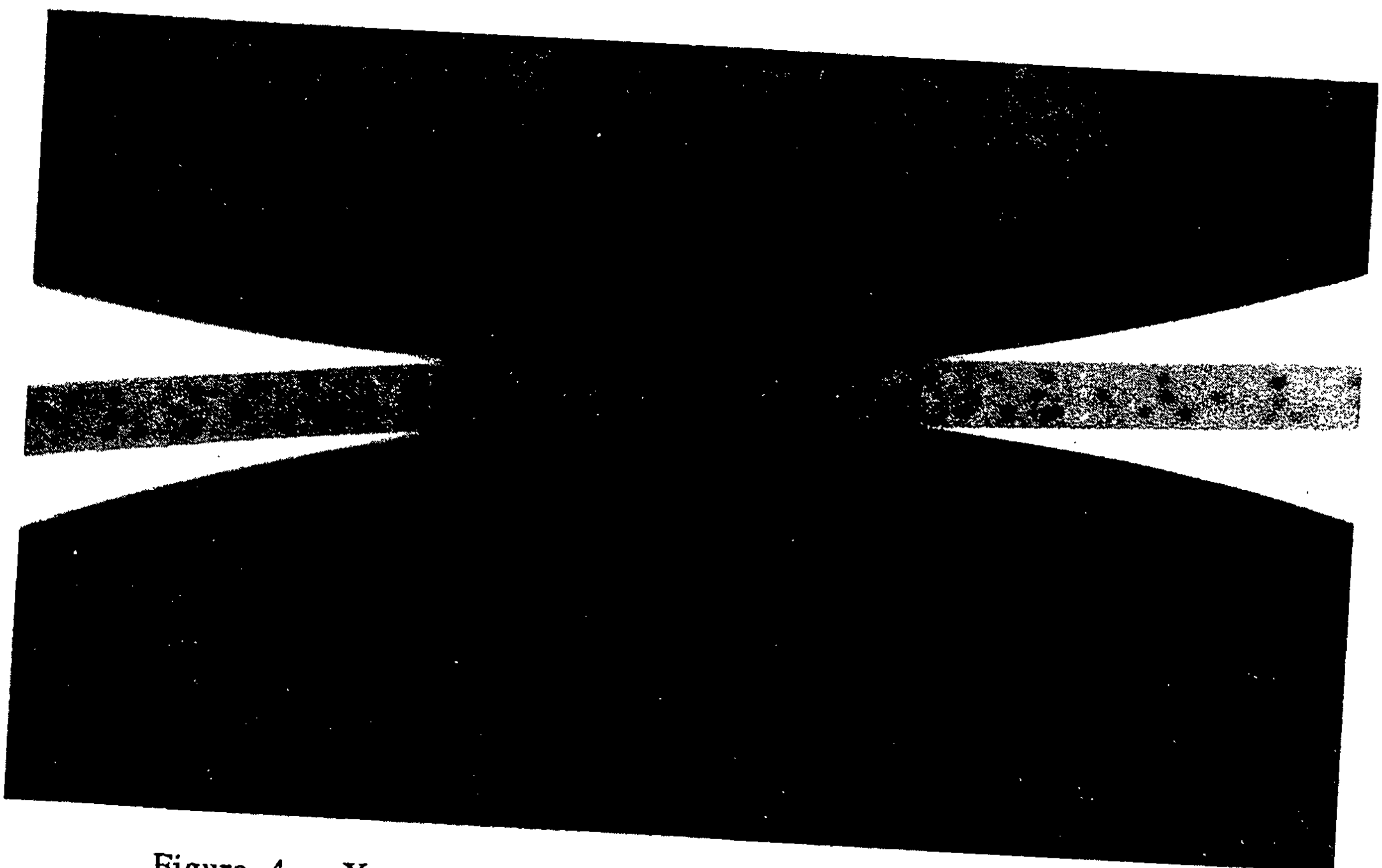

Figure 4. X-ray image of tracer particles in a deforming sheet.

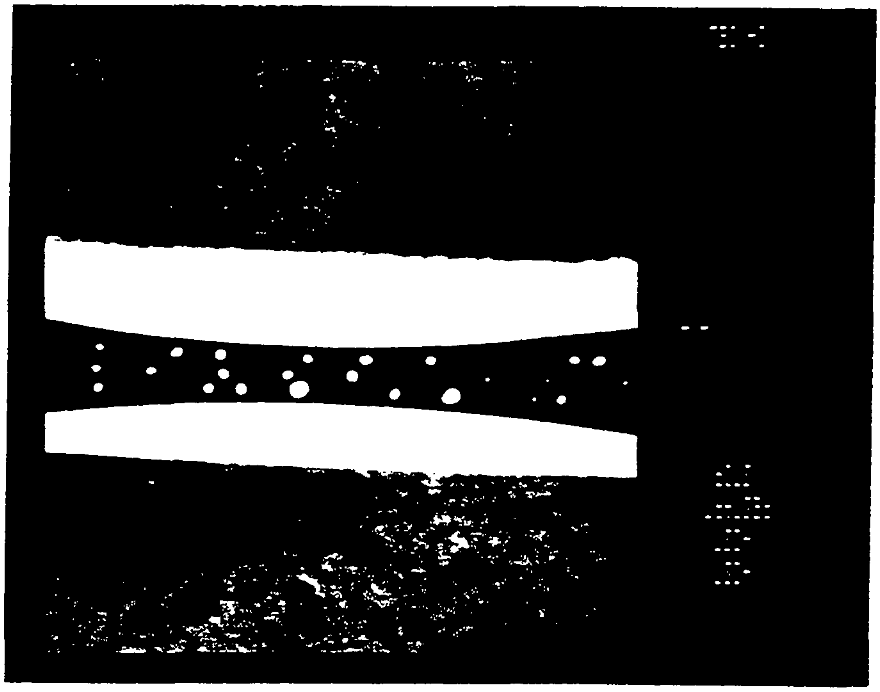

Figure 5. X-ray image of solid particle tracers in a sheet inside the nip of a roll press.

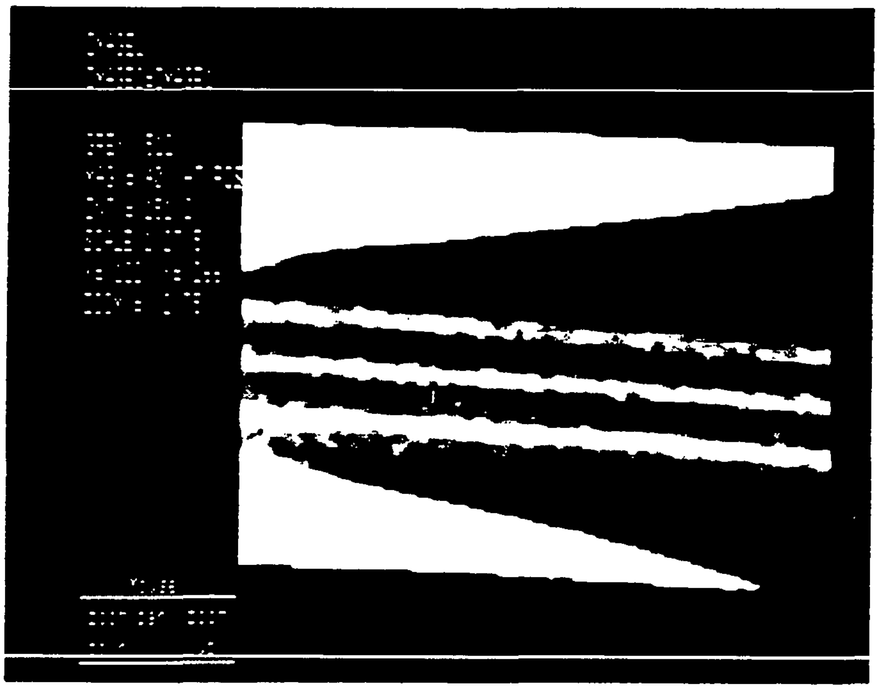

Figure 6. X-ray image of continuous tungsten wires in a sheet at the exit side of the nip.

(a)

(b)

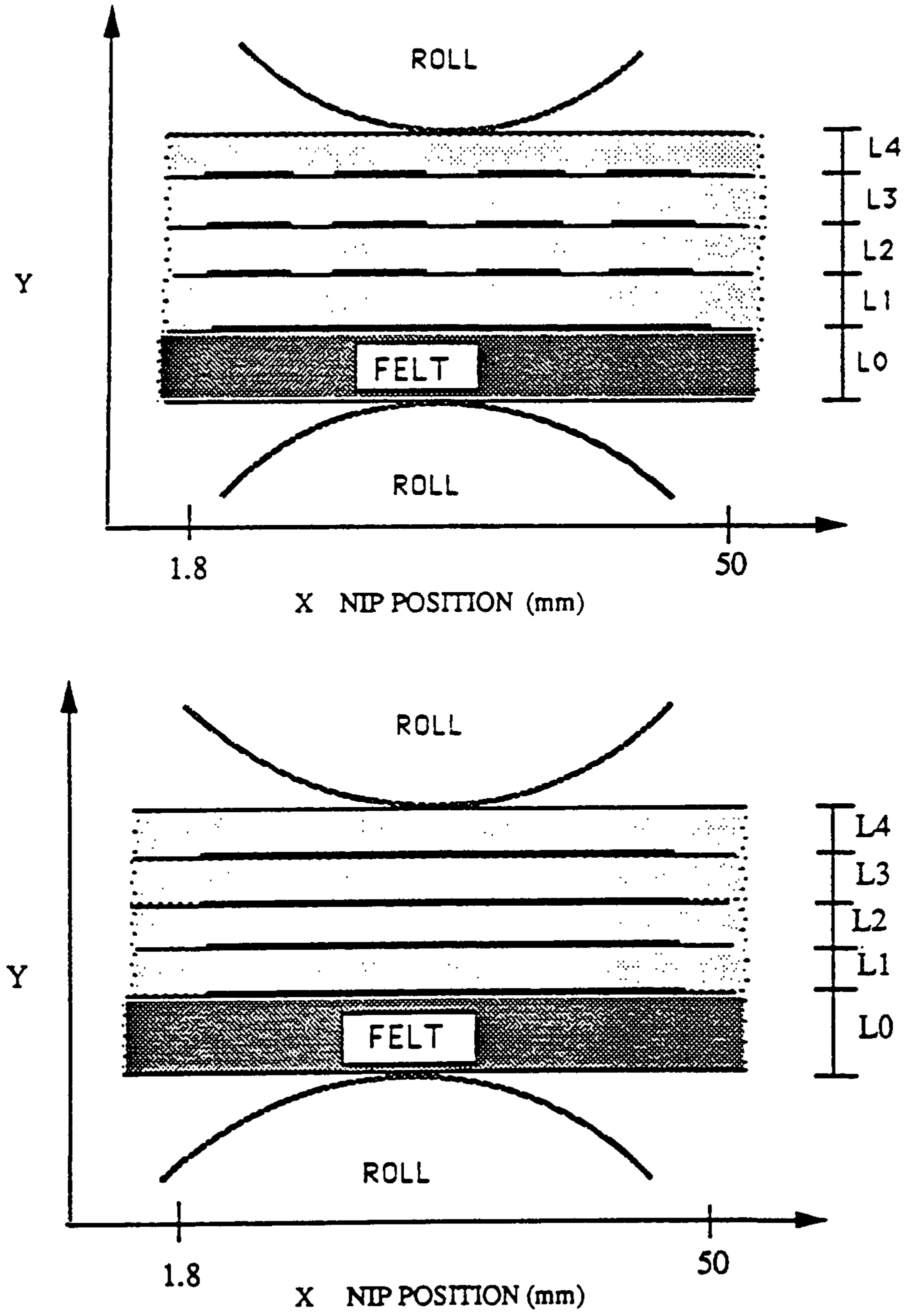

Figure 7. Schematic of the test samples.
4 layers of paper, L1 through L4, each with 150 g/m2 basis weight, 28% solids.
X-Ray shuts are at two different pressures, 50 and 60 psi. Roll press speed is at 17 ft/min.
Selection of axes for analyzing the x-ray films and the thickness measurements with the image analyzer are also shown. Targets : 50 microns, tungsten wires (99.95%) are located between the sheets in two different arrangements : (a) Discontinuous wires 5 mm long and 2 mm apart, and (b) Continuous wires 4 " long. Also a continuous wire is placed between the sheet and the felt in both sets.

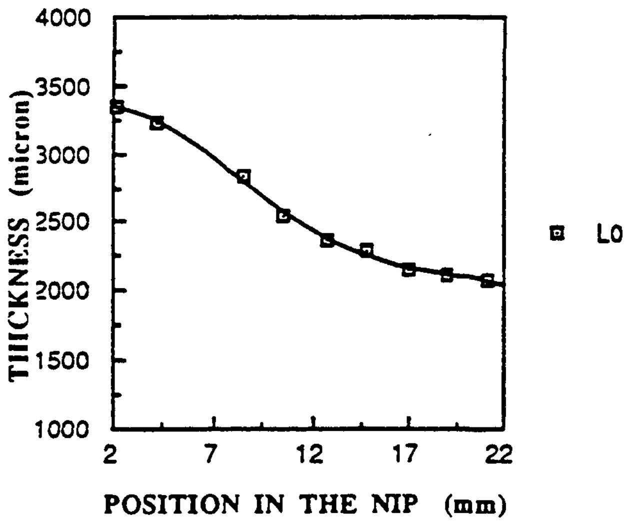

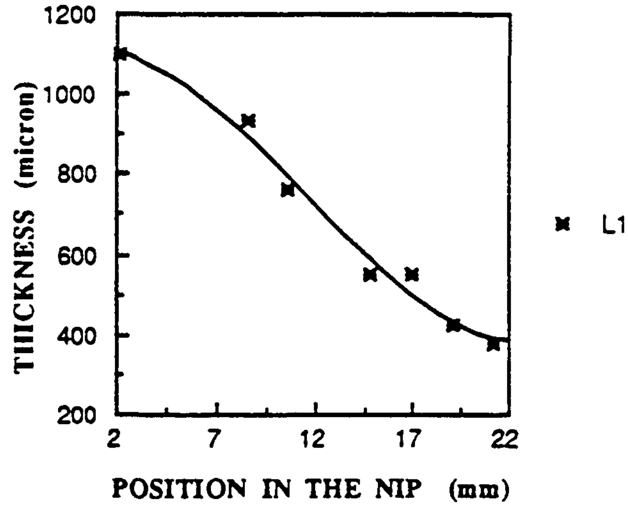

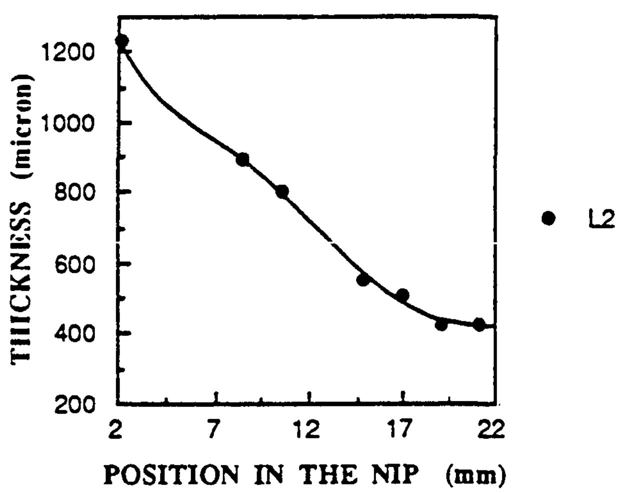

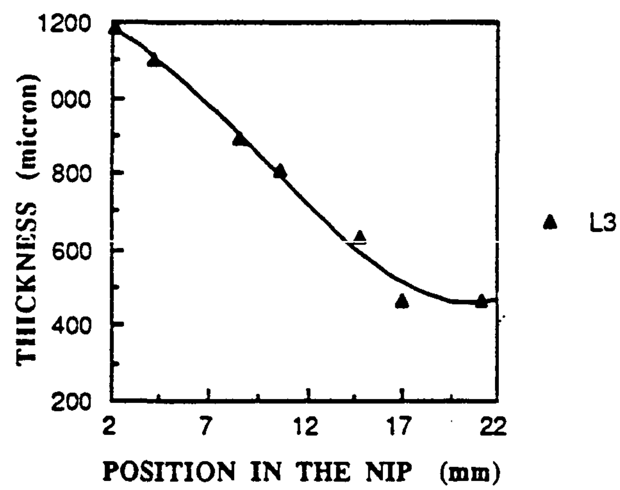

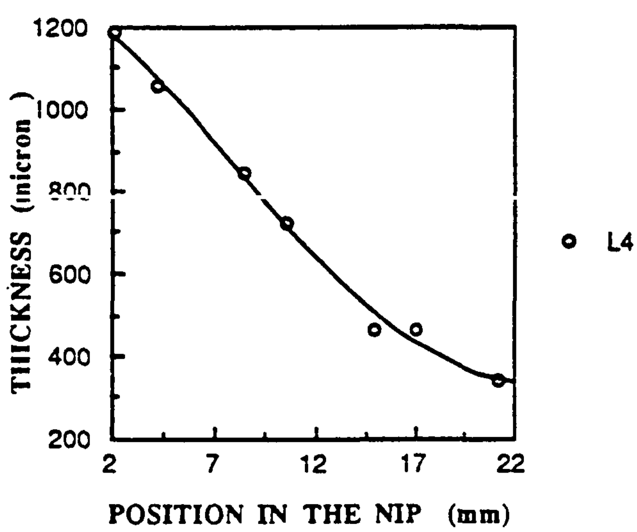

Figure 8. Thickness variation of individual free sheets in wet pressing at 60 psi, discrete target arrangement. For sample description, see Fig. 7a. Graphs show first half of the nip.

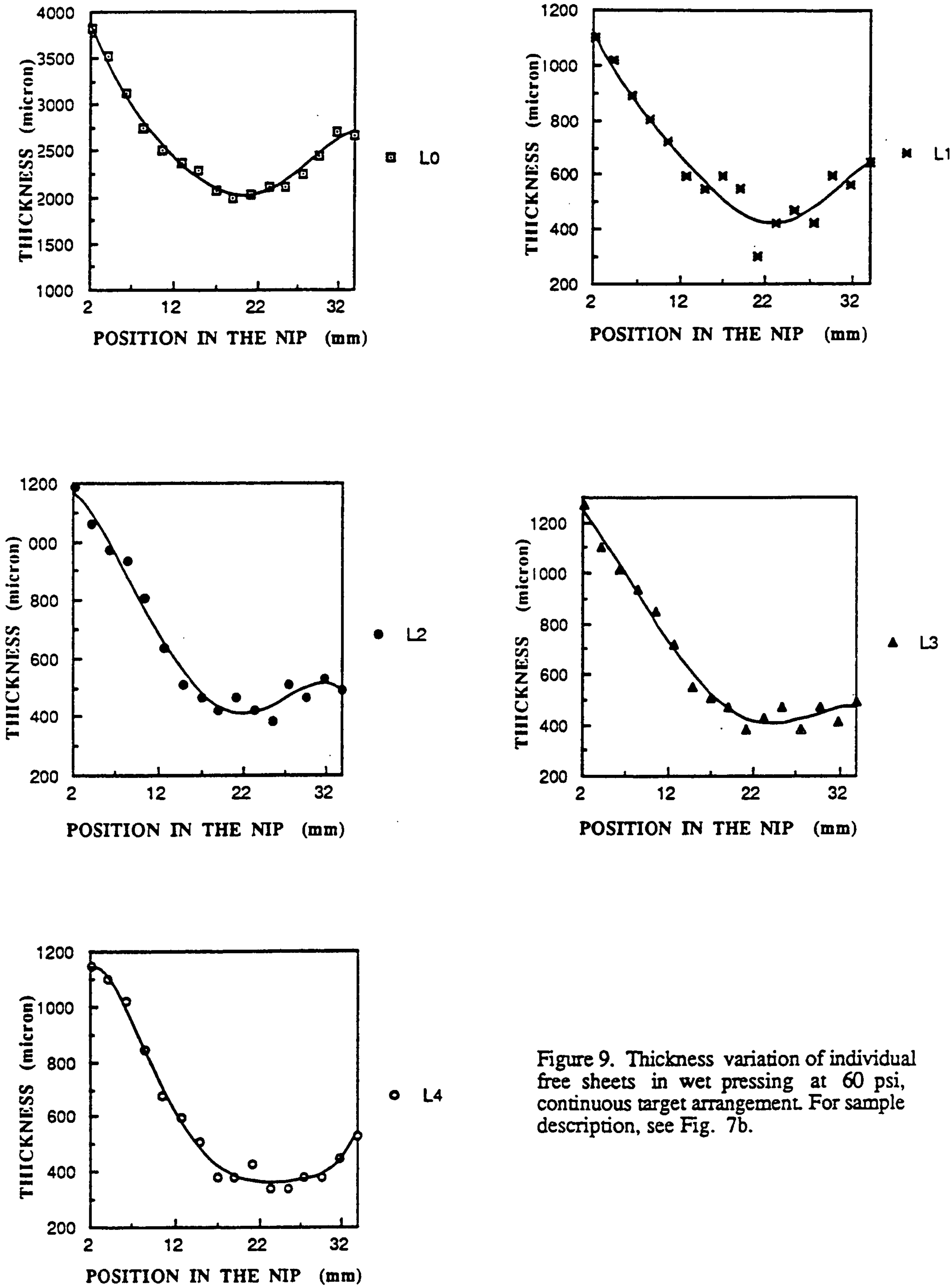

Figure 9. Thickness variation of individual free sheets in wet pressing at 60 psi, continuous target arrangement. For sample description, see Fig. 7b.

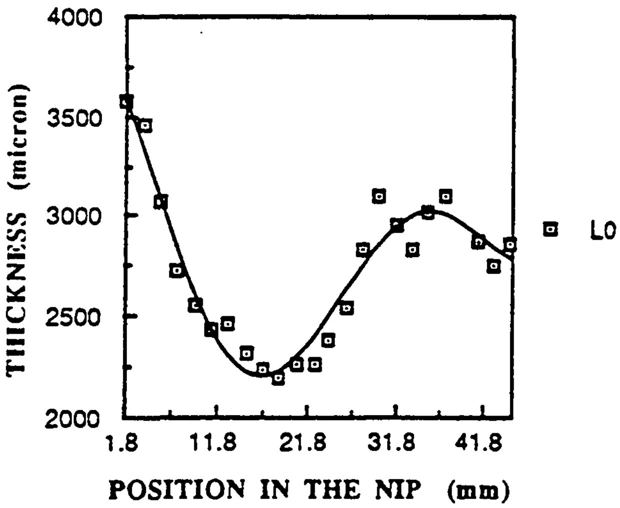

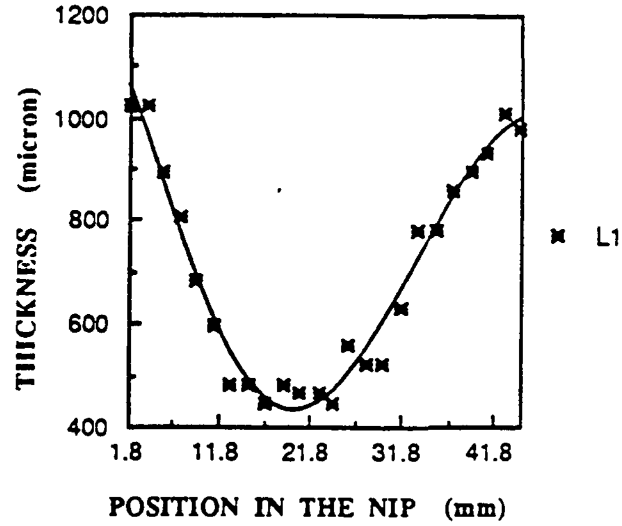

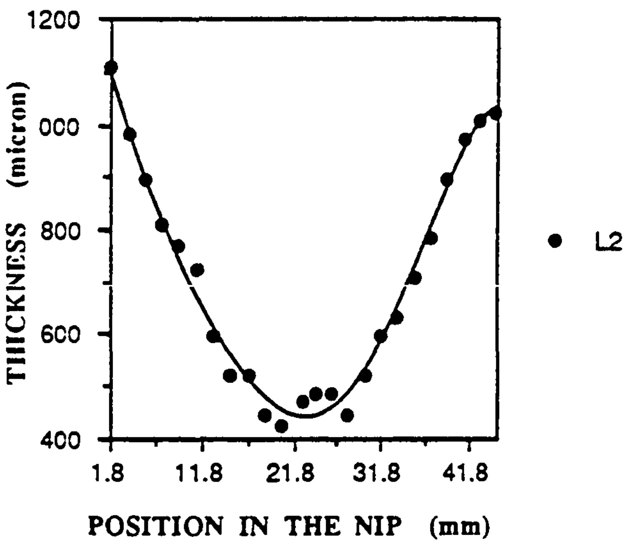

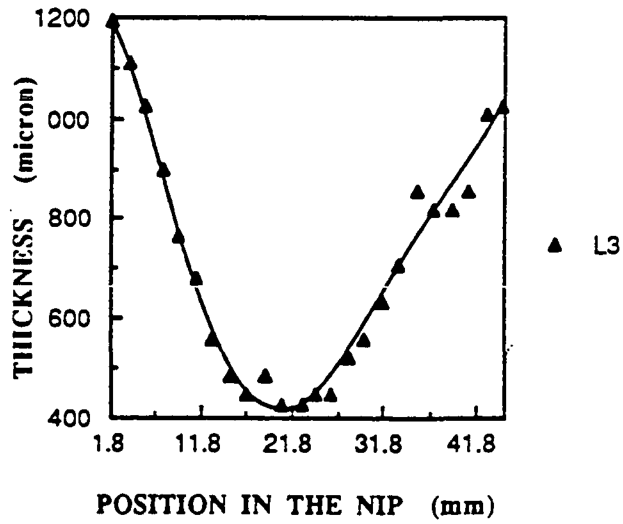

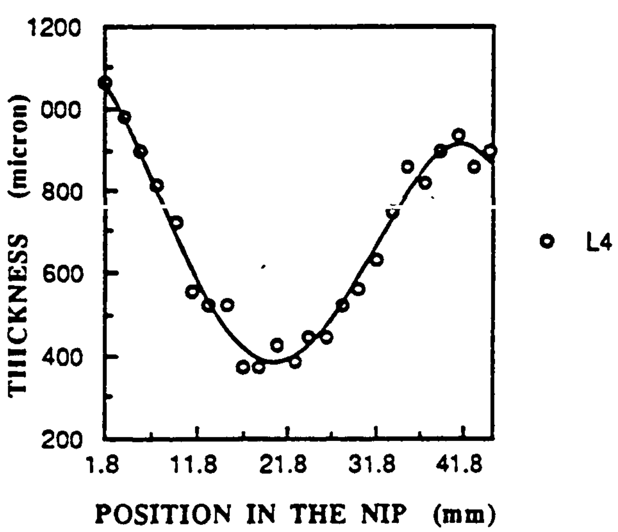

Figure 10. Thickness variation of individual free sheets in wet pressing at 50 psi continuous target arrangement. For sample description, see Fig. 7b.

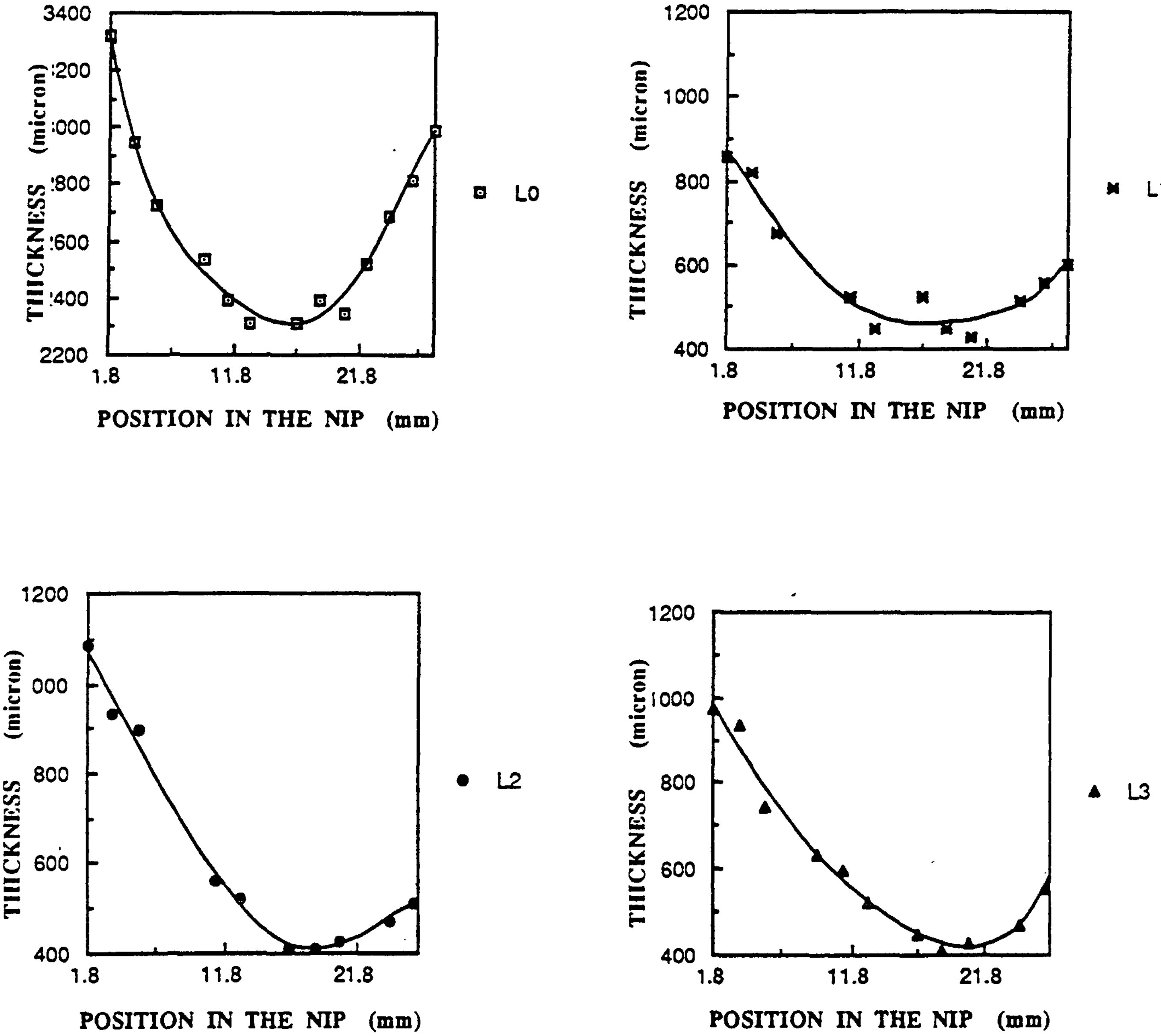

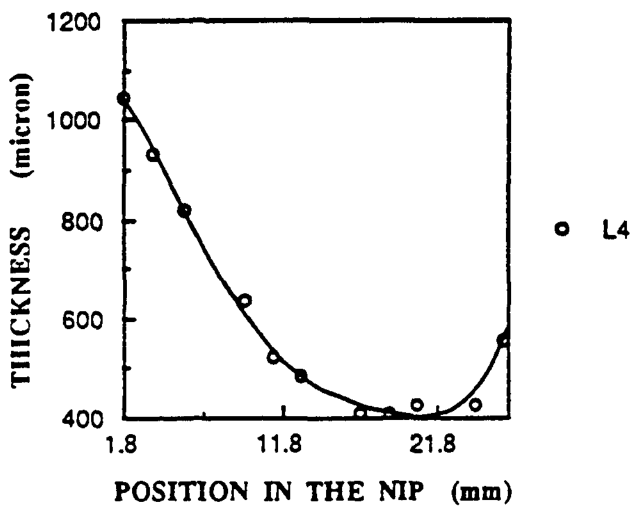

Figure 11. Thickness variation of individual free sheets in wet pressing at 50 psi, discrete target arrangement. For sample description, see Fig. 7a. Graphs show first half of the nip .

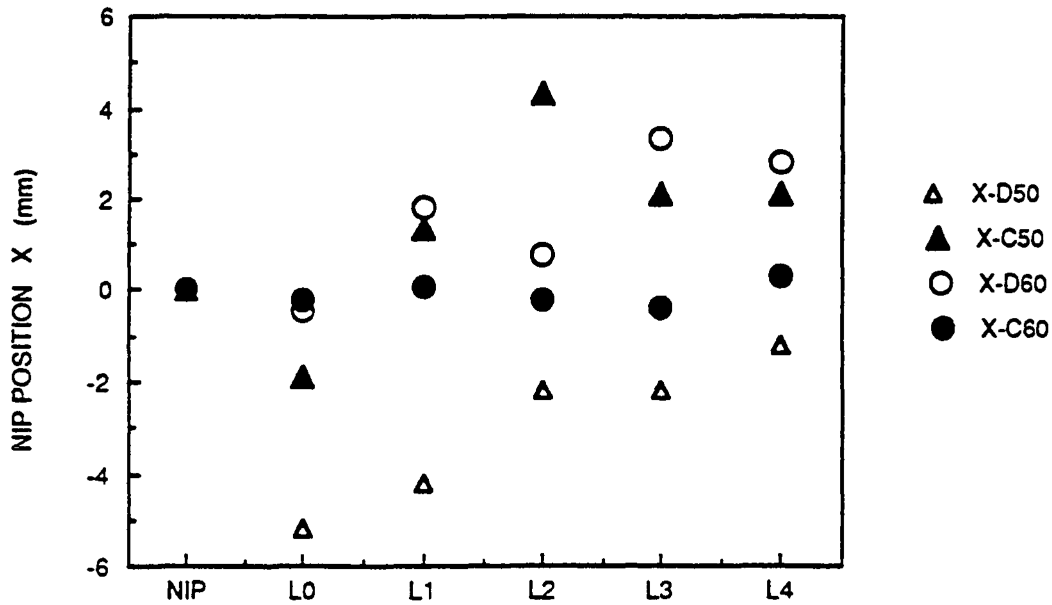

Figure 12. Location of the minimum sheet thickness relative to the mid-nip at 0.

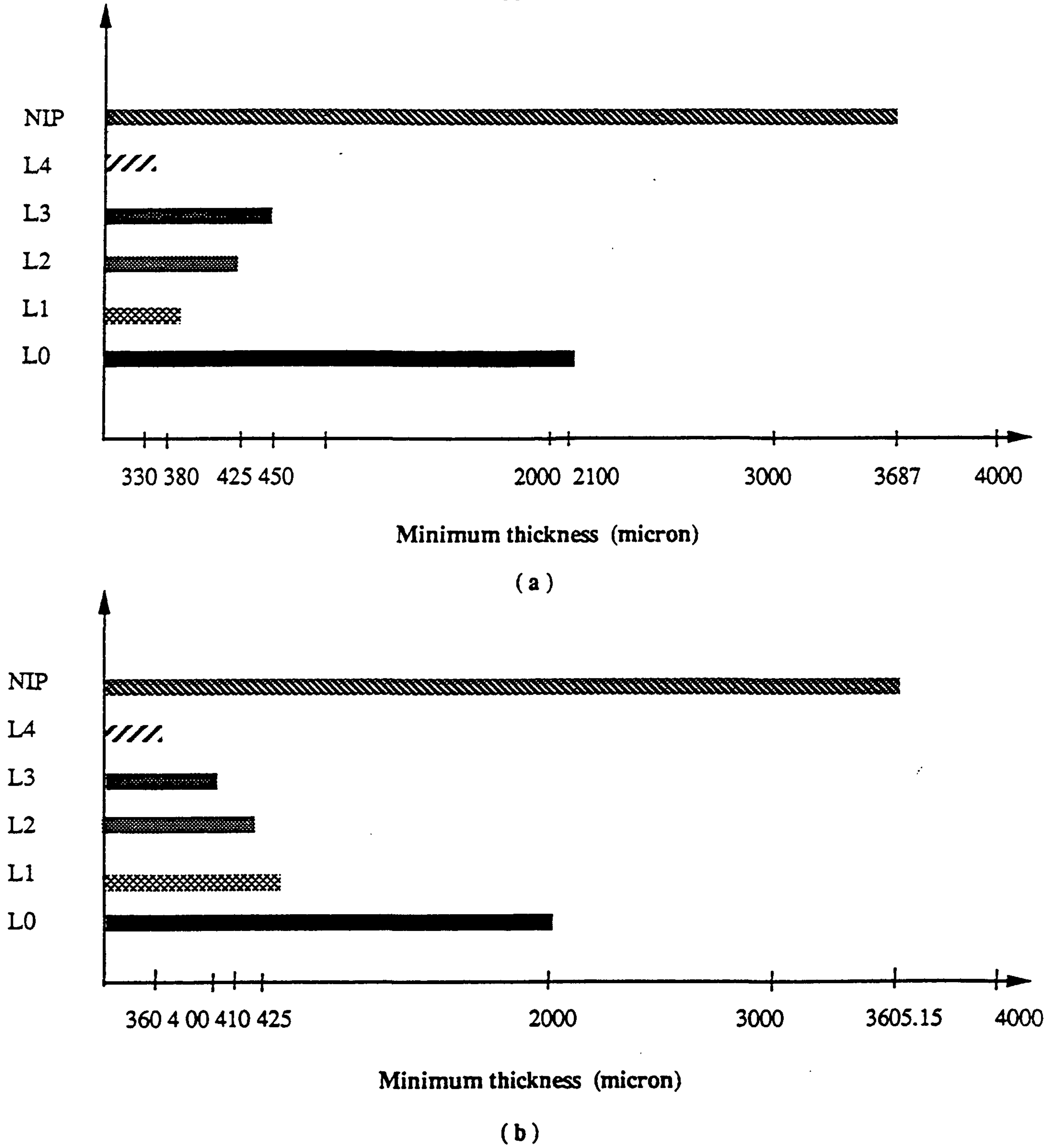

Figure 13. Minimum thickness of each individual sheet.
(a) Discontinuous wires at 60 psi and (b) Continuous wires at 60 psi.

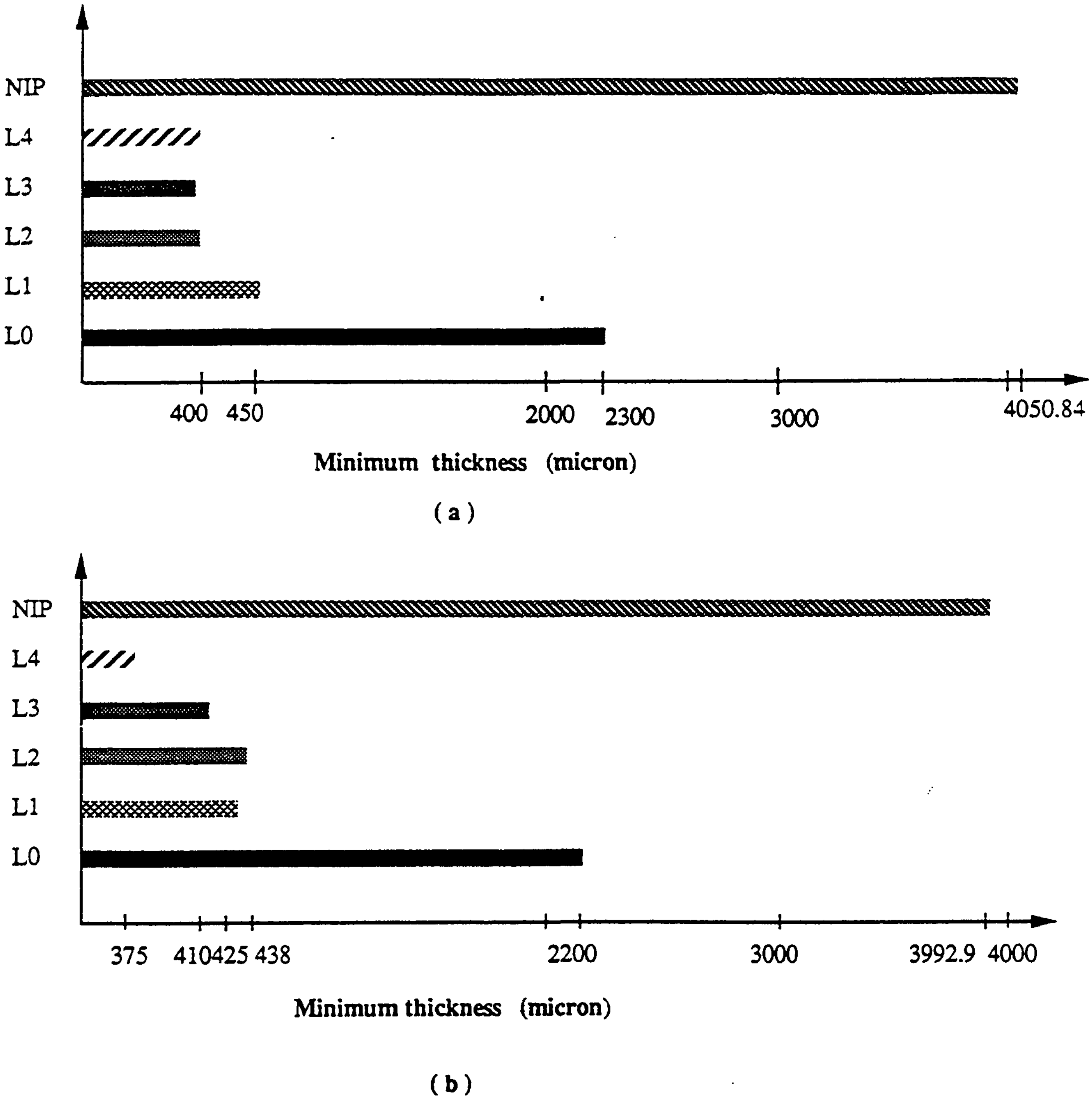

Figure 14. Minimum thickness of each individual sheet.
(a) Discontinuous wires at 50 psi and (b) Continuous wires at 50 psi.

CONCLUSIONS

- The thinnest target wire which can be resolved inside a sample sheet is 50 µm in diameter
- The resolution of the flash x-ray is not sufficient to measure deformations in single light-weight sheets
- The technique can be used to study multi-layer sheet pressing

FUNDAMENTALS OF COATING SYSTEMS
PROJECT 3674

April 4, 1991
Institute of Paper Science and Technology
Atlanta, Georgia

FUNDAMENTAL OF COATING SYSTEMS

PROJECT 3674

PROJECT LEADER

CYRUS K. AIDUN

OBJECTIVES

1. Investigate the cause and origin of coat weight nonuniformities in high-speed blade coating.
2. Explore novel coating systems for uniform coating at high machine speeds.

ORGANIZATION

- o BACKGROUND
- o RECENT RESULTS
- o FUTURE PLANS

BACKGROUND

CRITICAL HIGH-SPEED COATING PROBLEMS

1. COATING FILM THICKNESS NONUNIFORMITIES:

   (a) Large Scale (Striations, Streaks, etc.)

   (b) Small Scale (Microstriations)

2. AIR ENTRAINMENT
3. UNPREDICTABILITY

BLADE COATING SYSTEMS

1. Dynamics of Flow at the Blade

FLOW AT THE BLADE

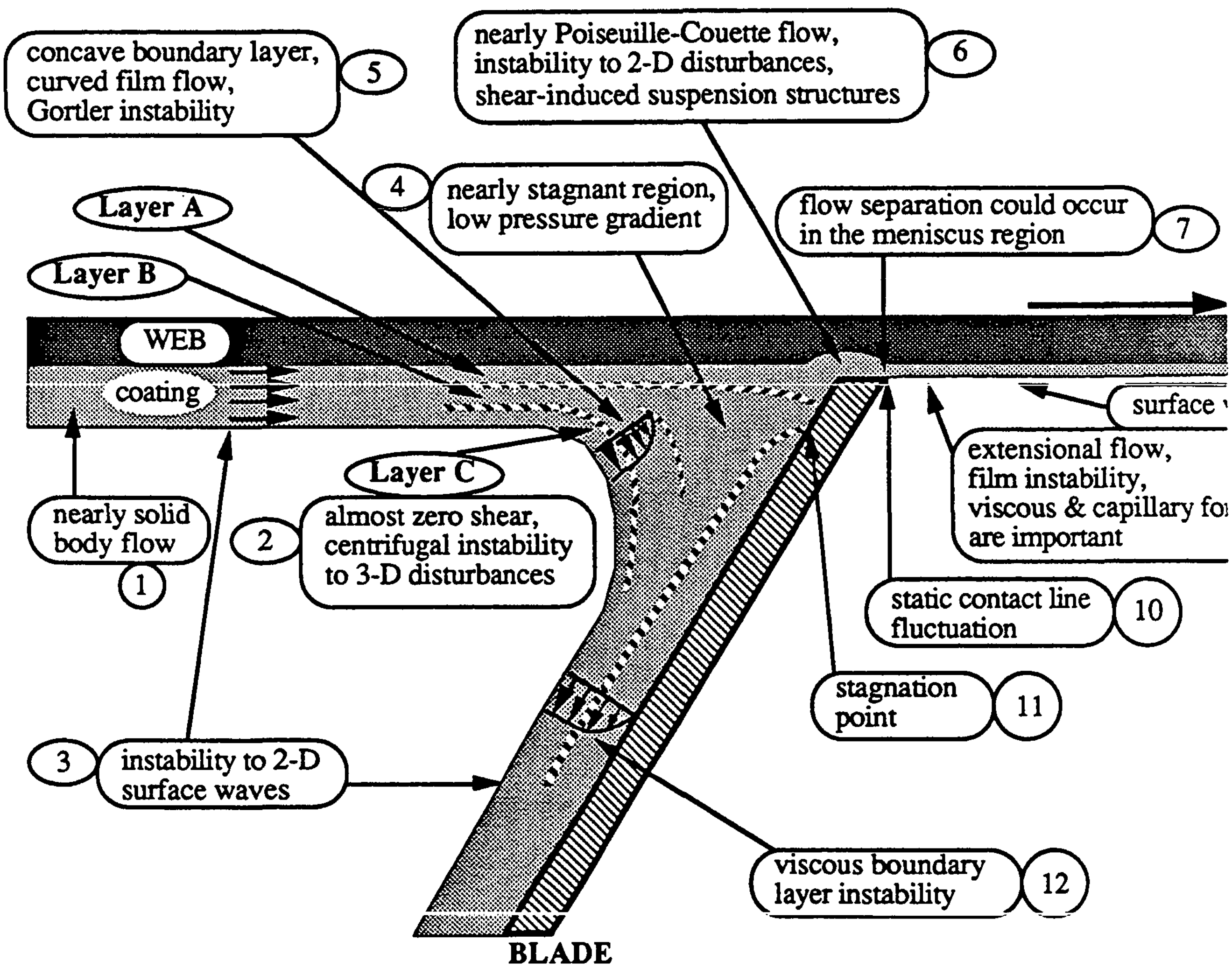

SHORT-DWELL COATER

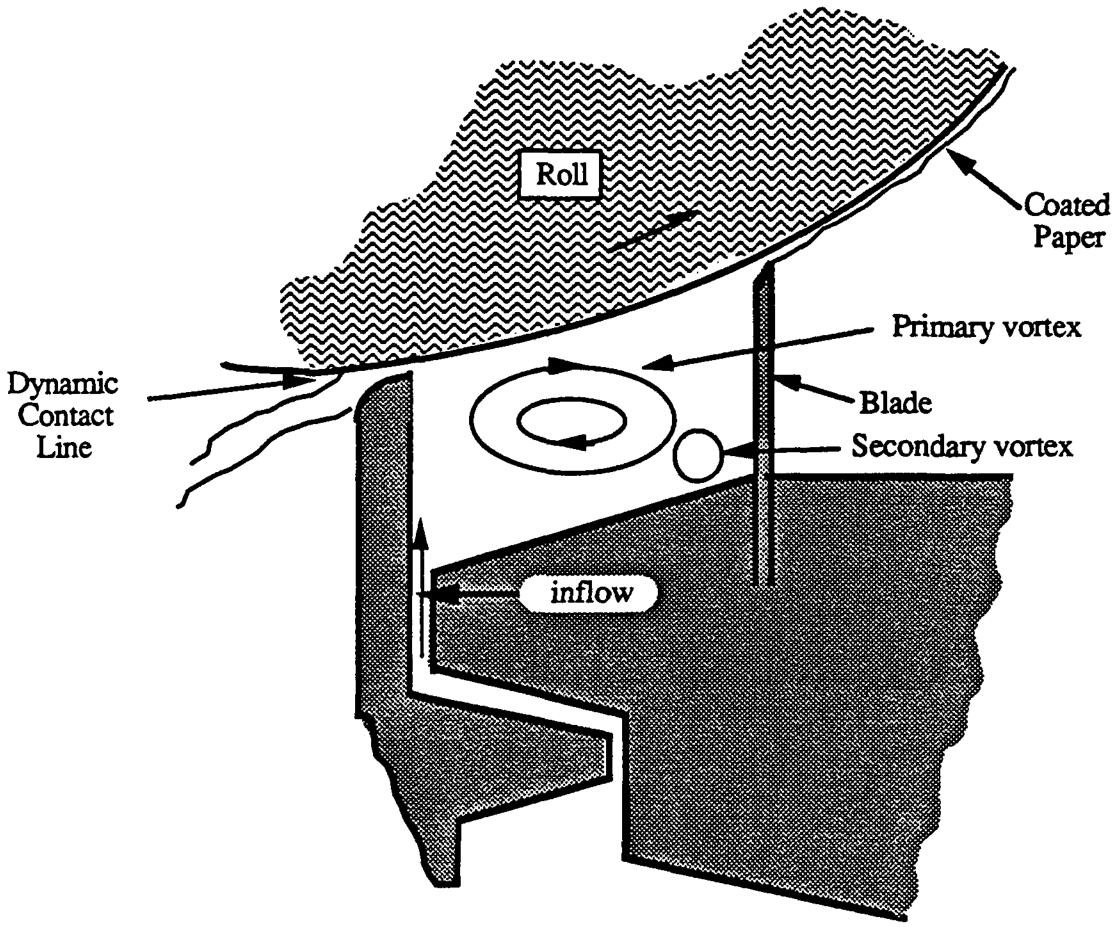

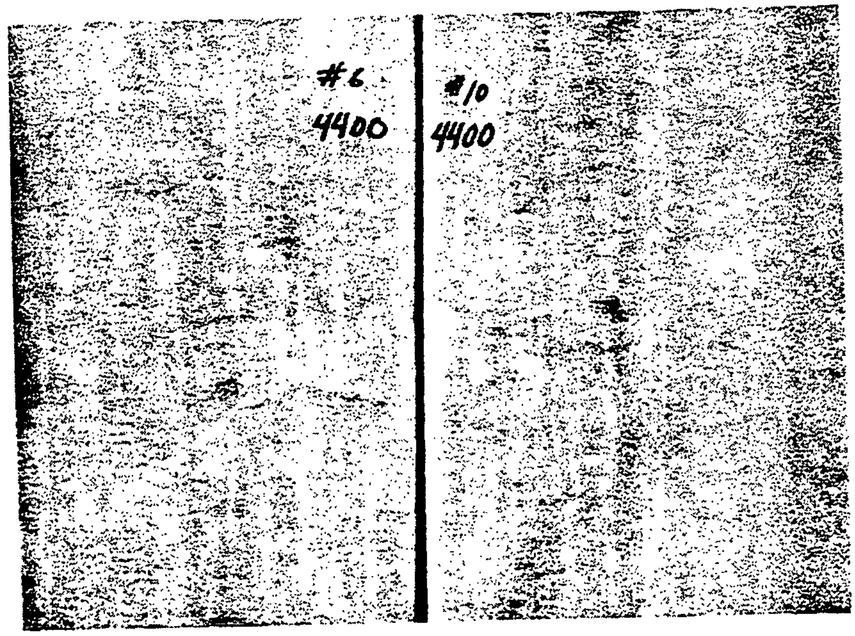

(a)

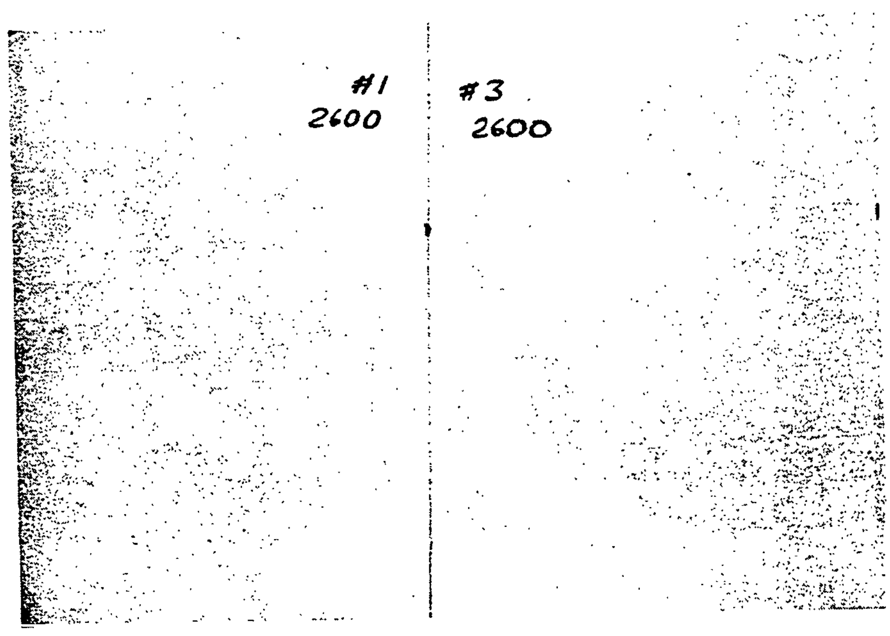

(b)

Figure 1. Macroscale and microscale nonuniformities in coat weight (or solids content) distribution for a LWC paper coated at (a) 4,400 fpm and (b) 2,600 fpm machine speeds.

BLADE COATING SYSTEMS

2. Flow Instability in the Pond of Short-Dwell Coaters.

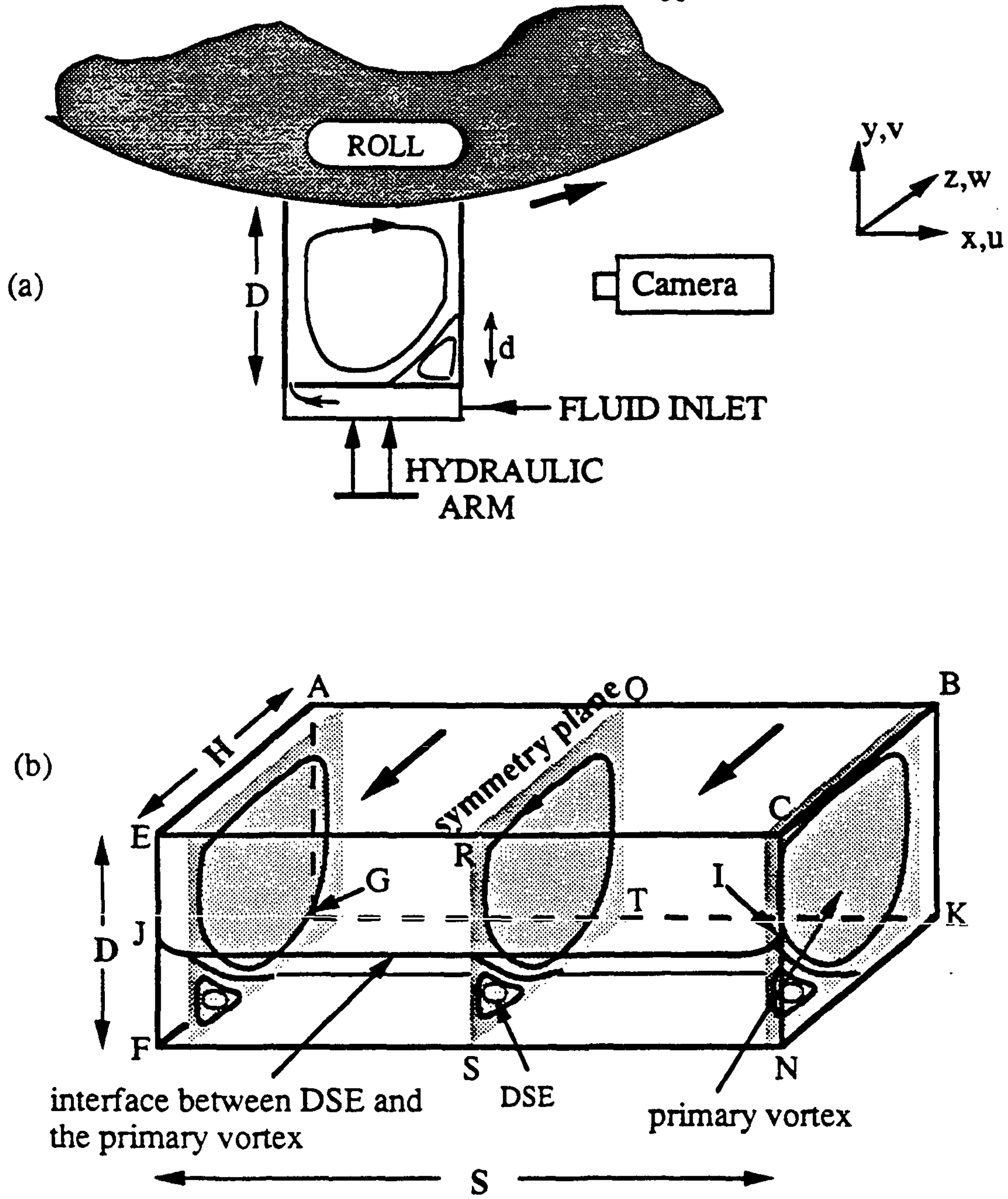
(a)
ROLL
y,v
z,w
x,u
D
d
Camera
FLUID INLET
HYDRAULIC
ARM
(b)
A
O
B
symmetry plane
H
E
C
R
G
I
T
J
K
D
F
S
N
interface between DSE and
the primary vortex
DSE
primary vortex
S

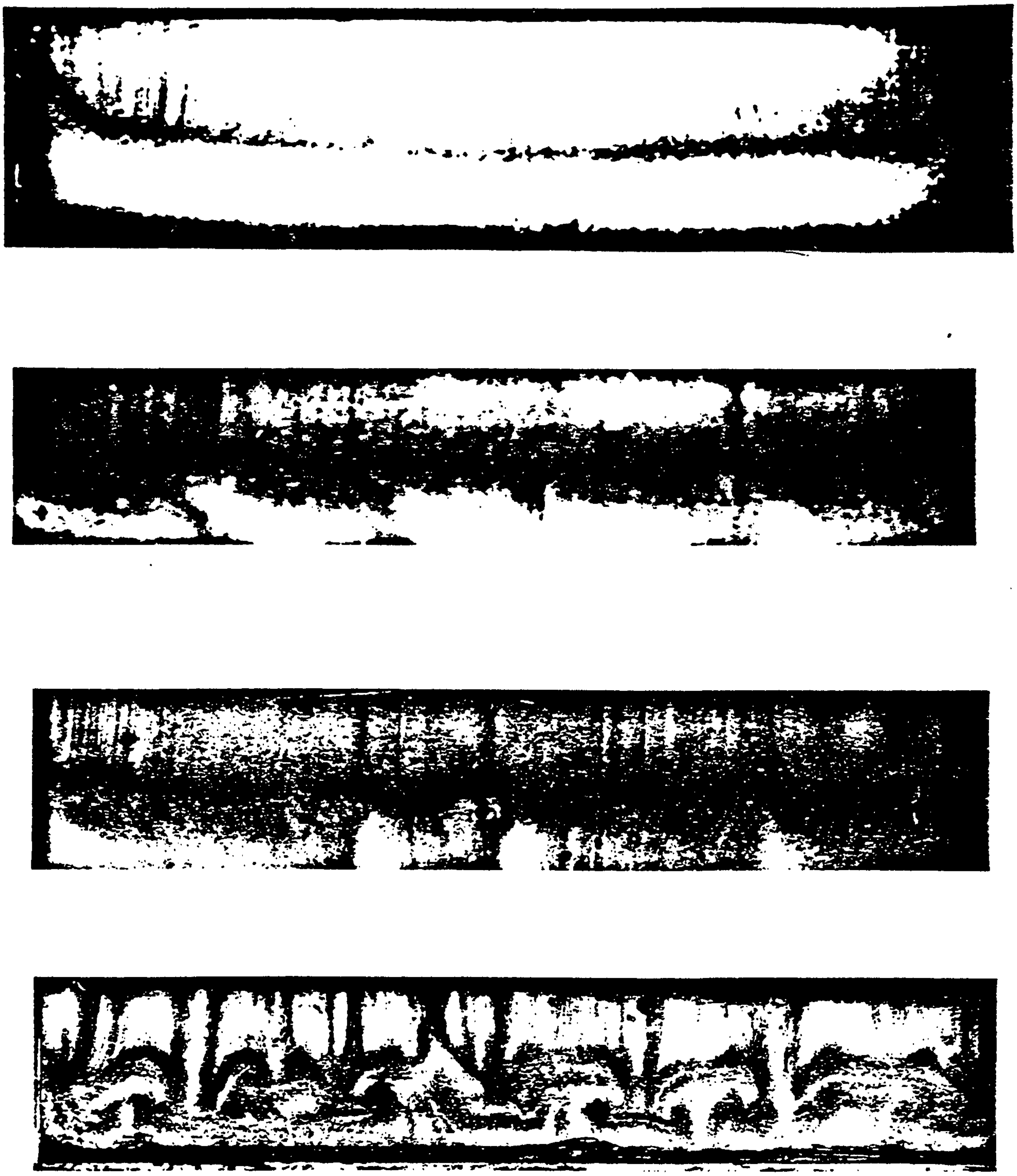

(a)

(b)

(c)

(d)

(a)

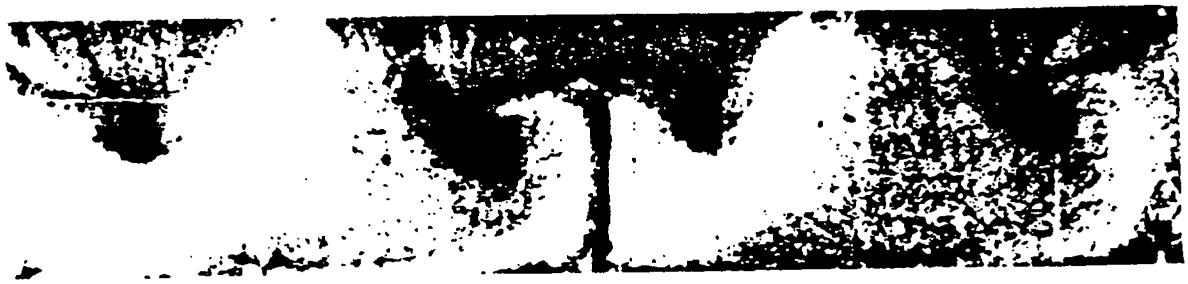

(b)

(c)

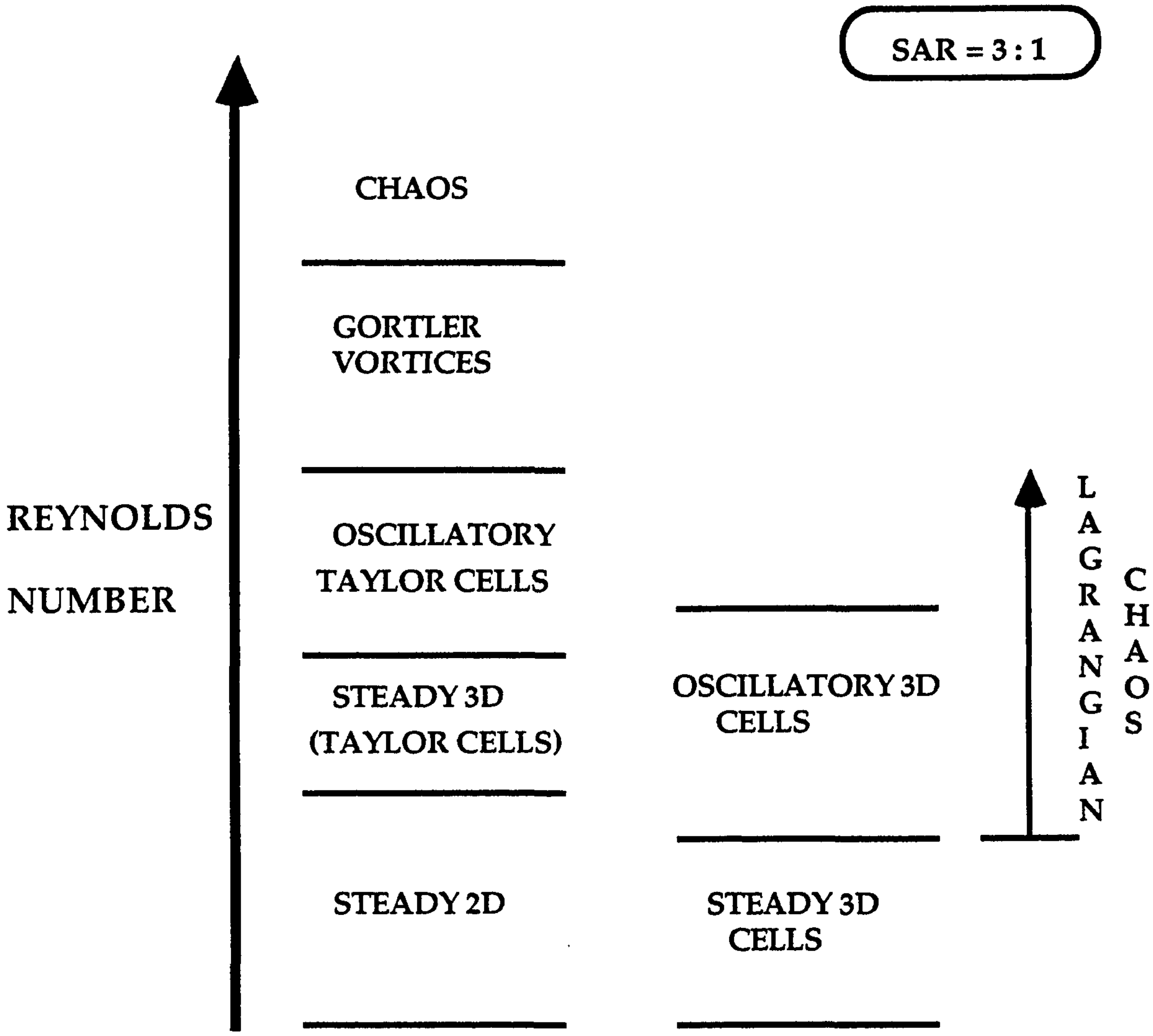
SAR = 3 : 1
REYNOLDS NUMBER
CHAOS
GORTLER VORTICES
OSCILLATORY TAYLOR CELLS
STEADY 3D (TAYLOR CELLS)
STEADY 2D
OSCILLATORY 3D CELLS
STEADY 3D CELLS
LAGRANGIAN CHAOS

CONCLUSIONS FROM LABORATORY EXPERIMENTS

- It is found that the flow inside the pond of a short-dwell coater is globally unstable
- At least three 3D flow patterns compete with the ideal "2D" flow pattern
- 3D unsteady flow patterns could generate streaks
- As the machine speed increases, the 3D flow patterns oscillate in CD

CONCLUSIONS FROM THEORETICAL ANALYSIS

- Due to the spanwise oscillation of the 3D flow patterns, the solid particles could follow chaotic trajectories (strong mixing) at the boundary of the recirculating vortices
- Stronger mixing at the boundary of the cells relative to the core could result in solid concentration gradient in CD
- Solid concentration gradient in CD will result in streaks

CONCLUSIONS FROM PILOT COATER TRIALS

- The instability of the primary vortex in the pond is partly responsible for the streaks
- Increasing the coating injection rate has a tendency to suppress the streaks

---

RECENT RESULTS

RECENT PROGRESS IN EXPERIMENTAL ANALYSIS

1. Modified the SDC Simulator for accurate quantitative measurements. Modifications include:

   - o a data acquisition system
   - o digital speed control
   - o accurate on-line flow meter

EXPERIMENTAL SETUP

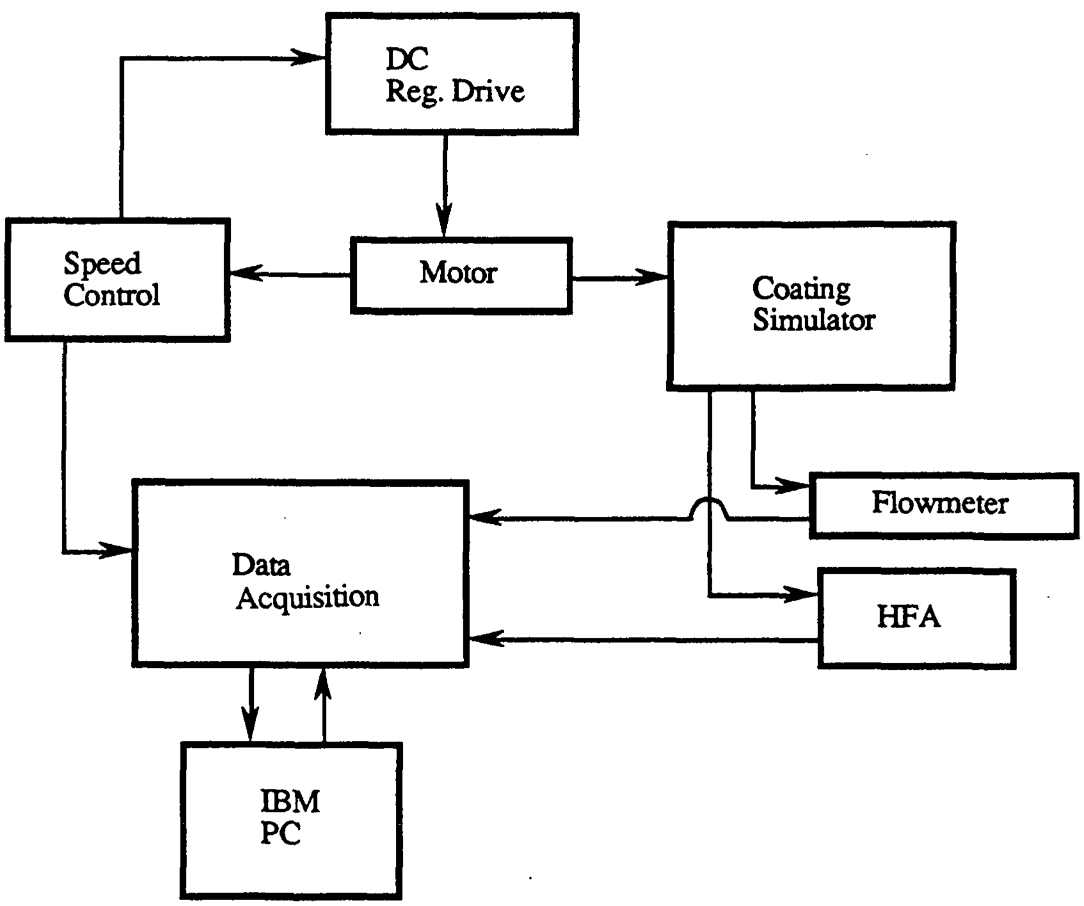

RECENT PROGRESS
IN
EXPERIMENTAL ANALYSIS (cont'd)

2. Measured critical roll speed for onset of unsteady flow as a function of fluid viscosity and net mass flow rate.

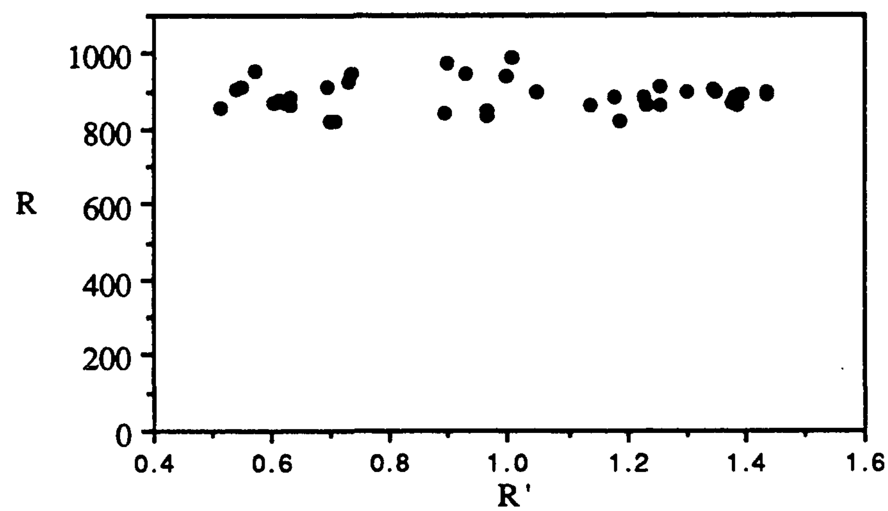

Figure 3. The critical cavity Reynolds number for transition to time-dependent flow as a function of through-flow Reynolds number.

RECENT PROGRESS
IN
EXPERIMENTAL ANALYSIS (cont'd)

3. Designed a cavity with variable aspect ratio (0>S/D>10) for measuring the influence of geometry on critical machine speed for onset of instability.

RECENT PROGRESS
IN
EXPERIMENTAL ANALYSIS (cont'd)

4. Completed the calibration loop for a hot-film anemometer.

HOT-FILM ANEMOMETER

- o Measures the shear stress of flow at the solid surface.
- o Can be used for measuring the dynamics of flow in a coater, headbox, or other sections.
- o Has to be calibrated for each specific fluid at a given temperature.

HOT-FILM ANEMOMETER

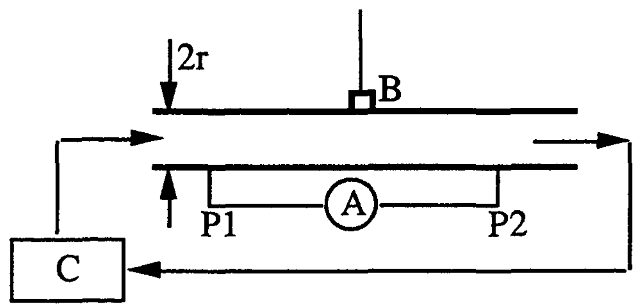

$$\tau = r\Delta p/2\iota$$

where: r , radius of the pipe;

ι , distance between the two pressure ports, P1 and P2;

τ, shear stress

$\Delta p = P1 - P2$;

A, pressure differential transducer

B, flush-surface hot-film sensor

C, temperature bath

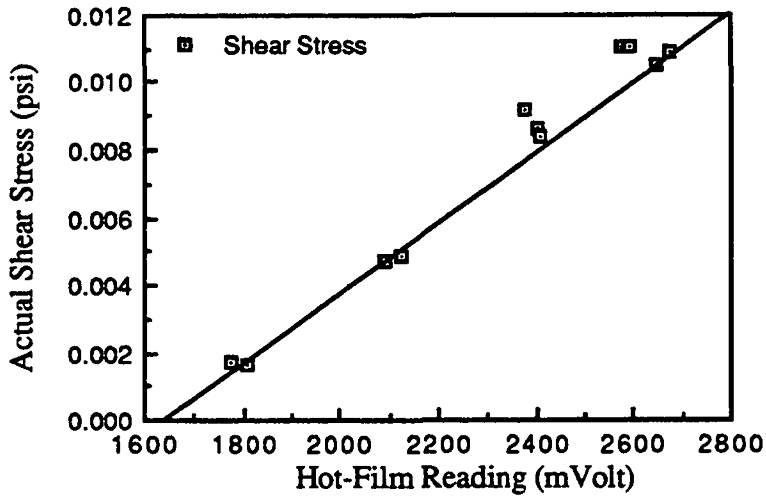

Figure 4. Hot-film calibration data at 20ºC

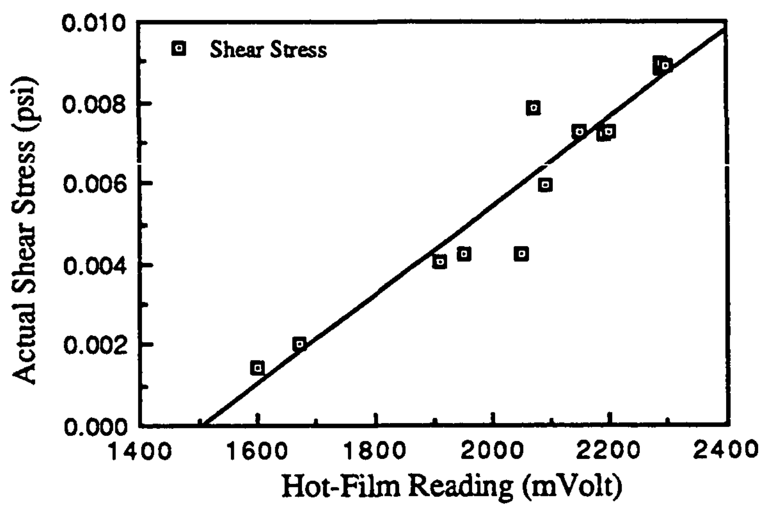

Figure 5. Hot-film calibration graph at 25ºC

COMPUTATIONAL ANALYSIS OF SHORT-DWELL COATERS

- First complete computational analysis of flow in the pond coupled with the free-surface flow through the blade.

COATING PARAMETERS

machine speed, $U = 1200$ m/min

net flow rate, $m = 166$ l/min.m

pond depth, $D = .05$ m

blade gap = .1 mm

viscosity, $\mu = 1{,}500$ mPa.s

surface tension, $\sigma = .05$ N/m

gravity = 9.8 m/s^2

density = 1000 kg/m^3

NONDIMENSIONAL PARAMETERS

Cavity Reynolds number, $R = \rho UD/ = 666.6$

Capillary number, $Ca = \mu U/ = 600$

Stokes number, $St = \rho g D^2/\mu U = .8167$

Through-flow Reynolds number, $R' = \rho m/\mu = 1.85$

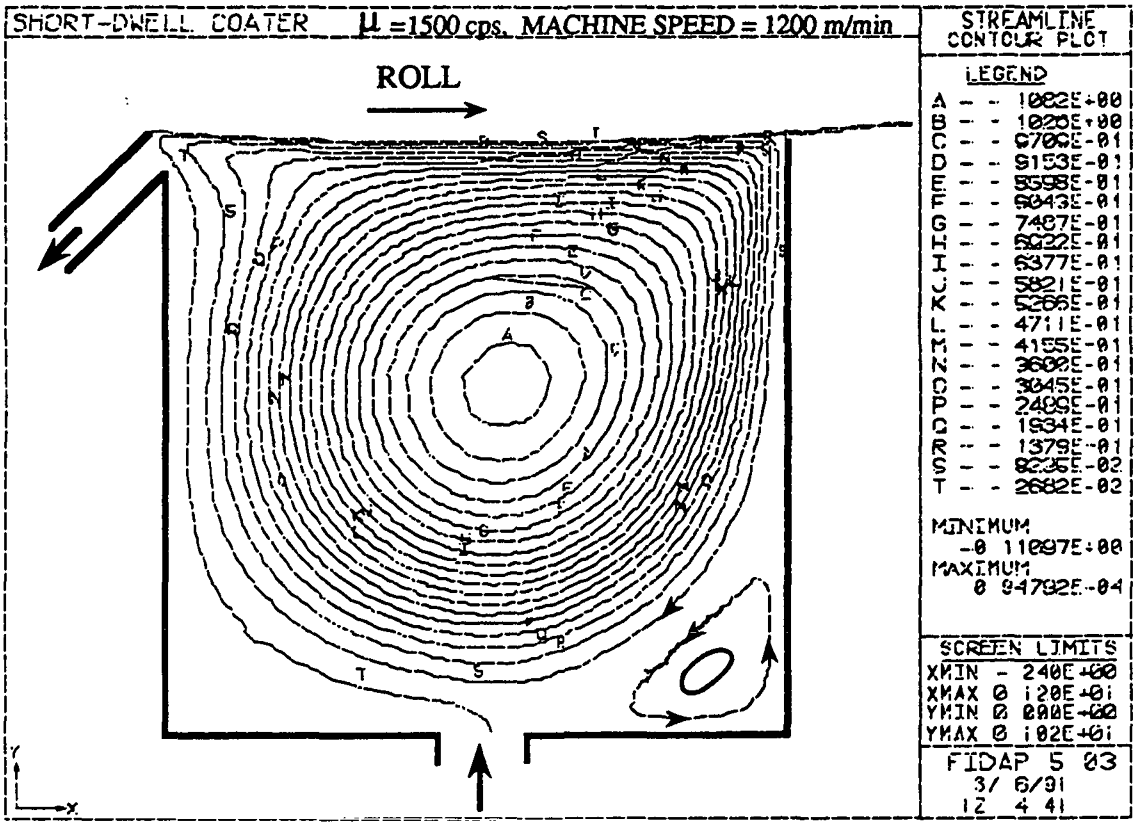

Streamline contour plot of flow in a short-dwell coater (constant viscosity).

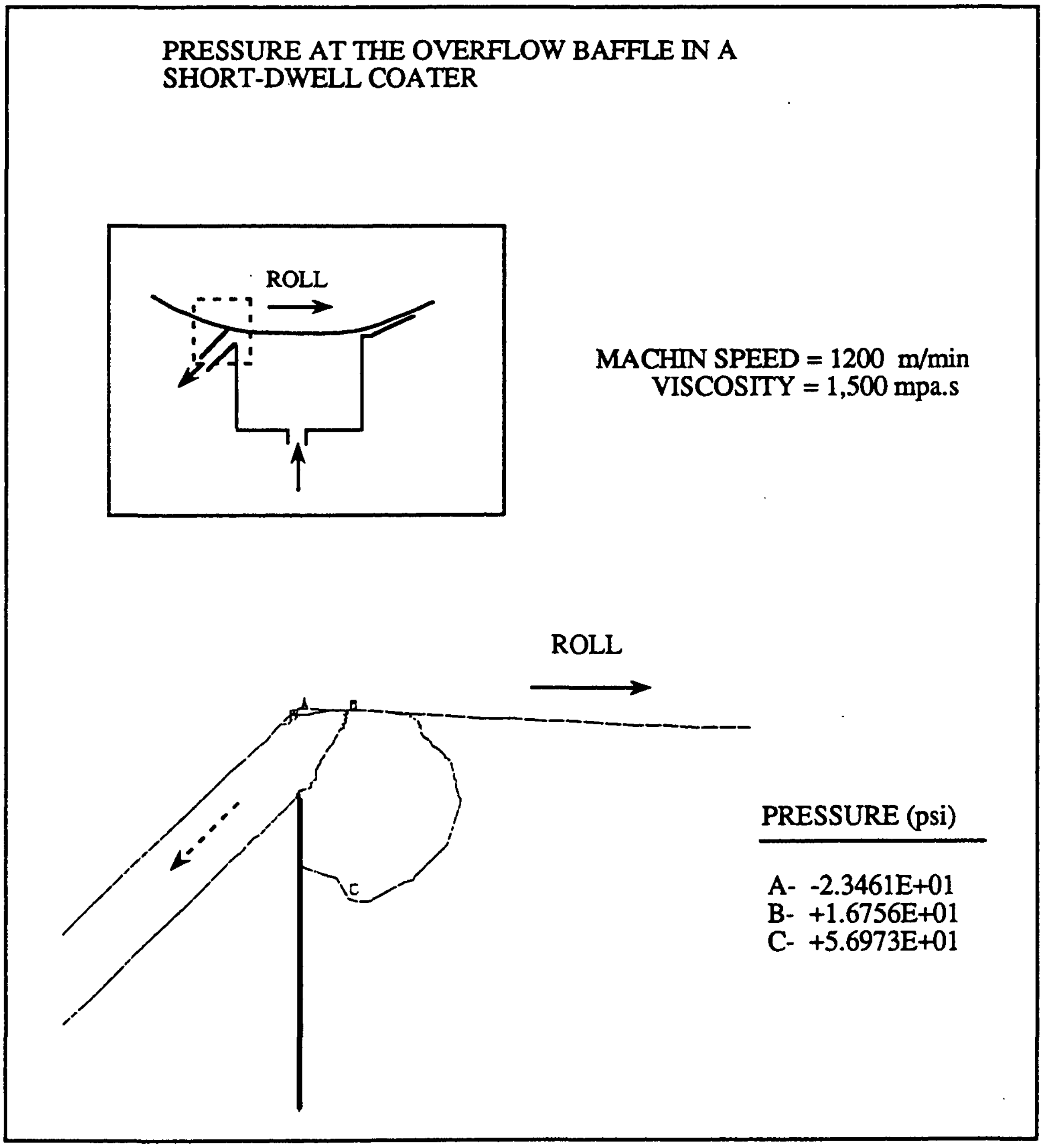

Subambient pressure at the overflow baffle in a short-dwell coater (constant viscosity).

DIVERGING BLADE IN A SHORT_DWELL COATER

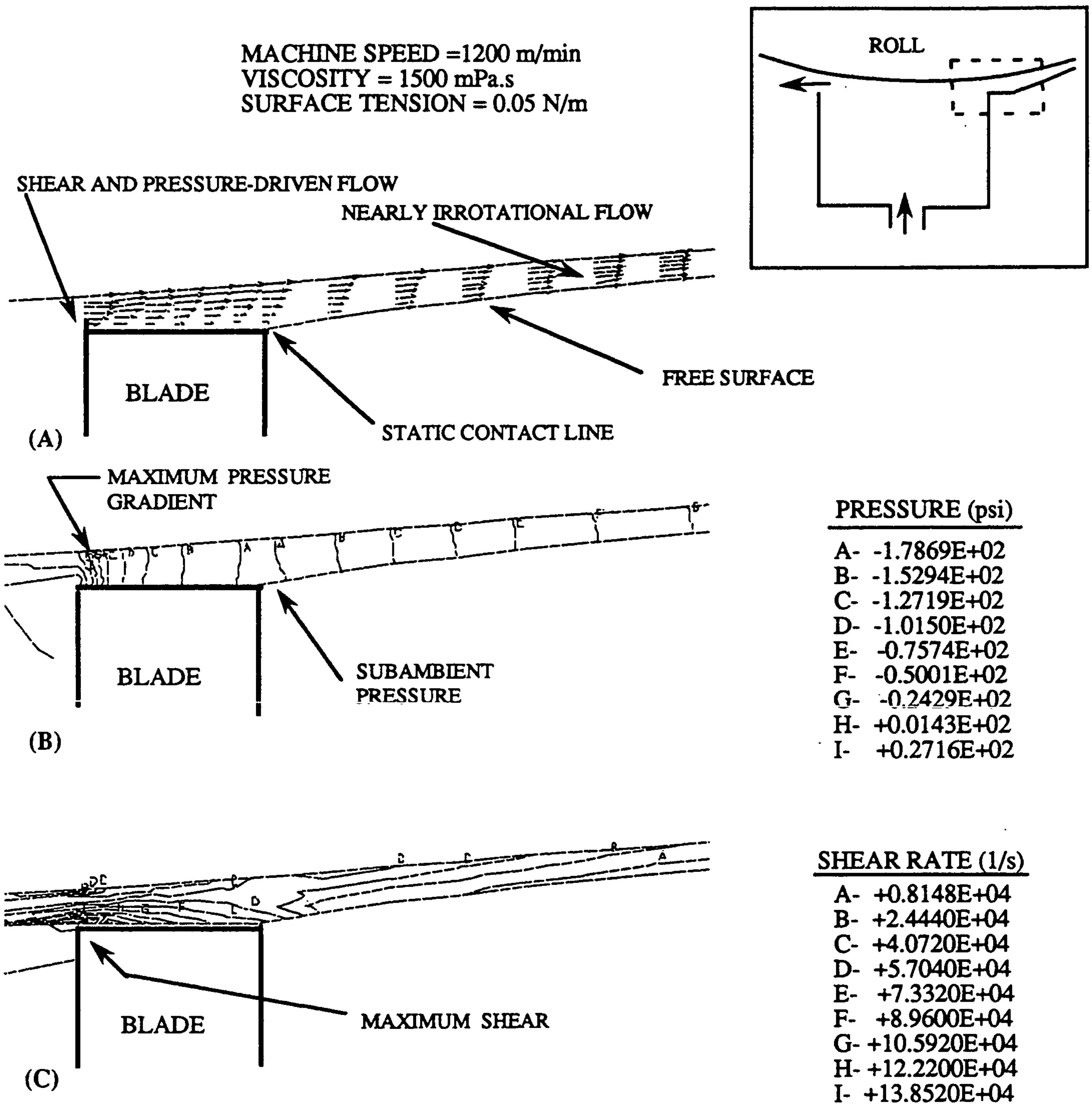

Constant viscosity fluid flow at the blade of a short-dwell coater; (A) velocity vector plot, (B) pressure contour plot, and (C) shear rate contour plot.

CARREAU MODEL

$$\frac{\eta - \eta_\infty}{\eta_o - \eta_\infty} = \left[1 + (\tau\dot{\gamma})^2\right]^{\frac{n-1}{2}}$$

where $\dot{\gamma}$ shear rate
τ time constant
n Carreau index
η_o zero-shear-rate viscosity
η_∞ infinite-shear-rate viscosity.

DIVERGING BLADE IN A SHORT-DWELL COATER

MACHINE SPEED = 1200 m/min
VISCOSITY; CARREAU MODEL

$\mu_o = 1500$
$\mu_\infty = 150$
$n = .7$
$\tau = .01$

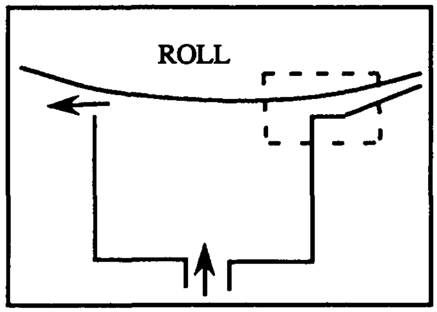

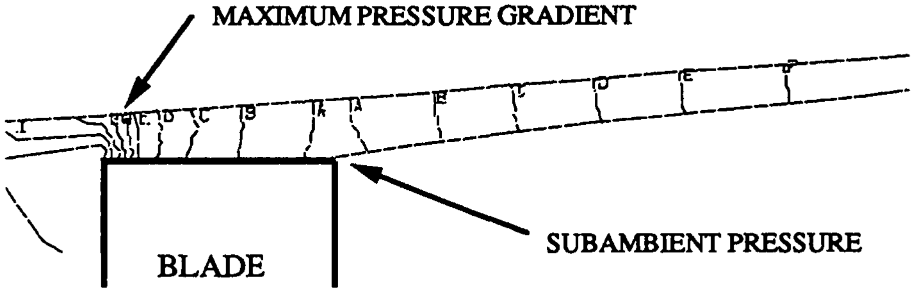

(A)

PTRESSURE (psi)

A- -1.4923E+02
B- -1.2702E+02
C- -1.0474E+02
D- -0.8253E+02
E- -0.6026E+02
F- -0.3803E+02
G- -0.1579E+02
H- +0.0645E+02
I- +0.0286E+02

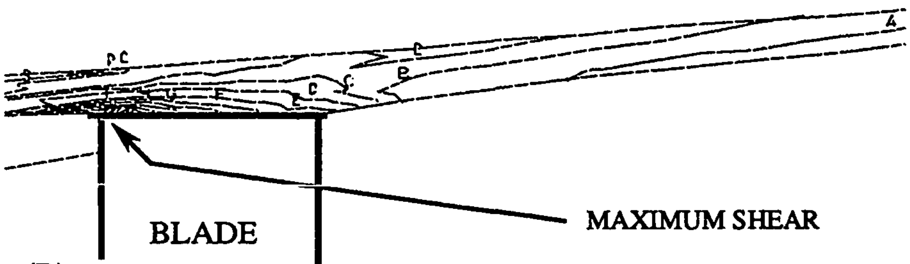

(B)

SHEAR RATE (1/s)

A- +0.9608E+04
B- +2.8824E+04
C- +4.8040E+04
D- +6.7240E+04
E- +8.6480E+04
F- +10.5680E+04
G- +12.4920E+04
H- +16.3360E+04

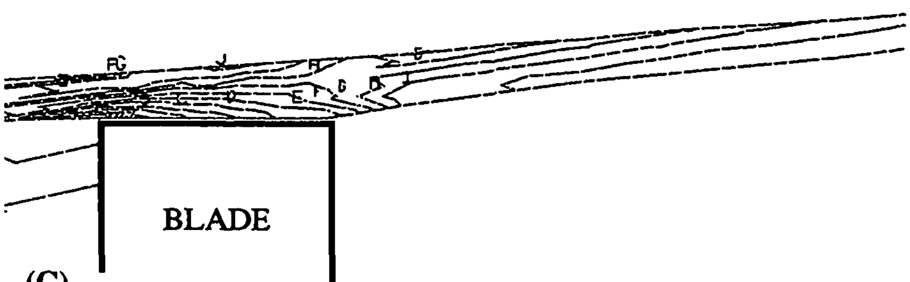

(C)

VISCOSITY (mPa.s)

A- +1.013E+03
B- +1.065E+03
C- +1.116E+03
D- +1.167E+03
E- +1.218E+03
F- +1.269E+03
G- +1.321E+03
H- +1.372E+03
I- +1.423E+03

Flow of shear-thinning coating color at the blade of a short-dwell coater; (A) pressure, (B) shear rate, and (C) non-newtonian viscosity contour plot.

HIGH-SPEED COATER

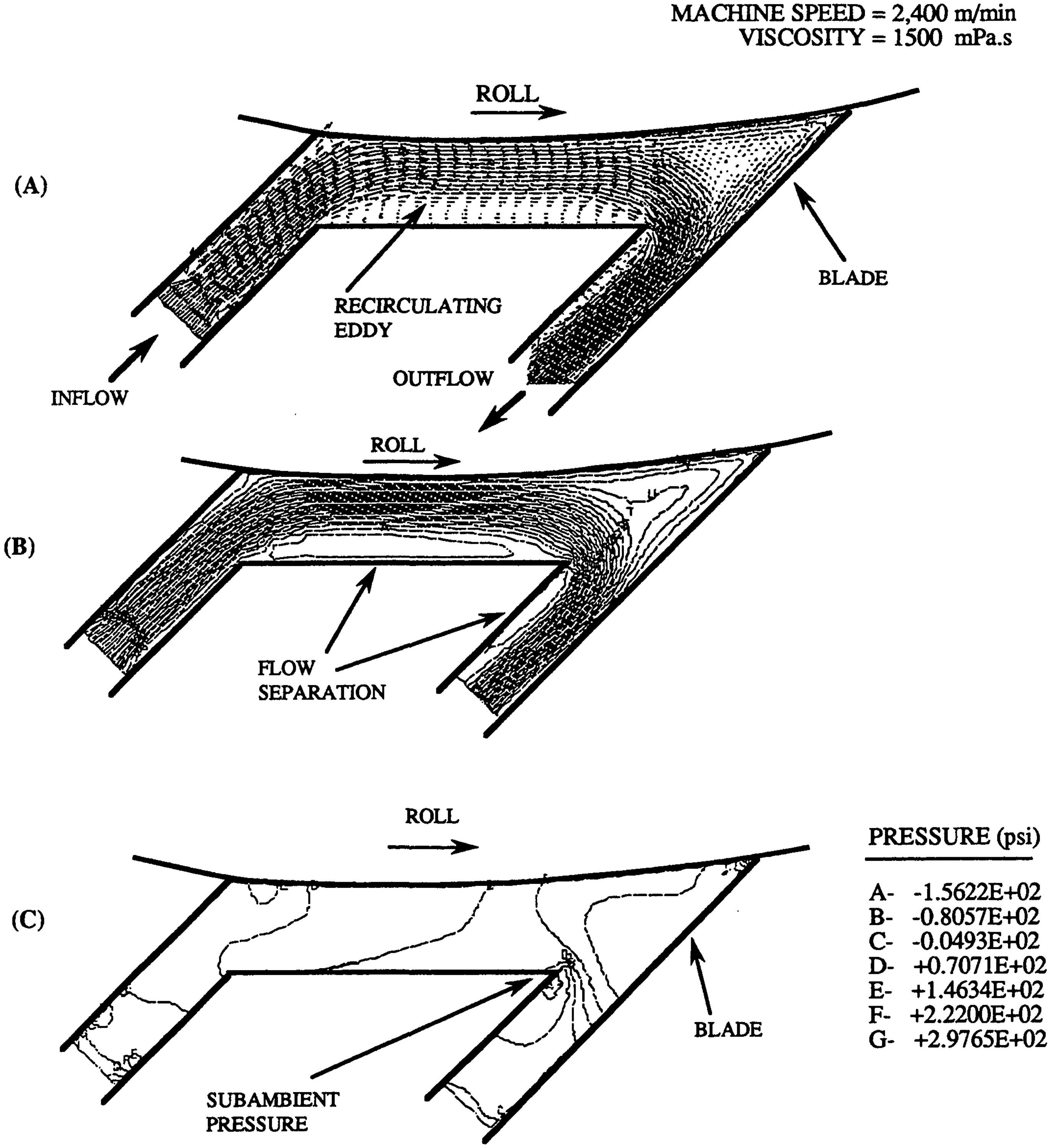

Parallel-flow coater; (A) velocity vector plot, (B) streamline contour plot and (c) pressure contour plot.

HIGH-SPEED COATER

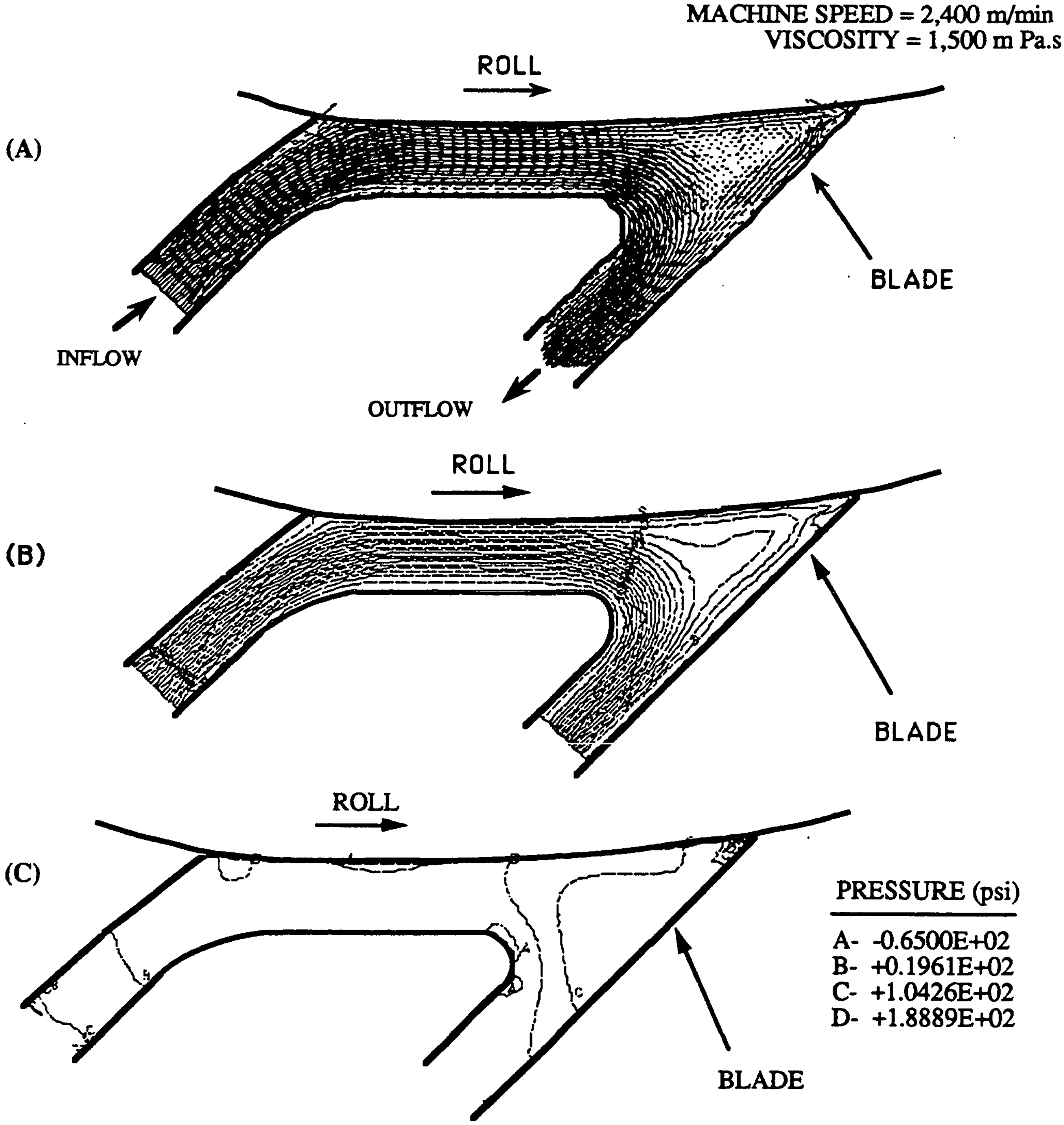

Modified parallel-flow coater; (A) velocity vector plot, (B) streamline contour plot, and (C) pressure contour plot.

FUTURE PLANS

1. Calibrate a hot-film anemometer (HFA) for non-isothermal conditions by attaching a thermocouple to the HFA probe.

2. Measure the effects of span aspect ratio on the critical speed for the onset of time dependent flow in the pond of short-dwell coaters using (a) viscous Newtonian fluid and (b) shear-thinning fluids with typical coating color rheological characteristics.

3. Extend the computational fluid dynamics techniques to study and compare the rheological behavior of coating colors in a SDC for various sets of parameters, such as blade angle and physical properties of the fluid.

4. Install an actual SDC head (being built by Beloit) on the experimental roll coater to investigate problems with flow cavitation.

Long-term:

5. Develop a computational technique based on spectral decomposition for stability analysis of rheologically complex coating colors in various coating systems.

6. Modify the application technique in a blade coating system for superior performance. This is an exploratory research within the project for development of novel coating systems. The current computer aided design techniques will be used to continue modification of the new coating head design.

DISPLACEMENT DEWATERING
PROJECT 3680

April 4, 1991
Institute of Paper Science and Technology
Atlanta, Georgia

Project 3680

Title:

Displacement Dewatering

Objective:

To remove liquid water efficiently while maintaining control over bulk.

Flat-bed Through Dryer

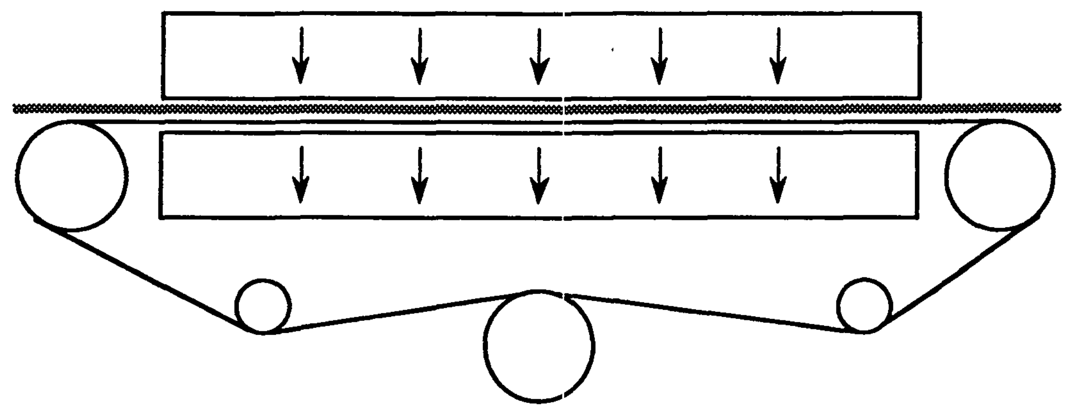

Rotary Through-dryer

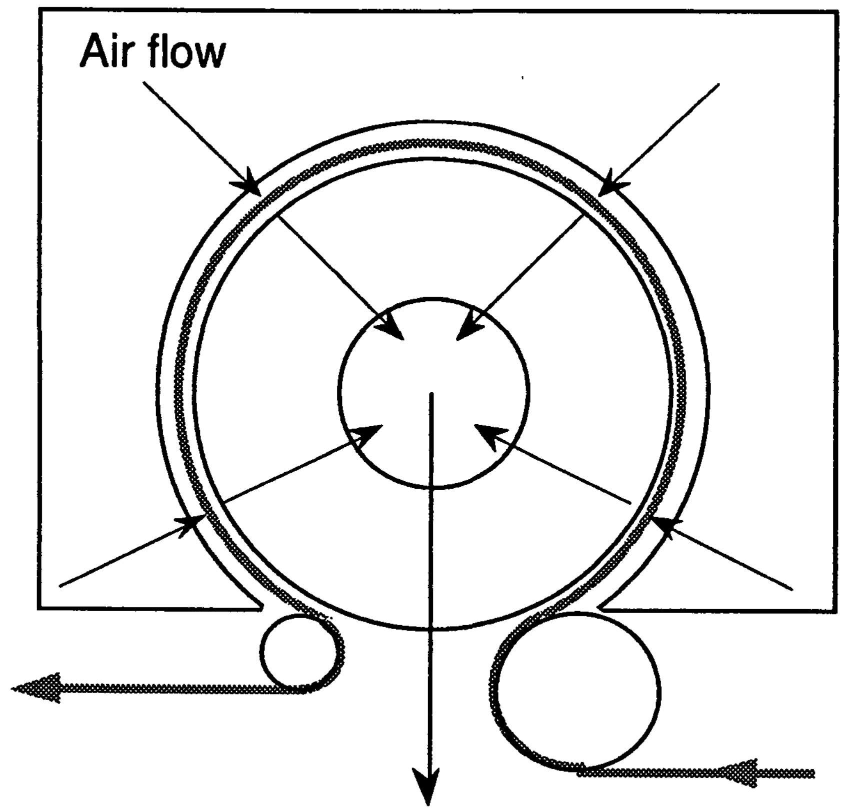

Early IPC Data

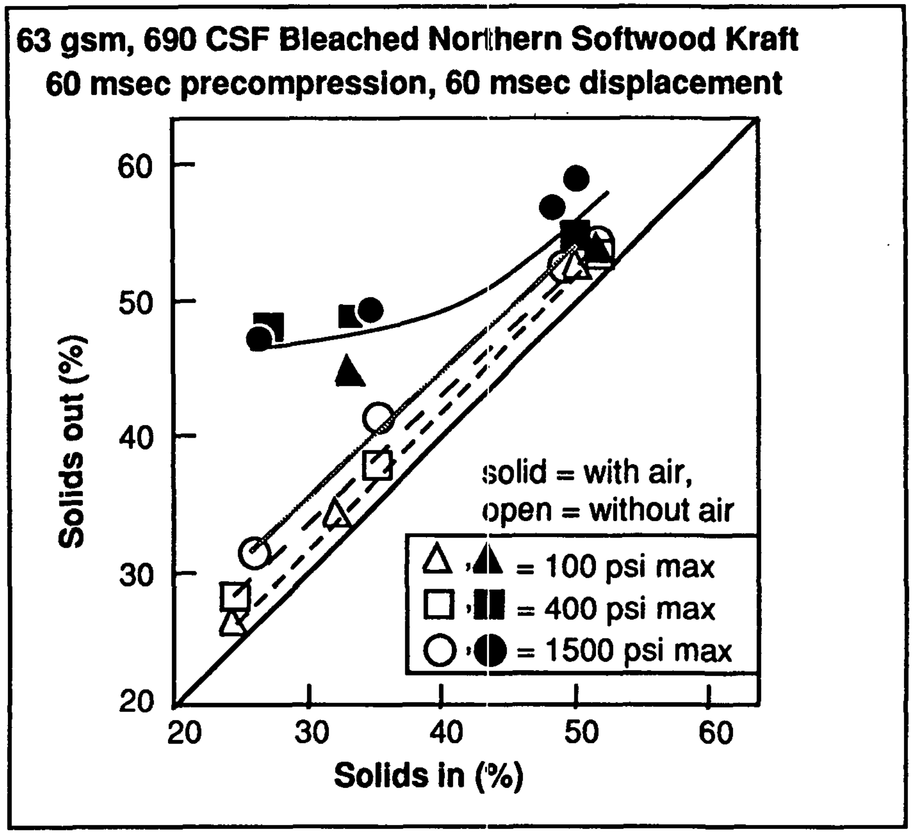

The Flaw in Early Analysis:

Wet pressing with a porous surface is much less efficient than wet pressing with a solid surface. Comparisons of such pressing to displacement dewatering are inappropriate.

White and Marceau Data

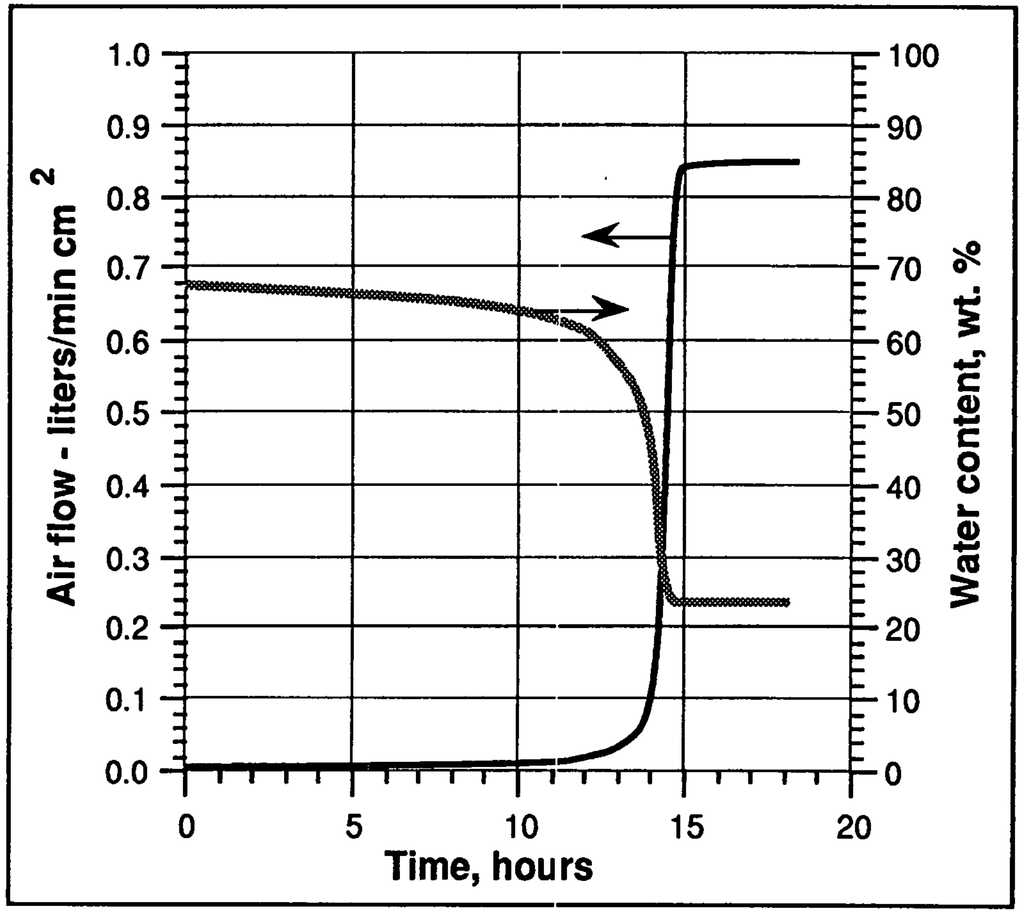

Viscous Fingering

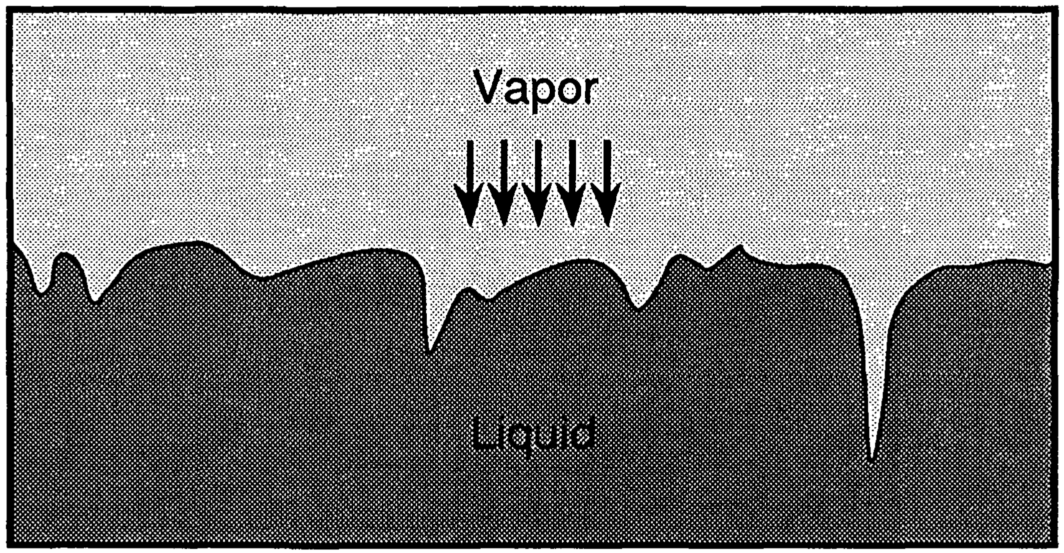

Equipment

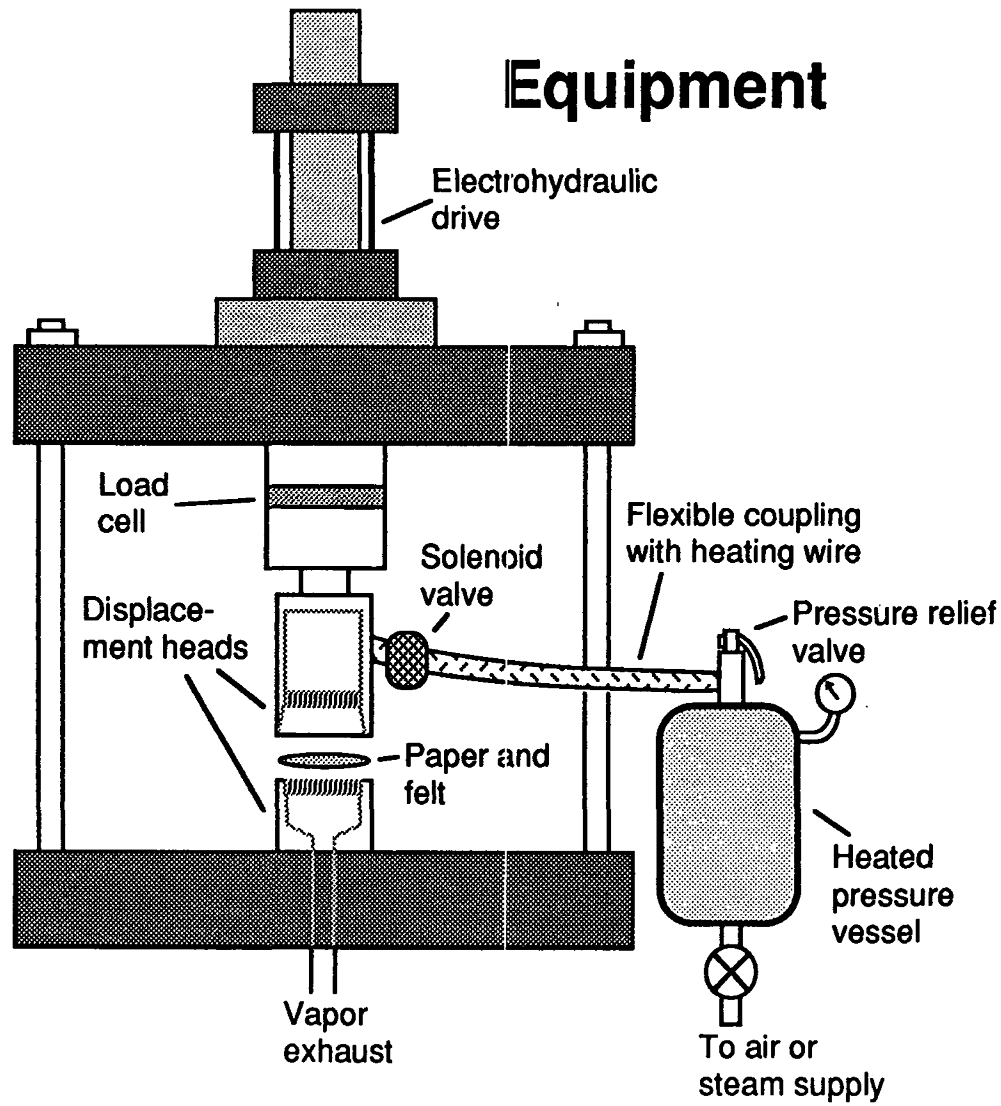
Electrohydraulic drive
Load cell
Displace- ment heads
Solenoid valve
Flexible coupling with heating wire
Pressure relief valve
Paper and felt
Heated pressure vessel
Vapor exhaust
To air or steam supply

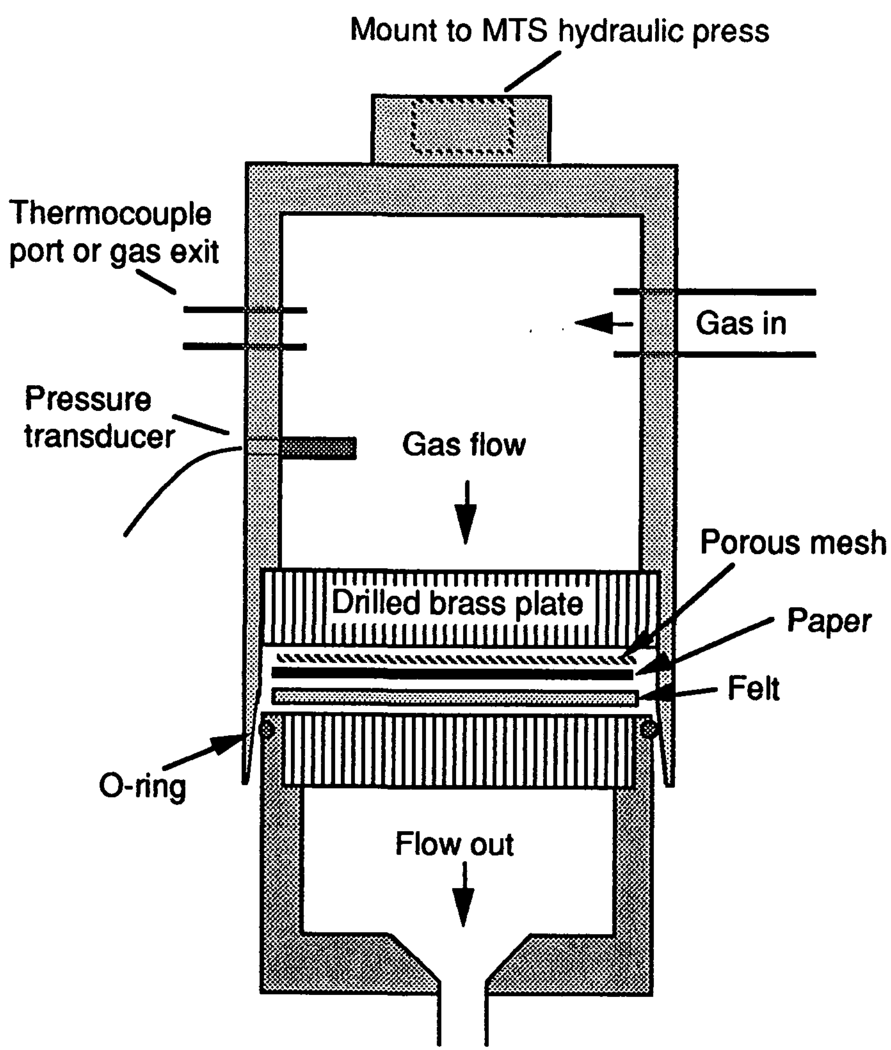

Displacement Heads

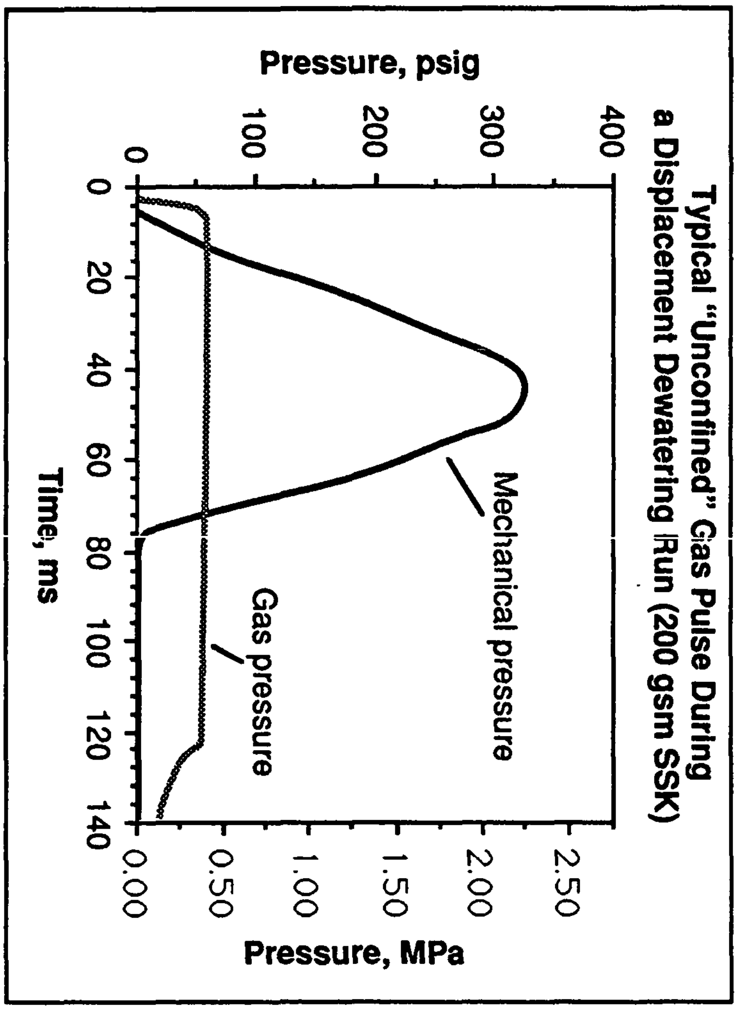
Typical "Unconfined" Gas Pulse During
a Displacement Dewatering Run (200 gsm SSK)
Pressure, psig
0
100
200
300
400
Time, ms
0
20
40
60
80
100
120
140
Mechanical pressure
Gas pressure
Pressure, MPa
0.00
0.50
1.00
1.50
2.00
2.50

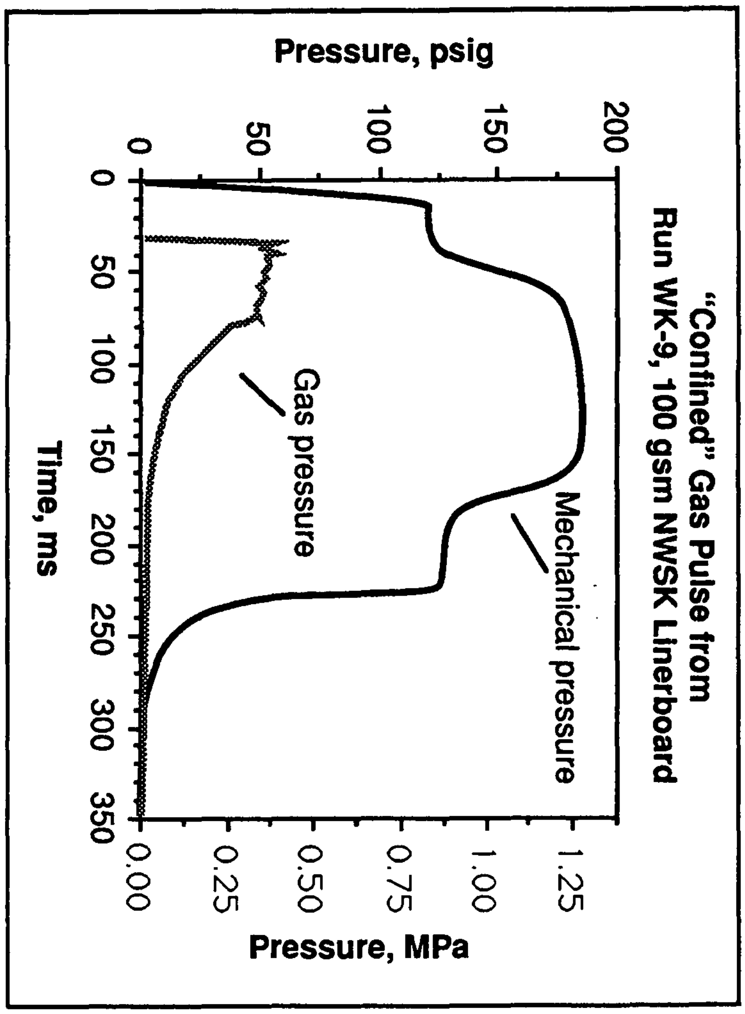
"Confined" Gas Pulse from
Run WK-9, 100 gsm NWSK Linerboard
Pressure, psig
0
50
100
150
200
0
50
100
150
200
250
300
350
Time, ms
Gas pressure
Mechanical pressure
0.00
0.25
0.50
0.75
1.00
1.25
Pressure, MPa

Definitions

"Low-pressure" wet pressing:

Wet pressing at low mechanical pressures (<300 psi peak) for long nip times (>50 ms)

"Normal" wet pressing:

Wet pressing with higher peak pressures and shorter nip times (ca. 20 ms).

Density Development in 100 gsm Handsheets During Unconfined Steam Displacement Dewatering

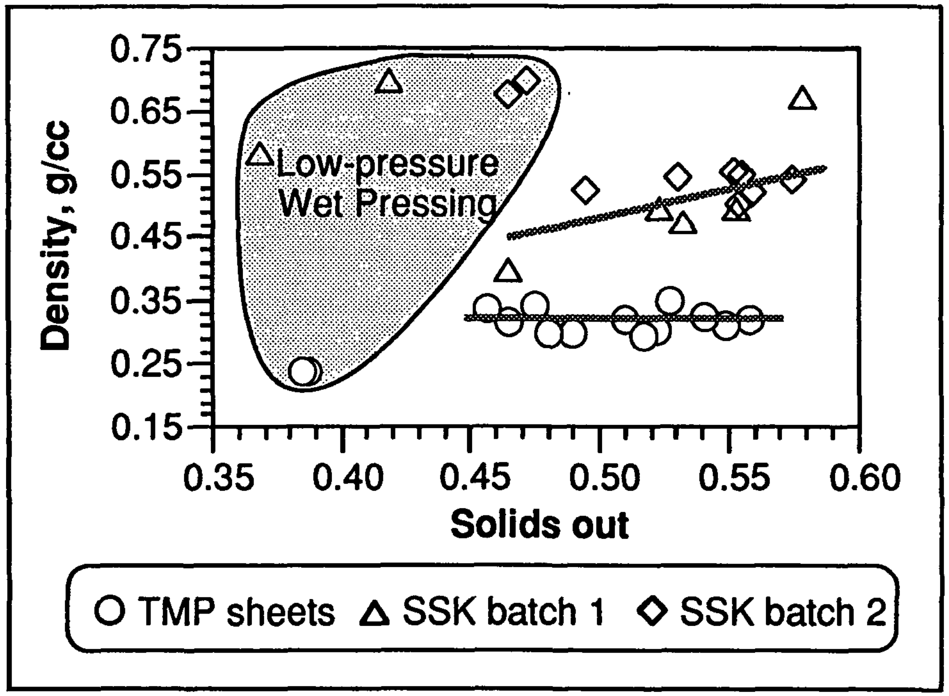

Unconfined Steam Displacement Dewatering in Several 100 gsm Handsheets

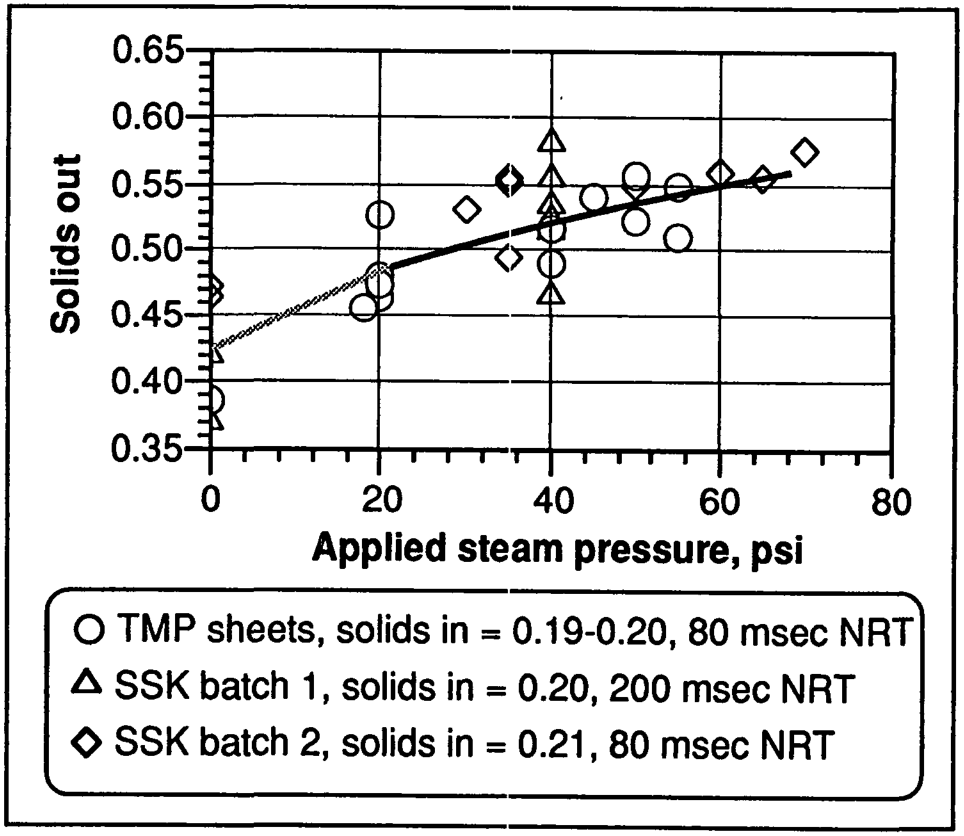

Air and Steam Displacement in 100 gsm NWSK Linerboard. Solids in = 0.25-0.26.

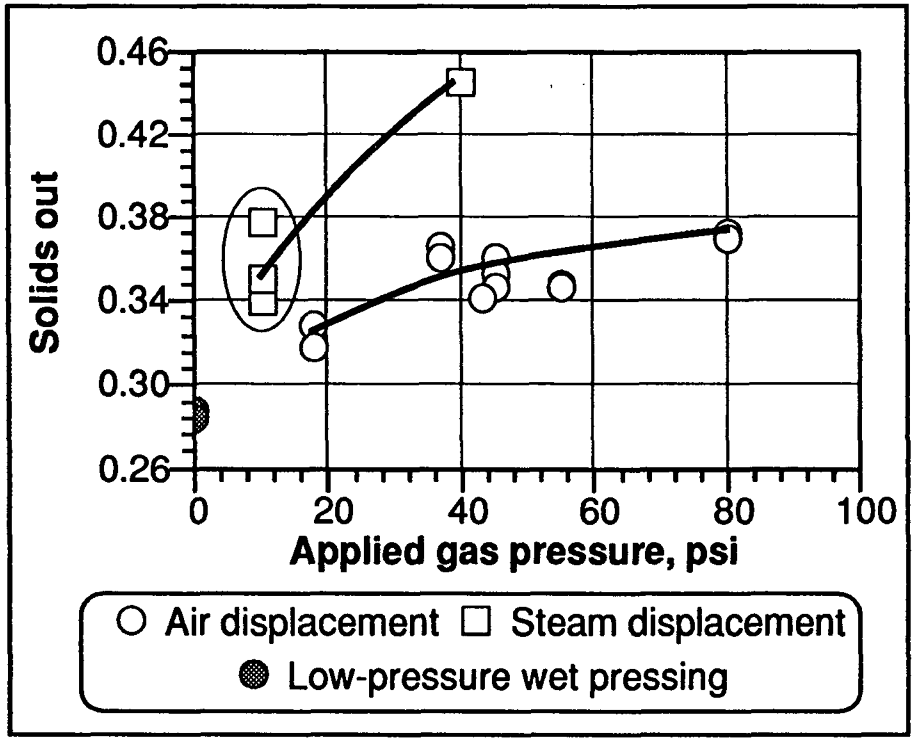

Confined Displacement Dewatering in 150 gsm NWSK Linerboard. Solids in = 0.24-0.25.

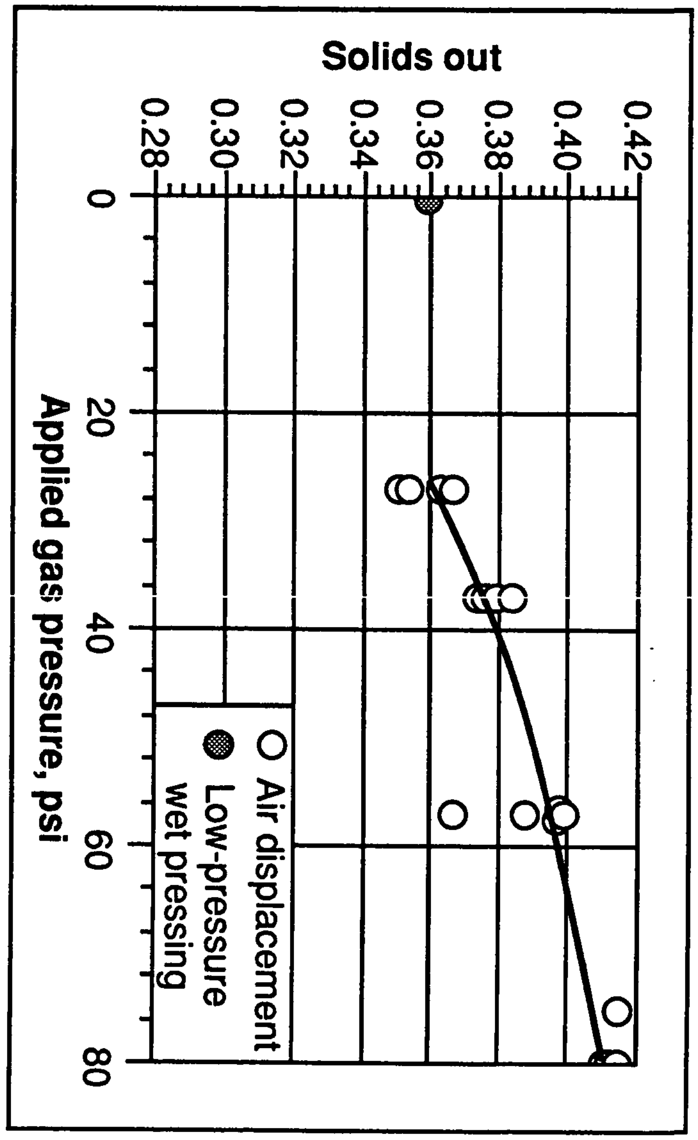

Confined Air Displacement in Saturated Blotter Paper. Solids in = 0.32-0.33.

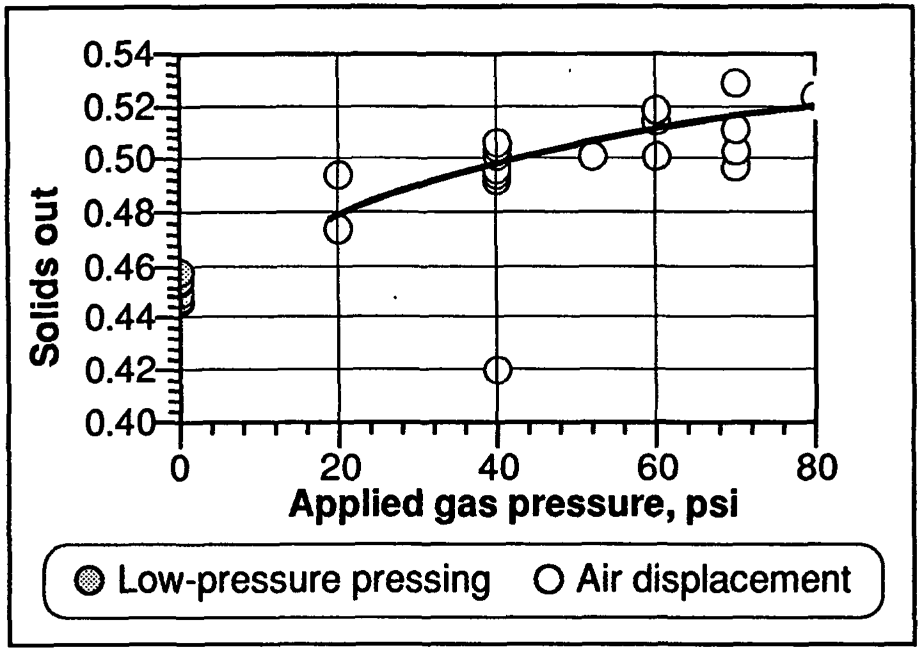

Normal Wet Pressing Density-Dryness Relation for NWSK Linerboard Sheets

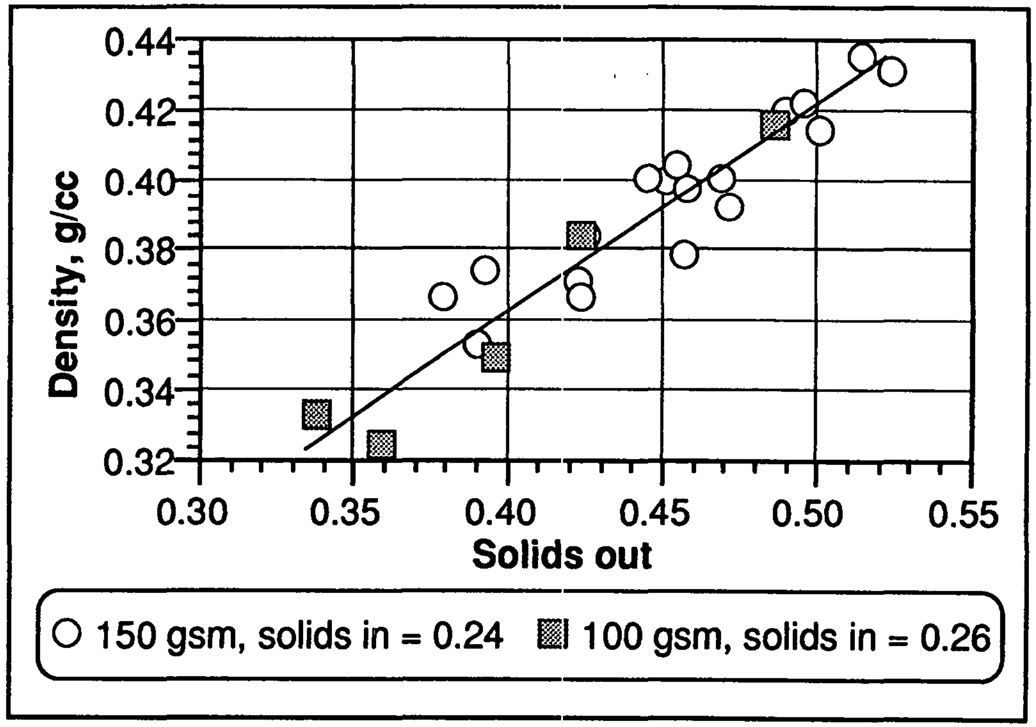

Density-dryness Relation in Displacement Dewatering of 150 gsm NWSK Linerboard Sheets

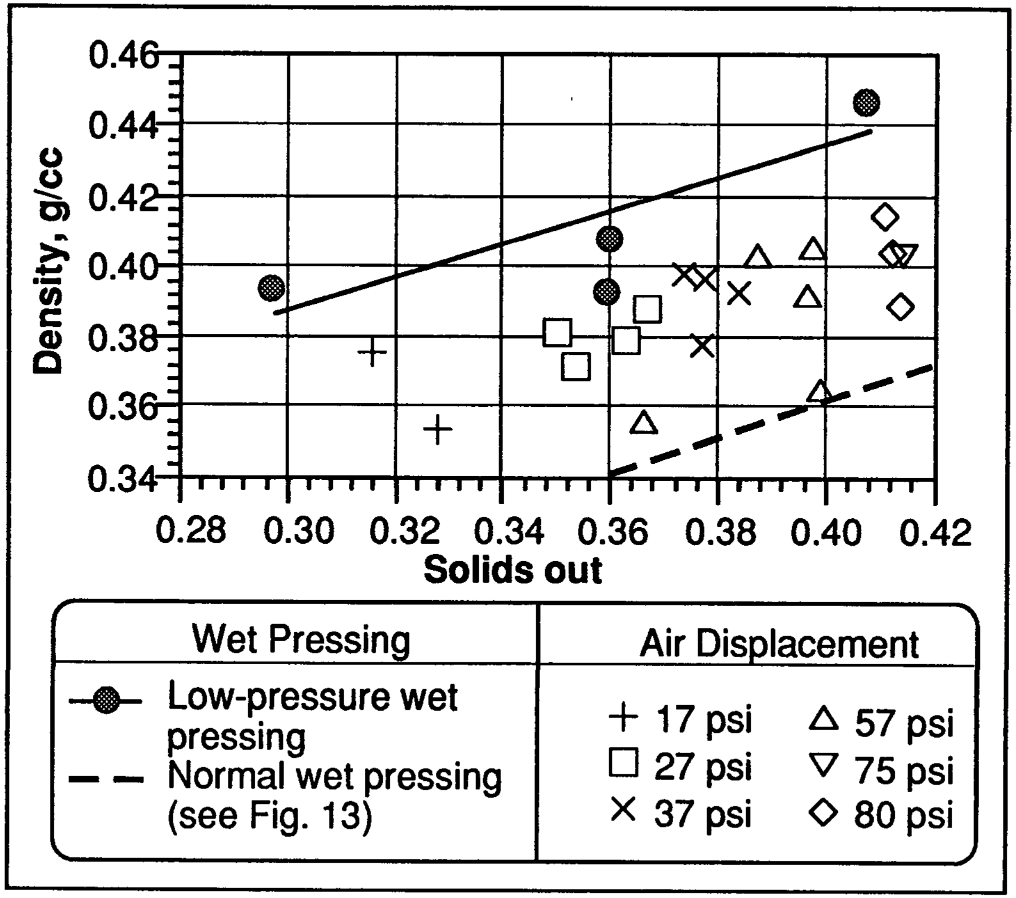

Density Development in Confined Displacement Dewatering of 100 gsm NWSK Linerboard Sheets

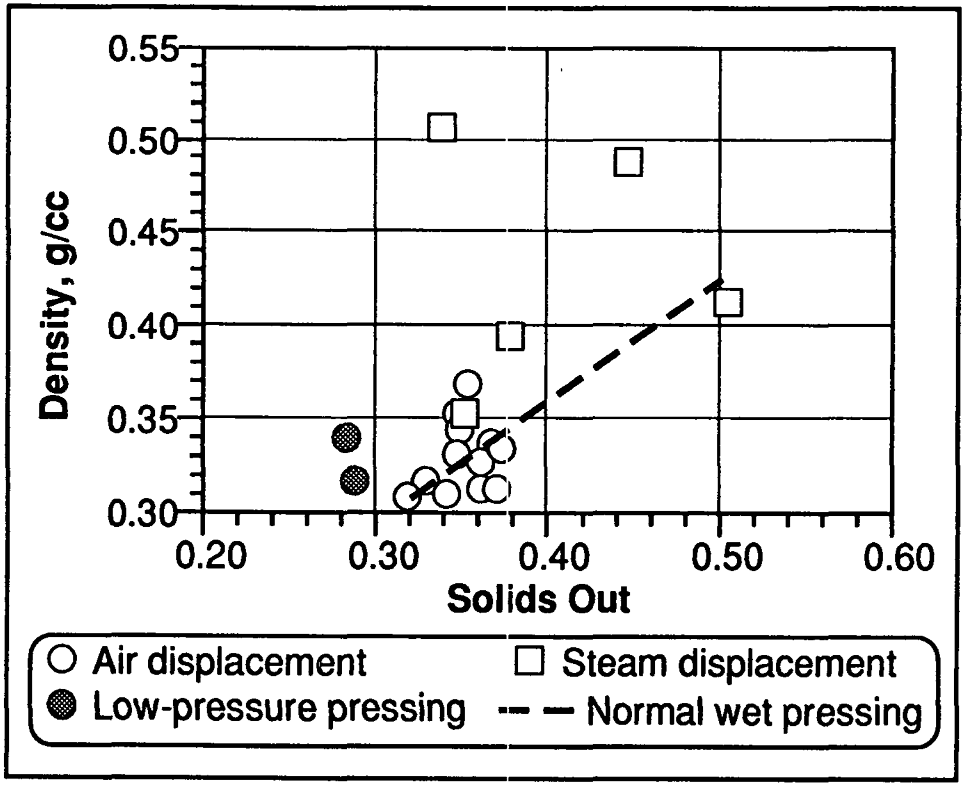

Path Dependent Consolidation

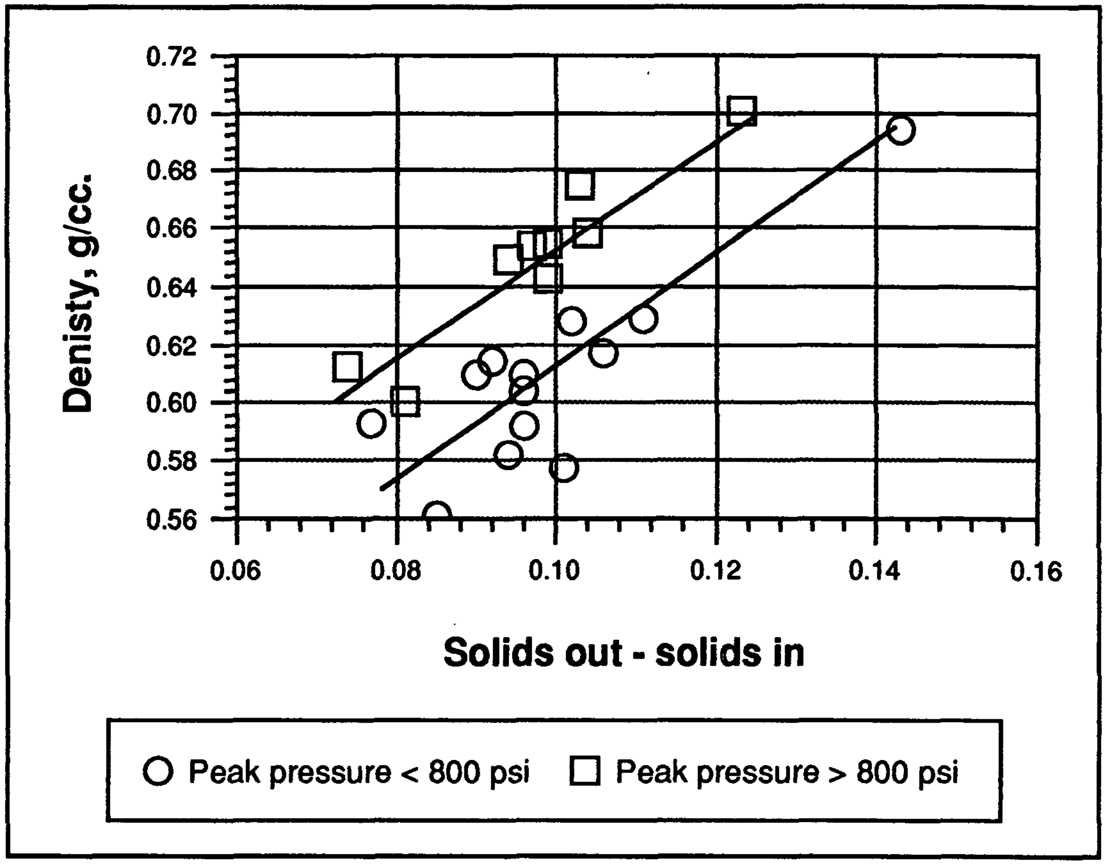

Path Dependent Consolidation

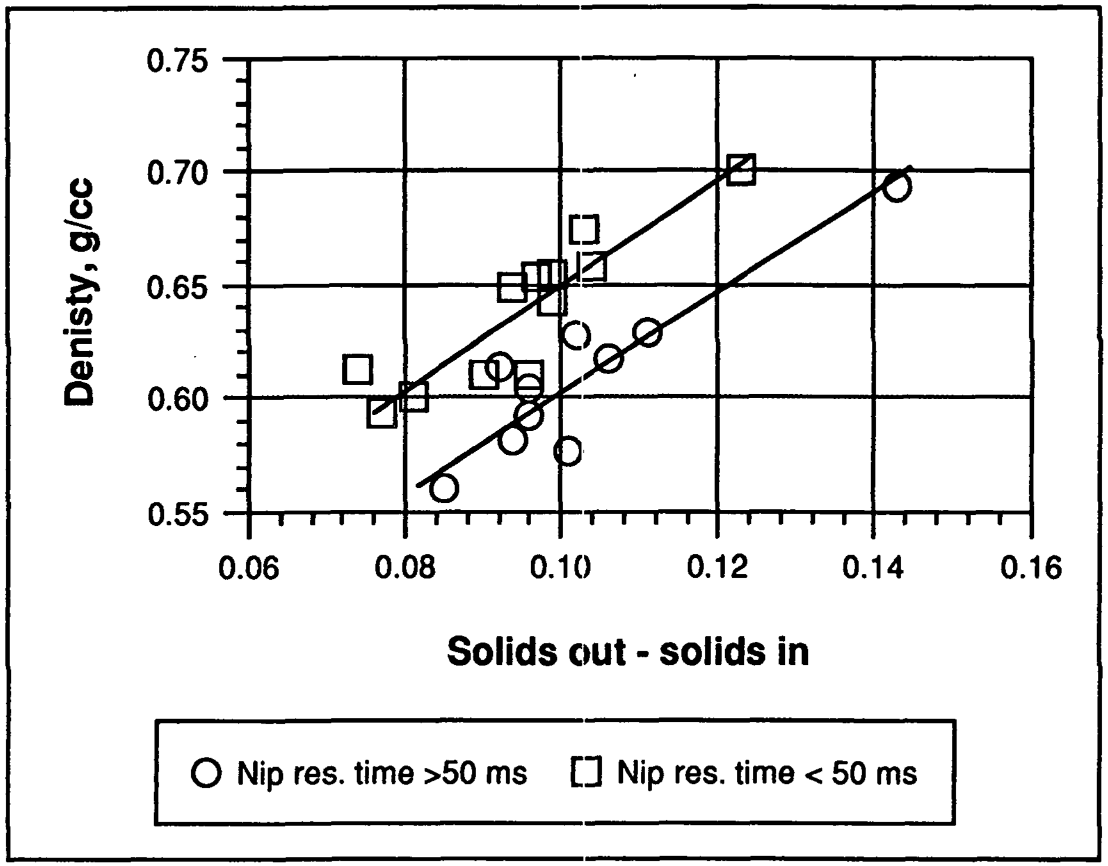

The Adverse Zone

At low gas pressures, displacement dewatering removes less water than a similar wet pressing process. The inefficiency of pressing with a porous surface is the cause.

Confined Displacement Dewatering in 150 gsm NWSK Linerboard. Solids in = 0.24-0.25.

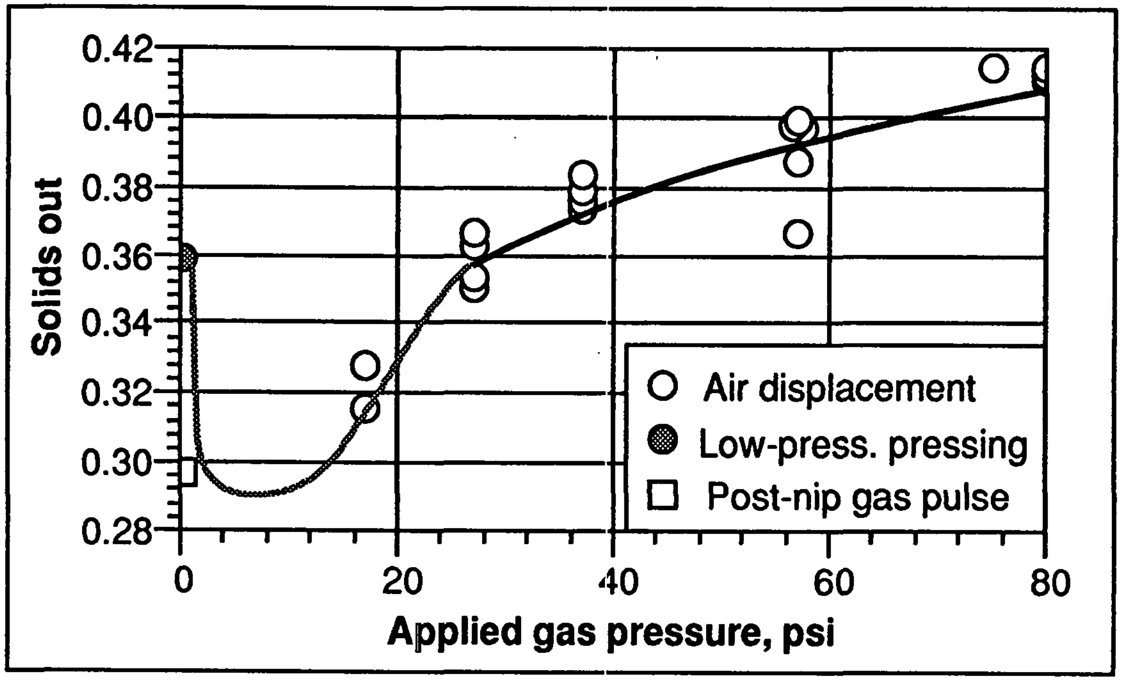

Confined Air Displacement in Saturated Blotter Paper. Solids in = 0.32-0.33.

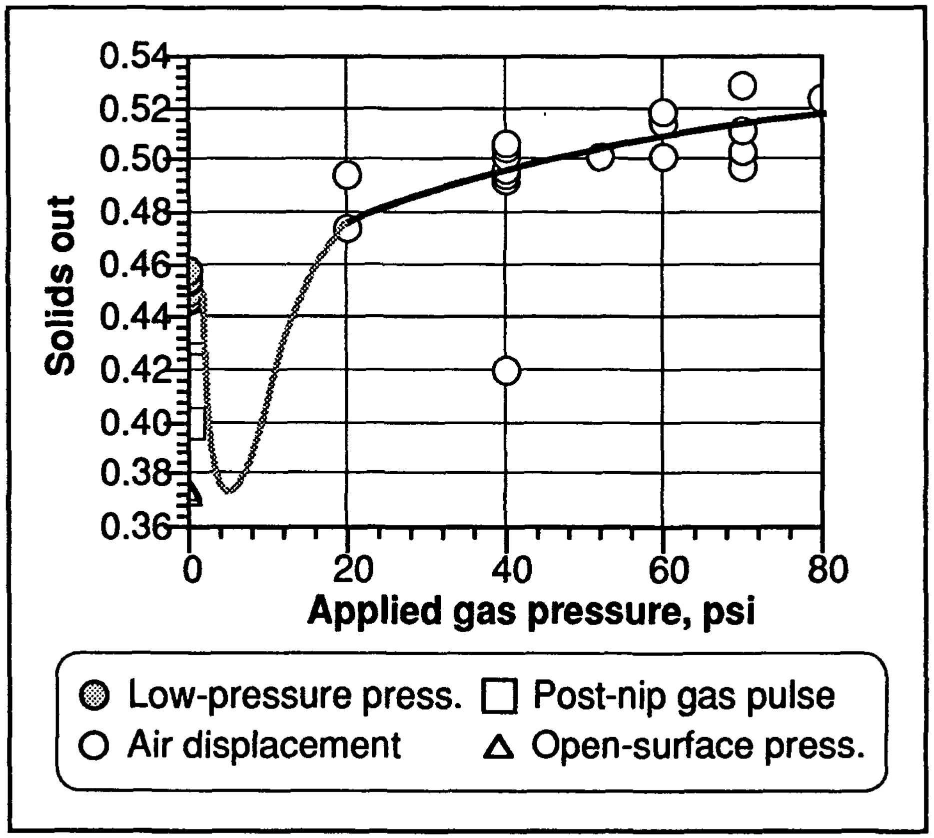

Plans for the next period

1. Carefully explore density-dryness relationships in displacement dewatering.
2. Determine optimum operating conditions.
3. Examine the effect of air temperature
4. Further explore the potential of steam.

Conclusions

- Displacement dewatering can remove additional water.
- Compared to a similar long-nip pressing process, the extra water removal is largely independent of bulk.
- Compared to regular wet pressing, the long nips required in displacement dewatering may be impractical and may lead to higher densification through creep consolidation.

IPST HASELTON LIBRARY
5 0602 01063891 6